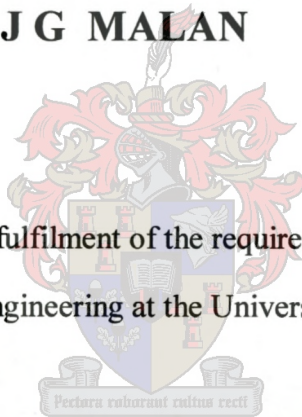


**FLOW RESISTANCE OF
LARGE-SCALE ROUGHNESS IN
MOUNTAIN RIVERS OF THE WESTERN CAPE**

By

J G MALAN

Thesis presented in partial fulfilment of the requirements for the degree of
Master of Science in Engineering at the University of Stellenbosch



Supervisor : Prof G R Basson

Declaration

I the undersigned hereby declare that the work contained in this thesis is my own original work and has not previously in its entirety or in part been submitted at any university in order to obtain an academic qualification.

Signature:

Date:

Abstract

This investigation arose out of the pressing need for alternatives to ineffective existing methodologies for low flow measurement in boulder bed rivers, with particular focus on the mountain streams in the Western Cape.

Both empirical and mathematical verification were regarded as important if progress was to be made towards identifying a suitable approach. Historically the inability to determine the frictional effect of the streambed on the flow rate has been a major obstacle limiting the accuracy of flow calculations. From literature, the most likely relationship appears to be a power function, utilising hydraulic variables derived from physical parameters characteristic of a section of stream.

Local Western Cape data was thus collected from various typical mountain streams, so that relevant analysis could be done. Testing of existing equations from literature sources on this set of data revealed limited applicability.

Subsequent empirical experimentation has shown that particle size is a dominant variable in determining boulder bed flow resistance under low flow conditions.

A mathematical approach was sought to provide a more suitable base for a locally applicable formula. Sediment transport theory, based on simple power conservation laws, was successfully implemented, partially bridging the gap between the applications for sand bed and boulder bed flow conditions respectively.

After a certain degree of empirical adjustment, an equation form was finalised that is believed to be the most suitable for Western Cape mountain streams, with definite potential for wider application, provided further research is done.

Opsomming

Hierdie ondersoek spruit uit die dringende behoefte aan bruikbare alternatiewe vir bestaande laagvloei meetmetodes in riviere met bodems bestaande uit spoelklip, met spesifieke klem op die bergstrome van die Wes Kaap.

Dit is as belangrik beskou om beide empiriese en wiskundige bevestiging te vind vir 'n verbeterde metode. Histories is die akkuraatheid van vloeitempo berekeninge hoofsaaklik beperk deur die onvoorspelbaarheid van die ruheidseffek van die rivierbodem op die vloei. Uit bestaende literatuur blyk dit dat die mees geskikte verwantskap waarskynlik 'n magsfunksie is, wat saamgestel is uit hidrouliese veranderlikes verkry vanaf fisiese parameters kenmerkend aan die spesifieke riviersnit.

Plaaslike Wes-Kaapse data is dus versamel op verskeie tipiese bergstrome in die gebied sodat geskikte ontledings gedoen kon word. Verskeie bestaende formules is getoets teen hierdie stel data en ongeskik gevind vir direkte aanwending.

Empiriese toetse het gevolg en getoon dat partikel grootte 'n dominante invloed het op die vloeiweerstand van spoelklip bodems onder laagvloei omstandighede.

'n Wiskundige benadering is daarna gevolg om 'n beter basis te verskaf waaruit 'n plaaslik bruikbare vergelyking kon volg. Sedimentvervoer beginsels, wat gebaseer is op basiese drywingsteorie, is suksesvol aangewend vir hierdie doel, en het in 'n mate die gaping tussen aanwending op sand en klip bodems oorbrug.

Na afloop van empiriese verstelling is 'n formule gefinaliseer wat beskou word as die mees geskikte vir Wes-Kaapse bergstrome, maar wat ook die potensiaal besit vir wyer aanwending, mits verdere navorsing gedoen sou word.

Dedicated to my parents, for their everlasting love and support

Acknowledgements

I hereby wish to express my sincerest gratitude to the following individuals who helped make this study possible:

The Almighty God for granting me the health, will and opportunity for this project.

Professor Gerrit Basson for his creative support, wisdom and encouragement throughout the duration of the project. His infectious enthusiasm and open-minded approach to difficult tasks is exemplary, and I would welcome any opportunity to work with him again in the future.

Professor André Görgens for initialising the opportunity to get involved with such an interesting and relevant project.

All the individuals who assisted during the field work process, without which data collection would have been impossible. They are (in no particular order):

Mia Barnard
Casper Brink
Roelof Le Roux
Frans Van Eeden
Sven (German student, surname unknown)
Jurgen (German student, surname unknown)

Cape Nature Conservation and SAFCOL for access to wilderness areas.

Francinah Sibanyoni of the Department of Water Affairs and Forestry, for the friendly assistance in acquiring gauging data.

The Department of Geography at Stellenbosch for supplying the map of the Western Cape.

All the individuals of the Water Division of the Department of Civil Engineering at Stellenbosch, for their general assistance and friendship.

Table of Contents

List of tables	iv
List of figures	v
List of symbols	viii
1. Introduction	1
1.1 Motivation	1
1.2 Purpose	4
1.3 Methodology	5
2. Flow resistance theory for boulder bed rivers	7
2.1 General hydraulic concepts concerning flow in mountain streams	7
2.1.1 Mountain stream flow regimes	8
2.1.2 Flow resistance in mountain streams	13
2.1.3 Bed roughness	15
2.1.4 Large-scale roughness	16
2.1.5 Energy losses in mountain streams	18
2.2 Existing theoretical basis for flow calculation	19
2.2.1 Basic laws of flow in open channels	19
2.2.1.1 <i>Conservation of Mass</i>	19
2.2.1.2 <i>Conservation of Momentum</i>	20
2.2.1.3 <i>Conservation of Energy</i>	20
2.2.1.4 <i>Conservation of Power</i>	21
2.2.2 Turbulent flow	23
2.2.3 General expression for steady uniform flow	24
2.2.4 The Chezy equation for steady uniform flow	24
2.2.5 Forms of the resistance equation	26
2.2.6 Factors affecting the resistance coefficient	29
2.2.6.1 <i>Roughness geometry</i>	29
2.2.6.2 <i>Channel geometry</i>	32
2.2.6.3 <i>Reynolds number</i>	33

2.2.6.4	<i>Froude number</i>	33
2.2.6.5	<i>Energy slope</i>	34
2.2.7	The approach of Simons and Senturk (1992)	35
2.2.8	Conclusion	36
3.	Data collection and processing	38
3.1	Field work methodology	38
3.1.1	Western Cape mountain stream characteristics	39
3.1.1.1	<i>Geomorphology</i>	39
3.1.1.2	<i>Physical characteristics</i>	40
3.1.1.3	<i>Hydraulic characteristics</i>	41
3.1.2	General criteria for selecting sites and sections	43
3.1.2.1	<i>River requirements</i>	43
3.1.2.2	<i>Logistic considerations</i>	44
3.1.2.3	<i>Sectional hydraulic requirements</i>	46
3.1.2.4	<i>Concluding remarks on criteria</i>	46
3.1.3	Selected sites	47
3.1.4	Data collection	56
3.1.4.1	<i>Data requirements</i>	56
3.1.4.2	<i>Collection process</i>	57
3.2	Data processing	65
3.3	The data set	68
4.	Methodology for deriving flow equation	71
4.1	Background	71
4.2	Initial testing of existing formulae	71
4.3	Empirical approach	75
4.3.1	Initial sediment transport investigation	76
4.3.2	Calibration procedures	78
4.4	Hydraulic theory considerations	79
4.4.1	Sediment transport theory	79
4.4.2	Hydraulic depth d versus hydraulic radius R	82
4.4.3	Bed material size distribution	84

4.4.4	Chezy's C versus relative roughness k/R	86
4.4.5	Comparison to existing formulae	87
4.5	Final proposal	88
5.	Variations on a theme	94
5.1	Sensitivity of slope in the chosen formulation	94
5.2	Averaged values of calculated discharge	96
6.	Verification of the derived equation	98
6.1	Background	98
6.2	Verification results	99
7.	Conclusions and recommendations	102
7.1	Conclusions	102
7.2	Recommendations	103
8.	References	105
	Appendix	108

List of tables

- Table 2.1 Parameters identified from literature.
- Table 3.1 Comparative general characteristics of selected sites.
- Table 3.2 Variables to be gathered from field visits.
- Table 3.3 Hydraulic parameter data set calculated from collected field data.
- Table 4.1 Empirical equations selected from literature.
- Table 4.2 Comparative discharge accuracies of equations tested (%).
- Table 4.3 Main parameters tested for significance.
- Table 4.4 The three best correlated equations.
- Table 4.5 Significant parameters.
- Table 4.6 Hydraulic radius R versus hydraulic depth d as a roughness parameter.
- Table 4.7 Addition of D_{84}/D_{50} to the roughness equation.
- Table 4.8 C instead of k/R as the roughness coefficient.
- Table 4.9 Accuracies of best existing equations in comparison to new equation.
- Table 5.1 Comparative accuracies of Equation (4.21) with different slopes.
- Table 5.2 Accuracies of original discharge values compared to averaged values.
- Table 6.1 Suitable data obtained from literature.
- Table 6.2 Accuracies of best existing equations in comparison to new equation.
- Table 6.3 Unsuitable data obtained from literature.

List of figures

- Figure 2.1 Upstream view of the Molenaars River, Du Toits Kloof.
- Figure 2.2 Range of bed material in alluvial channels (Simons and Senturk, 1992).
- Figure 2.3 Logarithmic velocity profile.
- Figure 2.4 S-shaped velocity profile.
- Figure 2.5 Form drag and surface distortion of a large boulder.
- Figure 2.6 Illustration of pool-riffle sequence of steep-sloped streams.
- Figure 2.7 Illustration of pool-fall sequence of very steep-sloped streams.
- Figure 2.8 Highly non-uniform flow conditions exhibiting more than one channel of flow in the Elandspad River, Du Toits Kloof.
- Figure 2.9 Plan view of a river showing various individual channels during a low flow period.
- Figure 2.10 Illustration of examples of form and grain resistance.
- Figure 2.11 Eddies fitting in with bed irregularities.
- Figure 2.12 Small-scale roughness (Simons and Senturk, 1992).
- Figure 2.13 Intermediate scale roughness (Simons and Senturk, 1992).
- Figure 2.14 Large-scale roughness (Simons and Senturk, 1992).
- Figure 2.15 Illustration of energy principle along a longitudinal flow section (Rooseboom, 2001).
- Figure 2.16 Stream power variation with depth (Basson and Rooseboom, 1997).
- Figure 2.17 Illustration of the ordinate of the centre of the boundary eddies R_0 .
- Figure 3.1 General map of South Africa.
- Figure 3.2 General map of the Western Cape Province.
- Figure 3.3 Schematic illustration of geomorphologic mountain ranges of the Western Cape (King, 1942).
- Figure 3.4 Suggested influences of different sized boulders under high and low flow conditions in a typical Western Cape scenario.
- Figure 3.5 Photo of gauging weir on the Berg River.
- Figure 3.6 Photo showing thick bush on the banks of the Berg River.
- Figure 3.7 Map of Du Toits Kloof catchment showing approximate location of Elandspad and Molenaars sites.

- Figure 3.8 Map of Jonkershoek catchment showing approximate location of Jonkershoek site.
- Figure 3.9 Map of Upper Berg River catchment, showing approximate location of Upper Berg site.
- Figure 3.10 Illustration of relevant terms.
- Figure 3.11 Photo of the Elandspad River looking upstream.
- Figure 3.12 Photo of the Jonkershoek River looking upstream.
- Figure 3.13 Photo of the Molenaars River looking upstream.
- Figure 3.14 Photo of the Berg River looking upstream.
- Figure 3.15 Illustration of cross-sectional measurements taken across a section of stream.
- Figure 3.16 Example of measured channel bottom in comparison to the top layer of boulders.
- Figure 3.17 Photo showing set up of measuring instruments on the Elandspad River.
- Figure 3.18 String spanned across the Molenaars River.
- Figure 3.19 A bottom reading being taken.
- Figure 3.20 Photo showing a water level reading being taken on the Berg River.
- Figure 3.21 Photo showing a close-up view of an estimated water level position being measured.
- Figure 3.22 Sampling of average water slope along a river reach.
- Figure 3.23 The median axis of a boulder.
- Figure 3.24 Grid system of particle sampling.
- Figure 3.25 Example of typical cross-section drawn with AutoCAD.
- Figure 3.26 Example of typical longitudinal profile drawn with Excel.
- Figure 3.27 Example of typical graph showing average particle sizes.
- Figure 4.1 Graphic representation of the three more accurate existing equations.
- Figure 4.2 v^*/v_{ss} plotted against $(gdS)^{1.5}/k$, with relative submergence the variable under observation.
- Figure 4.3 Illustration of relevant cross-sectional terms.
- Figure 4.4 Comparison of existing formulae with new equation.
- Figure 4.5 The quantitative effect of R on discharge.
- Figure 4.6 The quantitative effect of S_f on flow.
- Figure 4.7 The quantitative effect of D_{84}/D_{50} on flow.

- Figure 4.8 The quantitative effect of P on flow.
- Figure 5.1 Graph illustrating the minor influence of different slope values on the discharge calculated with Equation (4.21).
- Figure 5.2 Graph illustrating averaged discharge prediction in comparison to normal discharge prediction.
- Figure 6.1 Graph illustrating the fitting of the independent data sets from Tables 6.1 and 6.3.

List of symbols

A	=	Cross-sectional area of flow (m^2)
A_{bed}	=	Area of boundary per element (m^2)
A_F	=	Wetted frontal cross-sectional area of an element (m^2)
a	=	Constant
α	=	Coriolis coefficient compensating for velocity variation
b	=	Constant
C	=	Chezy's roughness coefficient ($\text{m}^{1/2}/\text{s}$)
C_D	=	Drag coefficient
C_r	=	Resistance coefficient
CS_a	=	Cross-stream axis (m)
c	=	Numeric constants
D_{84}	=	Particle size for which 84% of particles are of smaller size (m)
D_{50}	=	Particle size for which 50% of particles are of smaller size (m)
D_{xx}	=	Characteristic particle size (m)
d	=	Average or hydraulic flow depth (m)
d	=	Bed particle diameter (m)
$\frac{dv}{dy}$	=	Velocity gradient or angular velocity (s^{-1})
F	=	Froude number
F_x	=	Force component in x-direction (N)
f	=	Darcy-Weisbach's roughness coefficient
f_f	=	Friction factor
fn	=	"function of"
g	=	Gravitational acceleration (m/s^2)
H	=	Height of boulder (m)
h	=	Vertical elevation (m)
h_f	=	Frictional losses (m)
h_t	=	Transitional losses (m)
k	=	Roughness height (m)

k_s	=	Generated eddy size represented by roughness height (m)
κ	=	Von Karman coefficient, taken as constant = 0.4
L	=	Horizontal distance (m)
λ_l	=	Roughness spacing or concentration
n	=	Manning's roughness coefficient ($\text{s/m}^{1/3}$)
n	=	number of elements with the same drag coefficient
P	=	Wetted perimeter (m)
Q	=	Flow rate or discharge (m^3/s)
R	=	Hydraulic radius of cross-section (m)
R^2	=	Regression coefficient of correlation.
R_e	=	Reynolds number
R_0	=	Ordinate of the centre of the boundary eddies (m)
r	=	Outer radius of eddy (m)
ρ	=	Mass density of fluid (kg/m^3)
ρ_s	=	Average mass density of particles (kg/m^3)
S	=	Longitudinal slope
SF	=	Shape factor of element
S_f	=	Energy slope
S_0	=	Channel slope
S_w	=	Water slope
θ	=	Angle of channel bed to the horizontal (rad)
τ	=	Bed shear stress (N/m^2)
$\tau \frac{dv}{dy}$	=	Applied stream power (Nm/s)
U	=	Approach velocity at each element (m/s)
\bar{U}	=	Mean flow velocity (m/s)
v	=	Mean velocity of flow (m/s)
v_e	=	Velocity of fluid element (m/s)
v_x	=	Velocity component in x-direction (m/s)
v_{ss}	=	Average particle settling velocity (m/s)

v^*	=	Shear velocity (m/s)
ν	=	Kinematic viscosity ($\pm 10^{-6}$ m ² /s for water)
W	=	Surface width of section of flow (m)
X	=	Dimensionless independent variable
x,y	=	Constants
y	=	Depth of flow (m)
y_0	=	Mathematical distance from bed where velocity is theoretically zero (m)
z	=	Positional energy or head (m)

Chapter 1: Introduction

“Without water there is no life, and certainly no reconstruction and development.”

- Kader Asmal.

1.1 Motivation

South Africa is a water-scarce country. The result is an ever present striving towards more effective utilisation of the available resource, constrained by attempts to maintain the ecological health of the river systems. Accurate flow measurement, be it from an ecological or utilisation perspective, will always be an integral part of water planning if sustainable management of the limited natural supply is to be achieved. The maintenance of minimum water quality and flow standards in rivers and streams has been a state-supported issue in the USA for almost 20 years (Miller and Wenzel, 1985). In South Africa legislative protection has recently been provided for the first time, accommodating ecological considerations (National Water Act, 1998). *This new development makes the reliable description of stage-discharge relationships in the South African context all the more relevant.*

Accurate determination of the discharge for a specific stage in montane areas has been a major problem for hydrologists and ecologists alike. Where accurate recording of flows is possible such as at a properly functioning gauging weir, no need would exist for any other methods. However, weirs have certain practical and ecological limitations that can be summarised as follows:

1. The reaches that need recording are often located in inhospitable areas where inaccessibility could prevent the erection of gauging stations.
2. The high cost associated with constructing a proper gauging weir is always going to be a limiting factor, particularly in a developing country like South Africa that has many other pressing needs.
3. The hydraulic inability of weirs to sustain the normal downstream movement of bed materials diminishes their effectiveness. Weirs create an unnatural

disturbance to the flow regime, causing lower velocities and deposition of bed material. Constant removal of material and recalibration of the instruments are thus required to keep a weir effective.

4. The presence of weirs creates barriers to the natural movement and migration of aquatic life in a stream. Due to the adverse effects this could have on the ecological health of the river, alternative methods of measuring streamflow are urgently required.
5. Gauging weirs also detract from the aesthetic appeal of pristine environments. From a tourism or philosophical point of view, less obtrusive techniques are preferred for future usage.

The logical alternative to weirs is current meter gauging, which does not make use of a weir. However, apart from the fact that substantial effort will still be required to implement this technique in remote areas, the accuracies obtainable can vary significantly, and are at best of the order of 15% and at worst above 30%. The error involved is also likely to be higher as water levels fall and the stream splits up into various small channels. This method is thus not seen as a suitable alternative for low flow measurement. It has consequently become clear that other methods of flow measurement need to be investigated. *A less-invasive, non-damaging approach utilising easily measurable physical parameters is regarded as a desirable alternative. Finding such an alternative is the main focus of this study.*

Natural river flows are seen as the most complex and variable type of flow to be found in the hydraulic world, and are even likened to living organisms with “personality” (Kennedy, 1983). A main contributor to the descriptive difficulties concerning river flow is the frictional energy loss component. Friction is associated with the concept of hydraulic roughness, which is linked to river geometry, character of the bed material as well as the longitudinal energy slope. *The correct interpretation and description of the hydraulic roughness is central to the accuracy of river flow calculations.*

The shallow, cobble-bed mountain streams found in the Western Cape are considered in this study. Particular difficulties have been experienced in effectively measuring discharge in this area, mainly due to the rough nature of the terrain and the rivers

themselves. The streams that were selected are regarded as characteristic of and unique to the region. Steep slopes and a rough substrate contribute to high bed-friction that results in very turbulent flows. The retarding influence of the bed material is enhanced under low flow situations, which are common in the dry summer months. Previous research has shown that distinction between roughness description for low flows and higher flows is quite necessary if accuracy is to be improved (Bathurst, 1978). During low flow periods, so-called large-scale roughness conditions prevail, resulting in extreme values for empirical friction coefficients such as Manning's n and Chezy's C . It is also during these periods that water abstraction in the Western Cape is at its peak and aquatic life at its most vulnerable. The focus here is thus not on higher flows, but specifically on lower discharges, as it is of paramount importance that the mechanics of the lower flows be described more successfully if the proper balance between demand management and ecological well-being is to be found. *The extreme values of friction associated with low flows in the Western Cape require careful analysis and interpretation if progress is to be made concerning accurate large-scale roughness description and flow calculations.*

While bed roughness is one of the main causes of flow resistance in natural open channels, it is also the most difficult variable to quantify, particularly under large-scale roughness conditions. Mathematical uncertainties regarding the exact influence of the bed material on the flow resistance are increased under highly variable bed conditions such as those considered here. Empirically determined coefficient values are therefore used in such cases to fill the gap between rigorous mathematical description and the actual situation. Unfortunately, this approach has many obvious limitations. For instance, according to Miller and Wenzel (1985), the commonly used Manning's n does not provide a satisfactory description of variations in roughness with stage and discharge; neither does it accommodate frictional effects due to form drag. Extensive field calibration is usually required before a useful, but physically meaningless roughness parameter can be found. As Rouse (1938) pointed out as early as 1938, there is obvious merit in attempting to reconcile empirical evaluation with mathematical justification. *Both mathematical and empirical approaches have to be scrutinised so as to try and improve on large-scale roughness description.*

A number of studies have been carried out across the globe aimed at quantifying variables describing large-scale roughness. A multitude of different empirical friction formulae resulted, most of which have emerged from standard calibration techniques applied to particular data sets. However, equations derived in this fashion often tend to behave quite differently when applied directly to streams outside those they were calibrated on. *The need therefore arose to test the applicability of the more suitable foreign equations to local Western Cape Rivers, and to identify potential candidates for direct application or further analysis.*

1.2 Purpose

The preceding section establishes a definite need for an ecologically acceptable, cost-effective and easily applicable method of accurately measuring flow under large-scale roughness conditions. *The main purpose of this study is thus the evaluation of existing large-scale roughness formulae and applicable roughness parameters using a low-flow data set collected on Western Cape mountain streams, and the subsequent development of an improved expression for local large-scale roughness application that would allow reliable flow determination.*

This leads to the following specific aims for the study:

- *Literature review to identify roughness formulae and parameters used for describing large-scale roughness.*
- *Obtaining a dataset consisting of Western Cape mountain stream low-flow data.*
- *Testing well-known large-scale roughness formulae using the local dataset.*
- *Identifying the most suitable parameters for use in a large-scale roughness expression.*
- *Development of an improved empirical expression for large-scale roughness.*

- *Discussion of the main parameters and mechanisms identified empirically in terms of hydraulic theory fundamentals.*
- *Verification.*
- *Recommendations for practical application for the determination of stream flow in an ecologically acceptable and economically viable manner.*
- *Proposed further investigations.*

1.3 Methodology

Literature was reviewed to analyse applicable theory and identify potentially suitable friction equations for local large-scale roughness application. Such equations consist of different combinations of hydraulic parameters, which attempt to characterise a cross-section of a stream at a certain discharge. Parameters commonly used include hydraulic radius, hydraulic depth, energy slope, substrate size distribution and channel-width. Simons and Senturk (1992) evaluated large-scale roughness equations on their own set of data and recommended the most suitable version. It was decided that a similar approach was to be followed by measuring and fitting local data to selected equations, after which meaningful interpretation and proposed improvement could follow.

Applicable data were collected in the field over a period of time from various suitable catchments seen as significant in terms of runoff and where flow was being measured with weirs. Allocated field sites were visited under different discharge conditions ranging from $0.1 \text{ m}^3/\text{s}$ up to $4 \text{ m}^3/\text{s}$ so as to obtain a representative low-flow dataset. A raw data sample would typically consist of cross-sectional area, wetted perimeter, stream top-width, boulder sizes and average water slope. The necessary hydraulic parameters could then be extracted from the raw data and applied to friction formulae.

Various empirical roughness formulae as recommended in previous studies (Simons and Senturk, 1992; Thorne and Zevenbergen, 1985; Bathurst, 1978) were analysed by using the locally obtained data. Many of these formulae share the same variables, with

only emphasis and constants being different. The more significant dimensionless parameters were identified in the equations investigated and used as a basis for further analyses and recalibration.

This was done empirically through common regression techniques so as to try and determine those having the most significant influence on roughness description. All previously used combinations were tested along with some new but plausible alternatives. The parameter combinations and the final coefficient were kept dimensionless throughout so that independence from measuring units would ensure wide applicability (Simons and Senturk, 1992).

Significant mathematical and physical justification for the empirically derived expressions was regarded as a much sought after objective. The applicable stream-power theory was investigated to potentially provide a fundamental basis for the empirically determined relations. The power theory was chosen for analysis as it has been shown to describe sediment transport mechanisms effectively (Rooseboom, 1992), and the possibility of applying the same principles to larger bed materials was seen as an important step towards describing large-scale roughness mechanisms satisfactorily in a unified manner.

The final expression proposed for the large-scale roughness coefficient was tested for accuracy against the data set and supported by a comparison to various other known formulae, followed by an investigation concerning certain aspects surrounding the logic and practicality of the derived equation. Finally the applicability of the chosen formula was verified on independent sets of data selected from various literature sources.

Chapter 2: Flow resistance theory for boulder bed rivers

2.1 General hydraulic concepts concerning flow in mountain streams

Mountain streams are usually characterised by high gradients and coarse bed material. Very rough turbulent conditions prevail, particularly when flow is low and the bed material protrudes through the free surface. The roughness caused by the shallow depth combined with the large bed material dominates resistance to flow under these conditions. A typical example of a mountain stream in the Western Cape is the Molenaars River as depicted in Figure 2.1. Particular attention to some of the above concepts is given in this chapter.



Figure 2.1 Upstream view of the Molenaars River, Du Toits Kloof.

2.1.1 Mountain stream flow regimes

The hydraulic processes of rivers in mountainous regions differ from those found in lowland areas. The main reasons for this are the coarser bed material, steeper slopes and shallow depths in comparison to the size of bed material found there (Thorne and Zevenbergen, 1985). Figure 2.2 provides a visual interpretation of the character differences possible between mountain streams and lower lying areas. The various particle sizes and channel slopes (S_0) shown are overemphasised to illustrate the typical tendency of channel slope and bed material size to increase towards the mountain areas where the rivers originate from.

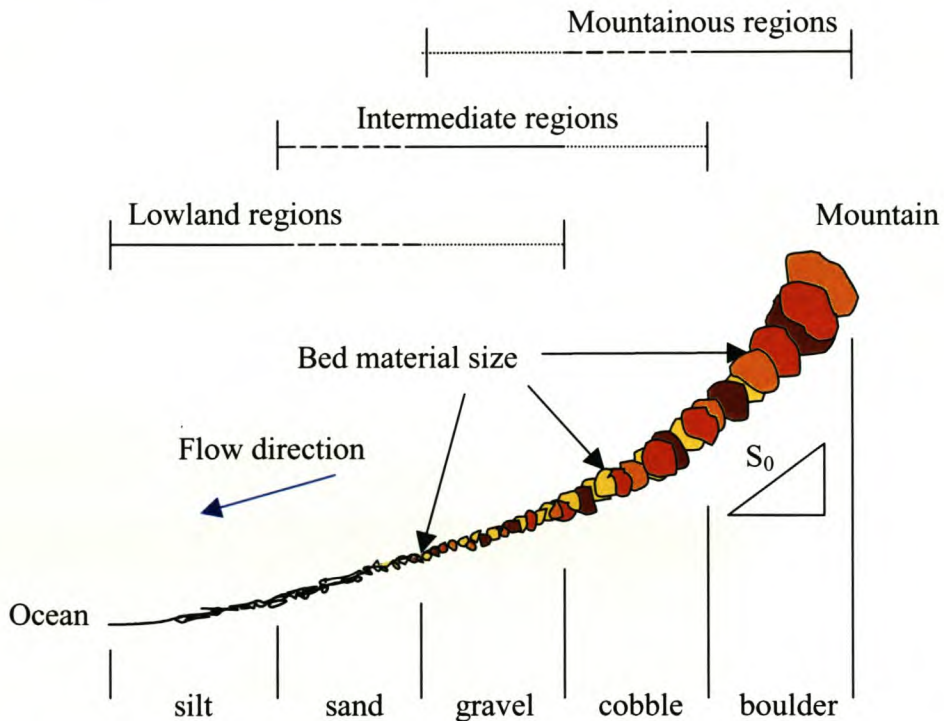


Figure 2.2 Range of bed material in alluvial channels (Simons and Senturk, 1992).

A logarithmic velocity profile is normally prevalent in steady uniform flow (Figure 2.3). However, in mountain streams the increased flow resistance due to bed roughness has a major impact on the flow profile. A logarithmic velocity profile is therefore not always to be found under these more adverse flow conditions (Smart, 1999). Drag and other resistive effects retard flow between major boulders and below the tops of these boulders, whereas flow is less impeded above the tops of the major

boulders and high velocities are possible there (Bathurst, 1987). The vertical velocity profile thus exhibits an S-shaped form (Figure 2.4), different from the familiar logarithmic profile present under less rough conditions and less turbulent flow. Ferro and Baimonte (1994) confirmed the S-shaped profile by conducting a flume study.

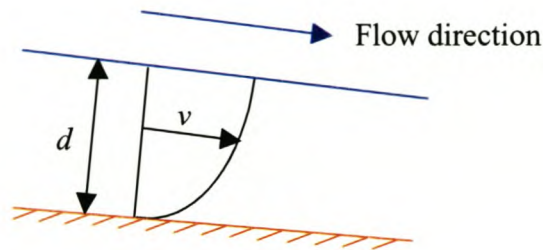


Figure 2.3 Logarithmic velocity profile.

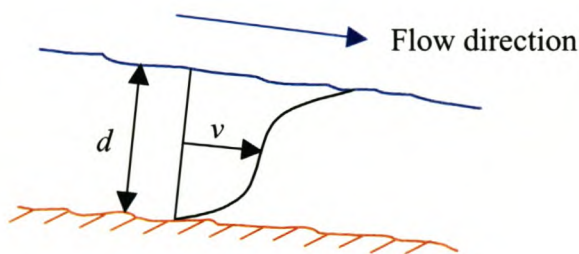


Figure 2.4 S-shaped velocity profile.

In Figures 2.3 and 2.4 the following apply:

- d = Average or hydraulic flow depth (m)
- = $\frac{A}{W}$
- A = Cross-sectional area of flow (m²)
- W = Surface width of section of flow (m)
- v = Mean velocity of flow (m/s)

As discharge decreases, the depth of flow decreases in relation to the size of the bed roughness particles. The resistance to flow begins to exert a dominant influence on the flow hydraulics, and the resistance due to bed forms becomes significantly greater than the surface drag (also known as skin friction) of the bottom (Miller and Wenzel,

1985). Whereas resistance in lowland streams is primarily a function of skin friction on the channel boundary, skin friction decreases in significance as slopes and bed material size increase (Simons and Senturk, 1992). According to Rouse (1965), at depths comparable to the size of the bed material, each boulder begins to act independently as a local non-uniformity influencing energy loss. Thorne and Zevenbergen (1985) state that for large relative roughness situations, i.e. bed material large in comparison to flow depth, flow resistance is mostly caused by the form drag of boulders, free surface distortion, and hydraulic jumps. Simons and Senturk (1992) describes form drag as a function of energy loss associated with turbulence and material size increase. A visual illustration of form drag and surface distortion by a large boulder is presented in Figure 2.5.

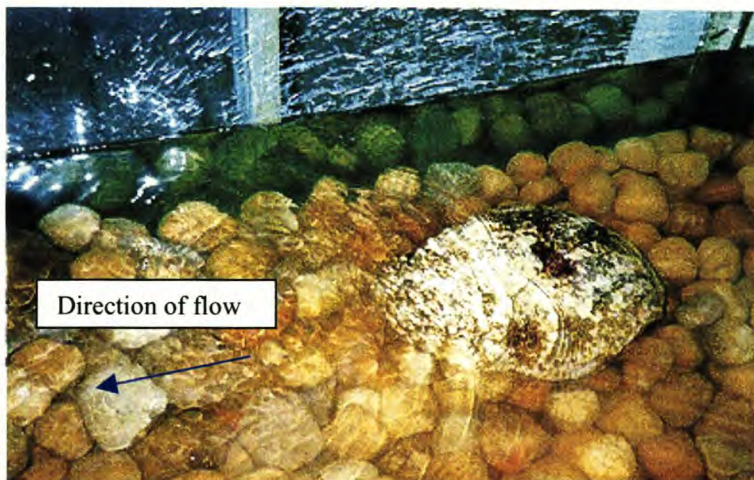


Figure 2.5 Form drag and surface distortion of a large boulder.

According to Smart (1999), coarse bedded rivers are hydraulically rough, with the thickness of a viscous sub-layer assumed to be insignificant. Bed form patterns as observed in sand-bed channels disappear completely in boulder bed streams, and the only bed form pattern distinguishable is the characteristic pool-riffle sequence as illustrated in Figure 2.6 (Simons and Senturk, 1992). Form resistance has a much smaller influence than is the case where bed forms are present, and grain resistance therefore dominates the flow (Simons *et al*, 1979). If the channel slope becomes very steep, a pool-fall configuration as shown in Figure 2.7 could replace the pool-riffle sequence (Bathurst, 1985).

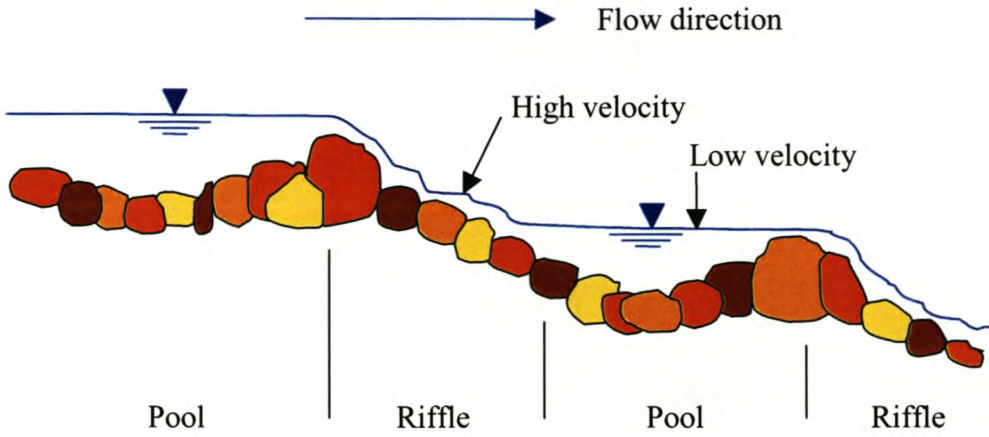


Figure 2.6 Illustration of pool-riffle sequence of steep-sloped streams.

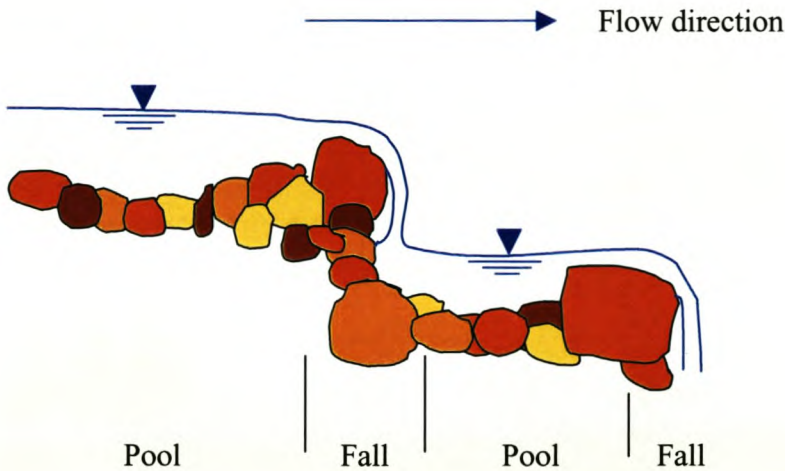


Figure 2.7 Illustration of pool-fall sequence of very steep-sloped streams.

Miller and Wenzel (1985) found the pool-riffle sequence to be the dominant channel feature during low flows. Pools are characterized by more depth and slower moving water, whereas riffles are generally shallow with rapid flow. Pools act similarly to reservoirs, with small slopes and low velocity, while riffles resemble chutes or broad-crested weirs with steeper slopes and high velocities. The channel geometry is highly non-symmetric under these circumstances, and the prevailing flow characteristics non-uniform, as can be seen in Figure 2.8.



Figure 2.8 Highly non-uniform flow conditions exhibiting more than one channel of flow in the Elandspad River, Du Toits Kloof.

It was observed in the field that a low-flowing stream often breaks up into various channels exhibiting individual riffle and pool configurations (see Figures 2.8 and 2.9). The velocities and slopes observed in the pool areas were very low, whereas the chutes exhibited high velocities and steep slopes (see Figure 2.6). What complicates the problem is that riffles and pools are often located in parallel across a single section of stream, implying significant transitional losses (Figure 2.9). Bathurst (1978) describes these zones of separation, acceleration, and deceleration around the roughness elements as local non-uniformity, but suggests that despite local effects the average flow along a reach could still be close to uniform.

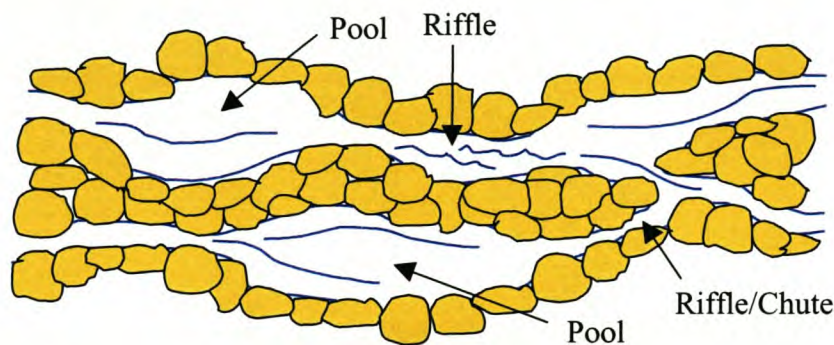


Figure 2.9 Plan view of a river showing various individual channels during a low flow period.

2.1.2 Flow resistance in mountain streams

Flow resistance is representing of the hydraulic processes by which the geometry and bed roughness of a channel determines the depth and mean velocity of flow (Thorne and Zevenbergen, 1985). When attempting to calculate the discharge, the hydraulic processes are represented by a flow resistance coefficient such as Manning's n , Chezy's C and Darcy-Weisbach's f . In steady uniform flows, these coefficients are related to velocity, hydraulic radius and energy slope as indicated below:

$$\text{Manning:} \quad n = \frac{R^{2/3} S_f^{1/2}}{v} \quad (2.1)$$

$$\text{Chezy:} \quad C = \frac{v}{\sqrt{R S_f}} \quad (2.2)$$

$$\text{Darcy-Weisbach:} \quad f = \frac{8gRS_f}{v^2} \quad (2.3)$$

From where:

$$\left(\frac{8}{f}\right)^{1/2} = \frac{C}{\sqrt{g}} = \frac{R^{1/6}}{n\sqrt{g}} \quad (2.4)$$

- where:
- n = Manning's roughness coefficient (s/m^{1/3})
 - C = Chezy's roughness coefficient (m^{1/2}/s)
 - f = Darcy-Weisbach's roughness coefficient
 - R = Hydraulic radius of cross-section (m)
 - = $\frac{A}{P}$
 - P = Wetted perimeter (m)
 - S_f = Energy slope
 - g = Gravitational acceleration (m/s²)

Ferro and Giordano (1991) distinguished between two main forms of flow resistance: *Grain resistance* is described as the resistance due to the shape, size, and arrangement of the roughness elements on the channel boundary (See Figure 2.10). In other words, it is resistance created by element geometry, which is primarily represented by bed roughness. Bathurst *et al* (1981) also referred to this as roughness geometry. *Form resistance* is linked to flow separation and macro-scale eddies as a function of channel alignment, cross-sectional shape, slope, and so on. It therefore mainly represents the resultant resistance effect of the channel geometry (Figure 2.10). For example, a specific boulder could be exposed and contribute more to channel shape and form resistance under low flows, but be submerged and become part of bed roughness and grain resistance under higher flows. This will be explained further in Chapter 3. Of these two forms of resistance, grain resistance is regarded as the main contributor to flow resistance under large-scale roughness conditions (Ferro and Giordano, 1991; Bathurst *et al*, 1981).

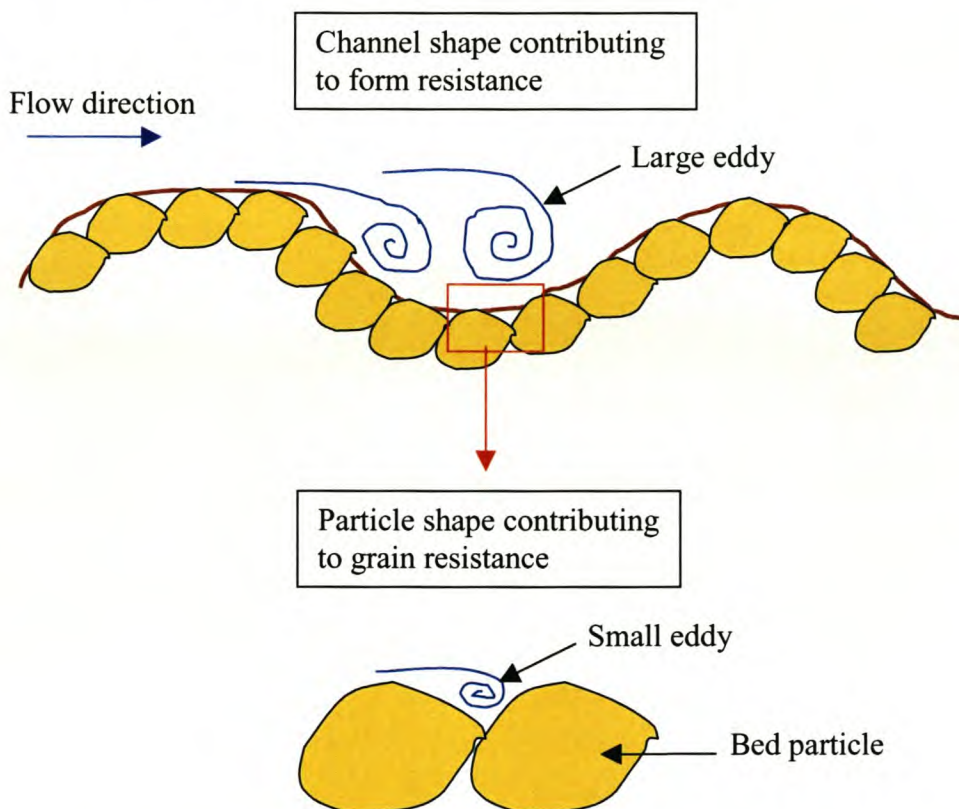


Figure 2.10 Illustration of examples of form and grain resistance.

The chief contribution to flow resistance in mountain streams under medium and low flow conditions is widely regarded to be drag around individual particles. This is so

because of the large size of the bed material in relation to the flow depth (Simons and Senturk, 1992). As mentioned above, roughness geometry is thus seen as the most important resistive factor, while channel geometry plays an indirect role in affecting the drag of the elements (Bathurst, 1978; Simons *et al*, 1979). According to Lopez and Falcon (1999) highly irregular bed material, wake turbulence, localized hydraulic jumps downstream from protruding boulders (implying varying energy dissipation) and a number of other lesser effects also contribute to the variable nature of flow resistance in mountain streams.

Due to the mathematical complexities accompanying turbulence description and the multitude of factors affecting mountain stream flow, rigid mathematical analysis is considered to be too difficult and cumbersome to apply in practice for the time being (Massey, 1989; Bathurst *et al*, 1981). Analysis of experimental data in determining flow resistance therefore remains an integral part of practical application. With grain resistance seen as the premier resistive factor in mountain streams, most proposed derivations focus primarily on calculating the effects of grain resistance on the streamflow.

2.1.3 Bed roughness

The size of the instantaneous eddies that characterise turbulent flow are depicted by the bed geometry where, as illustrated in Figure 2.11, those that are formed right next to the bed will have almost the same diameter as the bed irregularities present (Rooseboom, 1992). The size of the irregularities of the bed therefore influences the flow resistance that in turn affects the depth and velocity of flow.

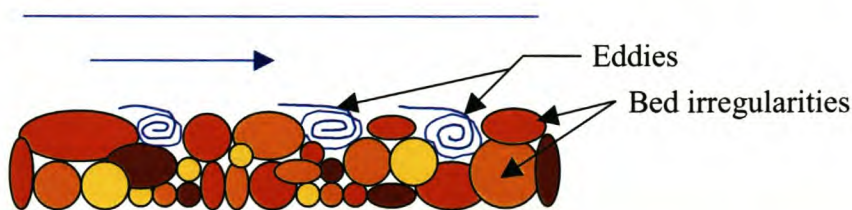


Figure 2.11 Eddies fitting in with bed irregularities.

The sizes of roughness elements in hydraulically rough channels vary widely, and are thus normally described by a representative grain size (Smart, 1999). The grain sizes are indicated by the percentage of elements smaller than a particular size, for example D_{84} represents the 84th percentile grain diameter, i.e. 84% of elements are of smaller dimensions.

The effective size of the prevailing eddies are equated through a roughness height parameter k (Rooseboom, 1992). There have been various attempts to relate the roughness height to the physical size of the roughness elements. For example, according to Smart (1999), the roughness height of gravel bed rivers is typically two to five times the bed particle size, whereas Hey (1979) was more precise and found the roughness height of gravel bed rivers to be $3.5D_{84}$. Nikuradse's roughness height k_s (a derivative roughness height parameter for sand grains experimentally derived by Nikuradse) has also been related by widely varying constants to representative grain size (Miller and Wenzel, 1985; Thorne and Zevenbergen, 1985; Smart, 1999).

It is thus clear that bed material size is related to roughness height in some way or another, but that uncertainty regarding this relation still exists, particularly under large-scale roughness conditions as defined in Section 2.1.4. Hey (1979) states that roughness height is substantially increased by wake interference. According to Chow (1959), k is representative of the roughness effect created by the roughness elements, and is therefore not only related to the dimensions of the elements, but also to their shapes, orientations and impact on flow. Bathurst (1978) and Ferro and Giordano (1991) emphasize that particle concentration or spacing could also be of significant importance.

2.1.4 Large-scale roughness

Because of the irregular nature of natural channel sections and the relatively large bed material found in mountain rivers, flow resistance is greater at low flows than at high flows (Bathurst, 1982). Large-scale roughness conditions occur at low relative submergence where the physical processes are dominated by form drag around individual particles and distortion of the free surface (Simons and Senturk, 1992), where relative submergence is defined as the ratio of the flow depth or hydraulic

radius to the characteristic bed particle size. Bathurst (1978) states that in the case of large-scale roughness, the roughness elements tend to act individually, with the total resistance produced mainly due to the sum of their form drags.

According to Bathurst *et al* (1981), the roughness is large-scale if the roughness elements affect the free surface. In these situations the bed material size, usually characterized by D_{84} , is of the same order of magnitude as the average flow depth d (also known as hydraulic flow depth), with boulders commonly protruding the free surface. Large-scale roughness is generally considered to prevail at relative submergence (d/D_{84}) values of smaller than 1.2 (Figure 2.14).

Figures 2.12 to 2.14 conceptually illustrate the distinguishable three roughness scales. Figures 2.12 and 2.13 could apply to high flow conditions in a boulder bed river, whereas Figure 2.14 could be representative of the same river during low flow conditions. Figures 2.12 and 2.13 could of course also represent a low flow situation in a sand or gravel bed river.

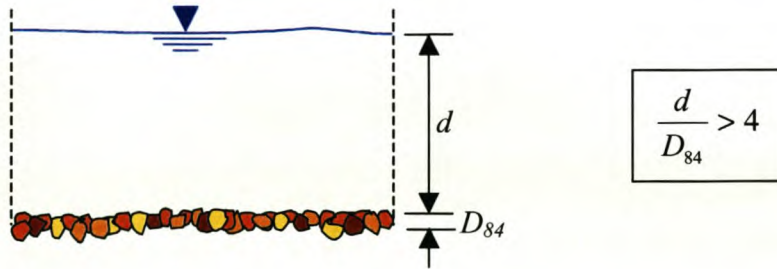


Figure 2.12 Small-scale roughness (Simons and Senturk, 1992).

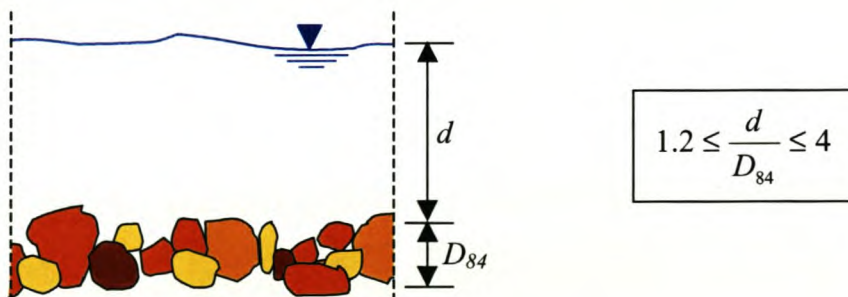


Figure 2.13 Intermediate scale roughness (Simons and Senturk, 1992).

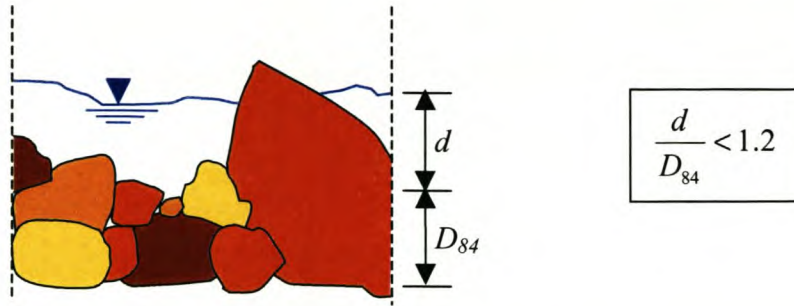


Figure 2.14 Large-scale roughness (Simons and Senturk, 1992).

where: D_{84} = Particle size for which 84% of particles are of smaller size (m)

2.1.5 Energy losses in mountain streams

Mountain streams are in general characterised by steep slopes and rough beds. Energy losses are severe and primarily due to the added flow resistance of the large bed material and local contraction or expansion around individual particles (Miller and Wenzel, 1985).

Of these the significant frictional effects associated with the bed material are the main causes of energy dissipation. A good example of this is the resultant form drags of individual elements protruding into the main flow area, where the velocity profile is completely disrupted by the presence of these elements (See Figure 2.5).

The continuously varying velocity components caused by channel slope variations between chute and pool reaches are responsible for transitional losses. Despite these prevailing losses, transitional effects are generally ignored in analyses, probably because calculation would be too complex and the results approximations at best. Furthermore, Bathurst (1978) states that local contractions and expansions might not affect the general uniform state of flow significantly.

2.2 Existing theoretical basis for flow calculation

The characteristics of the irregular flow behaviour typically prevalent in cobble and boulder bed streams are difficult to quantify effectively. It is therefore not surprising that no universally applicable resistance equation for high-gradient boulder bed rivers is available at present, and also no standard quantification of the wide variations in resistance at different flow rates exist (Chow, 1959; Bathurst, 1978; Bathurst, 1985). As Simons and Senturk (1992) points out, resistance to flow shows a marked dependence on flow rate, with resistance increasing as flow rate decreases. With errors of up to 100% possible in the calculated value of the resistance coefficient f according to Bathurst (1985) (and thus also significant errors for Manning's n and Chezy's C), it is clear that predicting the effects of the parameters influencing resistance still requires some attention.

2.2.1 Basic laws of flow in open channels

Flow in open channels is subjected to atmospheric pressure on the free surface. Since this pressure is constant, flow is the result of the force of gravity, i.e. a weight component of the fluid (Massey, 1989). In an ideal fluid the laws of conservation of mass, momentum, energy and power prevail, and are used to describe flow relationships (Rooseboom *et al*, 2001). These laws are discussed briefly.

2.2.1.1 Conservation of Mass

Assuming constant density of the fluid, conservation of mass in a specific time period is represented by the continuity equation:

The sum of inflows into a control volume = the sum of outflows from a control volume

or:

$$\Sigma Q_{in} = \Sigma Q_{out} \quad (2.5)$$

where: Q = Flow rate or discharge (m^3/s)

2.2.1.2 Conservation of Momentum

Assuming hydrostatic pressure and steady state conditions, the conservation of momentum can be defined as follows:

The sum of all external force components acting upon a body of fluid in a time period = the sum of the momentum flux components of the outflows minus the sum of the momentum flux components of the inflows during that time period

or:

$$\sum F_x = \sum \rho Q_{out} v_{x_{out}} - \sum \rho Q_{in} v_{x_{in}} \quad (2.6)$$

where: F_x = Force component in x-direction (N)
 ρ = Mass density of fluid (kg/m^3)
 v_x = Velocity component in x-direction (m/s)

2.2.1.3 Conservation of Energy

Conservation of energy is described by the Bernoulli equation:

$$\frac{\alpha_1 v_1^2}{2g} + y_1 \cos\theta_1 + z_1 = \frac{\alpha_2 v_2^2}{2g} + y_2 \cos\theta_2 + z_2 + h_{f_{1-2}} + \sum h_{l_{1-2}} \quad (2.7)$$

where: z = Positional energy or head (m)
 $y \cos\theta$ = Potential energy (m)
 $\frac{\alpha v^2}{2g}$ = Kinetic energy (m)
 h_f = Frictional losses (m)
 h_l = Transitional losses (m)
 α = Coriolis coefficient

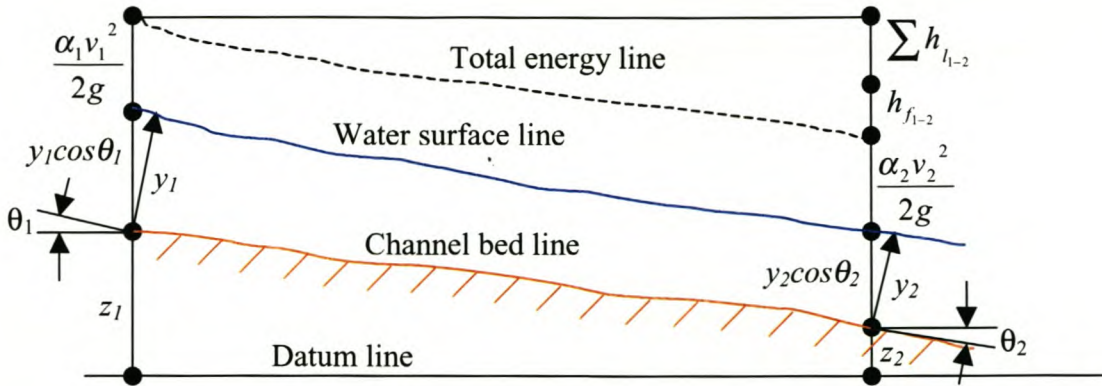


Figure 2.15 Illustration of energy principle along a longitudinal flow section (Rooseboom *et al*, 2001).

2.2.1.4 Conservation of Power

The law of conservation of power is mathematically related to momentum and energy conservation, and is therefore usually not treated separately. However, stream power theory as used to describe sediment transport mechanisms is specifically investigated elsewhere in this document as a possible fundamental link to empirical friction relationships (see Section 4.4). According to Rooseboom (1992), the law of conservation of power states:

The power made available due to potential energy expenditure = the power applied to maintain fluid motion

or (per unit volume):

$$\int_{y_0}^d \rho g S v_e dy = \int_{y_0}^d \tau_e \frac{dv}{dy} dy \quad (2.8)$$

- where:
- v_e = Velocity of element (m/s)
 - τ_e = Shear stress of element (N/m²)
 - $\frac{dv}{dy}$ = Velocity gradient (s⁻¹)
 - y_0 = Mathematical distance from bed where velocity

S = is theoretically zero (m)
 = Longitudinal slope

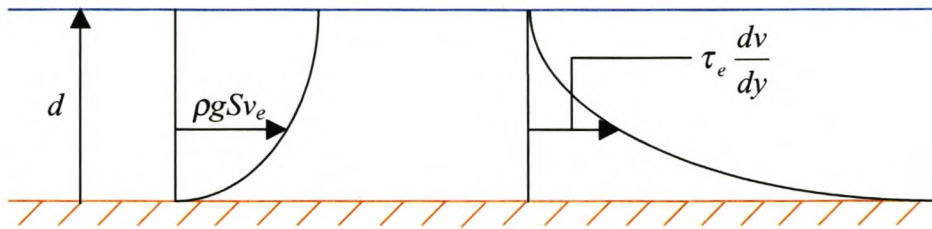


Figure 2.16 Stream power variation with depth (Basson and Rooseboom, 1997).

If power theory is applied to rough turbulent conditions, the unit stream power applied in maintaining motion along a bed with prevalent eddies of height $2R_0$ (See Figure 2.17) can be expressed as follows according to Rooseboom (1992):

$$\left(\tau \frac{dv}{dy} \right) \propto \frac{\rho g S_f d \sqrt{g d S_f}}{2R_0} \quad (2.9)$$

where: $\tau \frac{dv}{dy}$ = Applied power per unit volume
 R_0 = Ordinate of the centre of the boundary eddies (m)

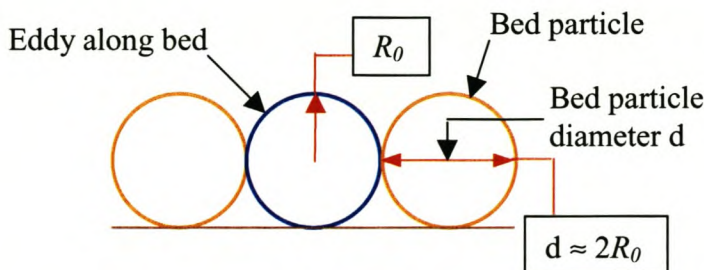


Figure 2.17 Illustration of the ordinate of the centre of the boundary eddies R_0 .

2.2.2 Turbulent flow

Erratic fluid particle movement characterizes turbulent flow. This random behaviour causes instantaneous fluctuations in the dimensional velocity components. Momentum exchange takes place whereby shear stresses additional to those found in laminar flow are set up (Featherstone and Nalluri, 1995). These apparent shear stresses existing between fluid elements have a retarding effect on the flow, and are thus a reflection of the flow resistance. According to power principles the shear stresses are generated by eddying motion on a much larger scale than the molecular movement found in laminar flow. Newton's law of viscosity governs laminar flow, and fluid particles move along smooth layers. According to Rooseboom (1992), the apparent shear stress of turbulent flow is directly related to the size of the prevailing eddies as follows:

$$\tau_t = \frac{\rho}{2\pi} r^2 \left(\frac{dv}{dy} \right)^2 \quad (2.10)$$

where:

τ_t	=	Average turbulent shear stress across eddy (N/m ²)
r	=	Outer radius of eddy (m)
$\left(\frac{dv}{dy} \right)$	=	Angular velocity of eddy (s ⁻¹)

Laminar and turbulent flow are distinguishable by the Reynolds Number for open channel flow:

$$R_e = \frac{vR}{\nu} \quad (2.11)$$

where:

R_e	=	Reynolds number
ν	=	Kinematic viscosity (10 ⁻⁶ m ² /s for water)

The Reynolds number is an indicator of the relative importance of inertial and viscous forces in a flow. If the Reynolds number is small, viscous forces dominate the flow resistance, and laminar conditions prevail. If the Reynolds number is large, viscous force becomes small in comparison to inertial force and turbulent conditions is found (Chow, 1979). Reynolds numbers can roughly be classified according to conditions as follows (Rooseboom *et al*, 1997):

- (i) Fully developed turbulent conditions - $R_e > 2000$
- (ii) Transitional conditions - $2000 \geq R_e \geq 500$
- (iii) Fully laminar conditions - $R_e < 500$

2.2.3 General expression for steady uniform flow

Steady uniform flow in open channels has generally been related to flow resistance in the following form (Chow, 1959; Hey, 1979):

$$v = C_r R^x S^y \quad (2.12)$$

- where:
- C_r = Resistance coefficient
 - S = Energy slope S_f
 - = Channel slope S_0
 - = Water slope S_w
 - x, y = Constants

The best known versions of the above expression are the Manning, Chezy and Darcy-Weisbach equations. Since it is theoretically sound and widely used in South Africa, particular further attention is given to the Chezy equation.

2.2.4 The Chezy equation for steady uniform flow

In the case of steady uniform flow, the hydrostatic forces acting on the fluid are in equilibrium and the resistance of the channel balances the forces due to gravity (Chow, 1959). Towards the end of the eighteenth century, Chezy experimentally

derived a relationship describing uniform flow (Massey, 1989). This formula was later proven theoretically and can be expressed as follows:

$$Q = vA = C\sqrt{RSA} \quad (2.13)$$

or:

$$h_{f_{1-2}} = \frac{Q^2 L_{1-2}}{A^2 C^2 R} \quad (2.14)$$

where:

$$S = \frac{h_{f_{1-2}}}{L}$$

$h_{f_{1-2}}$ = Frictional energy loss between section 1 and 2
(m)

L_{1-2} = Length of channel between section 1 and 2 (m)

From the studies performed on pipe flow, it was found that C is closely linked to the size of the generated eddies and accordingly the size of the bed material (Massey, 1989). The relationship of C to hydraulic radius R and roughness height k for rough-turbulent conditions can be written as follows (Rooseboom *et al*, 1997):

$$C = 5.75\sqrt{g} \log \frac{12R}{k} \quad (2.15)$$

where: k = size of eddies generated at bottom and sides of channel (m)

This expression for C , along with Manning's n and Darcy-Weisbach's f , describes flat gradient, sand- and gravel-bed streams adequately, but does not interpret the diverse conditions prevalent in steep sloped, boulder bed streams very well. According to Simons and Senturk (1992), analysis involving significant physical characteristics and parameters using a power function is generally considered more relevant for application on large-scale roughness situations. Prominent physical processes

controlling resistance to flow are considered to include bed material size, depth of flow and energy slope.

Although some previous studies focused on the Manning equation (Jarrett, 1984), Darcy-Weisbach's f was the most commonly encountered coefficient (Simons and Senturk, 1992; Thorne and Zevenbergen, 1985), mainly due to its dimensionless character aiding analysis and utilisation and its scientifically sound background (Bathurst, 1986). In the South African context, C or k is more widely used, and an effort was thus made to accommodate it in a proposed new formulation.

The Chezy coefficient relates to Manning's n and Darcy-Weisbach's f as follows (Thorne and Zevenbergen, 1985):

$$C = \left(\frac{8g}{f} \right)^{1/2} = \frac{R^{1/6}}{n} \quad (2.16)$$

or, in dimensionless form:

$$\frac{C}{g^{1/2}} = \left(\frac{8}{f} \right)^{1/2} = \frac{R^{1/6}}{ng^{1/2}} \quad (2.4)$$

2.2.5 Forms of the resistance equation

Friction factor relationships are commonly expressed in two forms (Bray, 1979):

$$\text{Semi-logarithmic: } \frac{1}{\sqrt{f_f}} = a_1 + a_2 \log X \quad (2.17)$$

or:

$$\text{Power: } \frac{1}{\sqrt{f_f}} = b_1 X^{b_2} \quad (2.18)$$

where: f_f = Friction factor
 X = Dimensionless independent variable
 a, b = Constants

The form of Equation (2.17) is similar to the theoretically derived semi-logarithmic relationship between grain resistance and the relative submergence as from boundary layer theory (Simons and Senturk, 1992):

$$\sqrt{\frac{8}{f}} = a + b \log \frac{d}{D_{xx}} \quad (2.19)$$

where: a, b = Constants
 D_{xx} = characteristic particle size (m)

However, it is important to note that this expression was derived for small-scale roughness, where the processes controlling resistance to flow are very different from that of large-scale roughness (Bathurst, 1978; Bathurst *et al*, 1981). Once the relative roughness enters the large-scale domain, the resistance to flow is higher than that predicted by Equation (2.19) (Bathurst, 1978). Ferro and Giordano (1991) stressed that the semi-logarithmic form of the flow resistance equation can only be applied to flow exhibiting large-scale resistance if it is the result of an empirical correlation.

Ferro and Giordano (1991) amended Equations (2.17) and (2.18) by substituting f with C and defining X as the relative submergence:

Semi logarithmic form:
$$\left(\frac{C}{\sqrt{g}} \right) = c_1 \log \left(\frac{R}{D_{xx}} \right) + c_2 \quad (2.20)$$

or:

Power form:
$$\left(\frac{C}{\sqrt{g}} \right) = c_3 \left(\frac{R}{D_{xx}} \right)^{c_4} \quad (2.21)$$

where: c_1, c_2, c_3 = Numeric constants

No clear distinction seems to be made between the use of hydraulic radius or hydraulic depth in the relation with particle size. Thorne and Zevenbergen (1985) defines relative roughness as the ratio of bed material size to flow depth, which implies hydraulic depth, but Simons *et al* (1979) and Chow (1959) define relative roughness with R instead of d . In rivers that are fairly wide in relation to depth, as are most of those experiencing large-scale roughness conditions, the values of hydraulic radius and hydraulic depth are assumed to be similar, which means the difference between the results will in all probability be negligible. For example, in the low-flow data set provided by Miller and Wenzel (1985), the values for hydraulic radius and hydraulic depth are almost exactly the same. This is also illustrated on local data later on. Hydraulic radius is preferred here, as it is a more commonly recognisable term, and may hold physical advantages over hydraulic depth.

Both the semi-logarithmic and power forms have been extensively investigated (Bathurst *et al* (1981), Thorne and Zevenbergen (1985), Ferro and Giordano (1991), Simons and Senturk (1992), Rosso *et al* (1990)). Although Ferro and Giordano (1991) found a semi-logarithmic equation to give the best fit to a flume study, Bathurst *et al* (1981) regarded the power law as more suitable than the semi-logarithmic law for large-scale roughness, as the resistance processes of small-scale roughness from which the semi-logarithmic law was derived differ from those of large-scale roughness. Bathurst (1985) stated that the S-shaped velocity profile implies very high surface velocities. This results in inaccurate answers due to overestimation of flow and thus underestimation of friction by the semi-logarithmic law. The irony of this statement is that the expressions he calibrated through the years were almost always semi-logarithmic. The comprehensive study by Simons and Senturk (1992) convincingly argued that the power form generally proves the most suitable basis for large-scale roughness application (see Section 2.2.7). From a practical perspective, it does seem wise to avoid logarithmic expressions, simply because of the possible mathematical complexities that could result in the calibration and application of such derivations. Theoretical justification of the power form will also be provided in Section 4.

2.2.6 Factors affecting the resistance coefficient

If accurate flow calculations under large-scale roughness conditions are to be done, the hydraulic processes causing resistance to flow and thus determining the resistance coefficient need to be successfully quantified. Bathurst *et al* (1981) emphasized the importance of individual form drag as main resistive factor, and stated that the processes of fluid mechanics under large-scale roughness conditions could be related to roughness geometry (affecting the effective roughness concentration), channel geometry (affecting the relative roughness area), Reynolds number (affecting the element boundary layer) and Froude number (affecting free surface drag). The influence of energy slope can also be significant (Bathurst, 1978; Jarrett, 1984; Rouse, 1965), and is added to the above factors for further discussion below:

2.2.6.1 Roughness geometry

The consequence of the variations in size and shape of roughness elements on a riverbed is that the flow resistance is strongly affected by roughness geometry (Ferro, 1999). Griffiths (1981) regarded internal distortion resistance associated with rugged and diverse bed topography as the most significant cause of error in friction coefficient estimation. These sentiments, along with the known prominence of form drag as a resistive factor in mountain stream flow, confirms that parameters representative of the roughness geometry are likely to have notable influence on the resistance coefficient. Various aspects related to roughness geometry, such as the relative roughness, roughness shape, size distribution and spacing could therefore prove to be significant.

The relationship between roughness height and hydraulic radius or hydraulic depth is known as **relative submergence** R/D_{xx} (also referred to in Sections 2.1.4. and 2.2.5), or in its inverse form relative roughness D_{xx}/R . Boundary layer theory showed this dimensionless relation to be the most important resistive parameter under small-scale roughness conditions. Although no theoretical justification for its presence in large-scale friction formulae exist, various studies seem to suggest that the relationship between roughness height and hydraulic radius or hydraulic depth remains an important descriptor of the resistance coefficient under large-scale roughness

conditions in open channel flow (Bathurst, 1978; Miller and Wenzel, 1985; Simons *et al*, 1979; Simons and Senturk, 1992).

Bathurst (1978) states that **roughness shape** is determined mainly by local geology, and the effect of shape is thus likely to be constant in a region of similar geology. This was proven at various sites where little variation, and thus little influence was observed. The Western Cape could be considered as a region of similar geology, with similar quartzite boulders present in all streams investigated. Thorne and Zevenbergen (1985) also discounted element shape as a notable parameter as a consequence of a flume study that revealed no marked influence of different shapes on the flow resistance. Bathurst (1978) defined roughness shape factor as the ratio of the boulder height to the cross-stream axis of the assumed semi-elliptical elements:

$$SF = \frac{H}{CS_a} \quad (2.22)$$

where: SF = Shape factor of element
 H = Height of boulder (m)
 CS_a = Cross-stream axis (m)

From literature the effect of shape on the resistance coefficient seems to be minor. From a practical point of view, it would be laborious and difficult to measure average boulder shape effectively in streams with extremely diverse bed material, as is the case in the Western Cape. Shape is therefore discarded as a potential friction parameter on the grounds of measuring difficulties and limited frictional influence.

As pointed out earlier in Section 2.1.3, the **bed material size distribution** is an important variable influencing roughness height and determining the amount of developed form drag. Bed material size usually appears in a dimensionless relationship such as relative submergence (R/D_{84} , R/D_{50} , d/D_{84}) or size distribution (D_{84}/D_{50}). Whereas Bathurst (1978) states that the resistive effect of the roughness size distribution should be approximately constant in rivers, Simons and Senturk (1992) advocates the inclusion of a bed material gradation factor (D_{84}/D_{50}) in friction expressions. The significance of bed material gradation is explained by its

representation of the coarse portion of the bed material. These larger elements have a major impact on flow through form drag, localized hydraulic jumps and transitional energy loss, and a reflection of their presence should prove noteworthy, particularly in reaches containing a diverse tapestry of particle sizes.

Various conducted studies mention **roughness spacing** or concentration as a possibly notable resistance variable (Bathurst, 1978; Simons *et al*, 1979; Ferro and Giordano, 1991). Under the assumption of longitudinal uniform flow, Bathurst (1978) equated resistive stresses in terms of form drag and element concentration to arrive at a basic flow resistance relationship:

$$\sqrt{\frac{8}{f}} = \left[\frac{1}{\frac{1}{2} C_D \lambda_1 \left(\frac{U}{\bar{U}} \right)^2} \right]^{1/2} \quad (2.23)$$

- where:
- C_D = Drag coefficient
 - λ_1 = Roughness spacing or concentration
 - = $\frac{\sum_1^n A_F}{A_{bed}}$
 - n = number of elements of the same drag coefficient
 - A_F = Wetted frontal cross-sectional area of an element (m²)
 - A_{bed} = Area of boundary per element (m²)
 - U = Approach velocity at each element (m/s)
 - \bar{U} = Mean flow velocity (m/s)

Equation (2.23) highlights the importance of the drag coefficient, roughness spacing, and the ratio of the approach velocity U at each element to flow velocity \bar{U} . The quantification of concentration or spacing in this manner is however considered to be cumbersome and impractical (Thorne and Zevenbergen, 1985). In later years,

Bathurst (1985) did relate λ to relative submergence to try and improve the utility of his equations. This resulted in the following, highly empirical relation:

$$\lambda = 0.039 - 0.139 \log \left(\frac{R}{D_{84}} \right) \quad (2.24)$$

From flume experiments, Ferro and Giordano (1991) found that the effect of particle concentration could be implicitly included in friction expressions if D_{84} or D_{90} were used as characteristic particle diameter in the relative submergence relationship, as is unwittingly illustrated by Bathurst in Equation (2.24). A bed gradation factor such as (D_{84}/D_{50}) could possibly also include this effect. The potential of roughness concentration as a noteworthy and readily applicable parameter in friction relationships therefore appears limited.

2.2.6.2 Channel geometry

Bathurst (1978) found that the resistance coefficient is influenced to a certain degree by channel geometry. The inclusion of a channel geometry factor in the friction formula is thus considered. Simons *et al* (1979) stated that channel shape is one of three main factors influencing the resistance coefficient, the other two being relative roughness and roughness spacing. Myers (1991) focused specifically on channel geometry, and found its influence to be significant, with wide sections exhibiting much higher friction factors and lower flow capacity than narrow sections.

In contrast to these findings, Griffiths (1981) stated that the influence of wide channel cross-section shape on friction factors is minor, and that spurious correlation limits the applicability of shape factors like P/R ; P being the wetted perimeter and R the hydraulic radius. Furthermore, apart from Bathurst's equation, no other studies included channel shape in friction expressions. The implicit inclusion of the influence of channel shape in roughness equations through the presence of hydraulic radius $R=A/P$ is probably the main reason for this. It seems therefore as if divided views exist regarding the importance of channel geometry as a roughness parameter.

2.2.6.3 Reynolds number

The Reynolds number reflects the effects of viscosity on the flow. Bathurst (1982) stated that the Reynolds number could significantly affect the flow resistance, as the form drag varies according to the state of the boundary layer on the element and therefore the flow type, i.e. laminar, transitional or turbulent. This might be so for variable flow type, but in natural gravel or boulder bed streams the flow is always completely turbulent, which should diminish the influence of Reynolds number. Graf (1987) concluded that the effect of Reynolds number could be safely ignored in rough streams. Furthermore, an important point to keep in mind when considering Reynolds number, is that its presence in a roughness expression would mean that velocity v is found on both sides of the discharge equation. This can be illustrated as follows:

$$R_e = \frac{vR}{\nu} \quad (2.11)$$

Say: $f = fn(R_e)$

where: $fn = \text{“function of”}$

Then: $Q = vA = \sqrt{\frac{8gRS_f}{f}}A = \sqrt{\frac{8gRS_f}{fn(R_e)}}A \quad (2.25)$

The existence of velocity on both sides of the equation means that spurious correlation would result from calibration of such an equation, and an iterative approach will be needed to solve it. Consequently, the usefulness of the Reynolds number seems limited.

2.2.6.4 Froude number

Distortions of the free surface are called free surface drag and vary with Froude number (Bathurst *et al*, 1981). Rosso *et al* (1990) further emphasized that the Froude number affects the value of the friction factor in open channels under unstable flow

conditions. In contrast to the above, Graf (1987) stated that the effect of Froude number is minor and could be readily ignored. Afzalimehr and Anctil (1998) based their friction formulation on a relationship between the Froude number and the friction factor f . However, in subsequent discussions, both Aberle *et al* (1999) and Rennie and Millar (1999) pointed out that Froude number already defines the friction factor f :

$$f = 8SF^{-2} \quad (2.26)$$

where:

$$F = \text{Froude number}$$

$$= \frac{v}{\sqrt{gR}}$$

This means that spurious correlation could result from including the Froude number in a calibrated equation. It would thus appear that the Froude number (or rather its parameters) indeed has an influence on flow resistance, but that its inclusion as such in a friction formula could result in unnecessary complications.

2.2.6.5 Energy slope

Jarrett (1984) emphasized that the effect of slope must be allowed for in high-gradient streams if reasonable agreement with real flow rates is to be had. Bathurst (1985) agreed that slope has some sort of influence, but avoided going into detail. Bray (1979) also suggested the significance of slope in determining frictional relationships, although no specific inclusion in roughness formulation is advocated.

The general impression gathered from literature is that apart from Jarrett (1984) and Simons and Senturk (1992), most publications reviewed tend to be fairly vague in discussions surrounding slope and its importance as a roughness parameter. Many noteworthy studies (Bathurst *et al*, 1981; Simons *et al*, 1979; Thorne and Zevenbergen, 1985) either discard or neglect its influence on the friction factor, mostly in favour of focussing on relative roughness as a key parameter. Despite this fact, it was felt that the possible significance of slope must not be unduly

underestimated. The steeper slopes associated with mountain streams and large-scale roughness conditions is one of the main characteristics defining this type of flow, and along with the larger bed material is what separates it from other types of river flow. This in itself suggests enough relevance to warrant further investigation.

2.2.7 The approach of Simons and Senturk (1992)

The methodology followed by Simons and Senturk in their 1992 study was regarded as central to the further investigation of large-scale roughness mechanics, and thus plausible enough to be mentioned specifically in this section. Simons and Senturk discussed the processes of natural stream flow, and more particularly flow under large-scale roughness conditions in Chapter 6.8 of “Sediment Transport Technology”. Equations from various publications spanning more than a decade were displayed there to highlight the studies’ exclusive focus on large-scale roughness conditions in contrast to previous works, where intermediate scale roughness conditions were also included in analyses.

They then evaluated the factors affecting resistance to flow so as to determine the most appropriate form for a large-scale roughness equation. The resultant conclusion was that the most influential parameters that can be easily obtained are the hydraulic radius, bed-material gradation and channel gradient. The suitability of the semi-logarithmic relationship for large-scale roughness conditions was also discussed, and it was stated that expressions of this form have some applicability, but that the power form could more readily express the relevant parameters. This was proven through various calibrations, where the power form consistently gave the best fit to the data set. It was also mentioned that relative roughness, the chief parameter of the semi-logarithmic equation, decreases in importance with increasing gradient, while at the same time the gradation coefficient increases in significance as slope increases. The following equation was thus advocated (Simons and Senturk, 1992):

$$\sqrt{\frac{8}{f}} = 1.11 \left(\frac{d}{D_{84}} \right)^{0.46} \left(\frac{D_{84}}{D_{50}} \right)^{-0.85} S_f^{-0.39} \quad (2.27)$$

As can be seen, three of the notable parameters discussed in Section 2.2.6 were regarded as significant to describe large-scale roughness adequately, namely the relative submergence, bed material size distribution and energy slope. Equation (2.27) gave the best correlation of the numerous formulations analysed by Simons and Senturk, and verification by an independent study further proved its applicability. Consequently, a strong case is made for the relevant parameters. It was also stated that the relatively simple form and use of commonly available variables makes it a relatively easy equation to apply in practice.

Whereas the exact form of the above equation may prove not to be the best option for local or general large-scale roughness application, it does point out the more significant parameters involved. As for the Simons and Senturk study as a whole, notable progress was made concerning the general approach most suitable to these extreme roughness environments and the roughness parameters most likely to be of influence.

2.2.8 Conclusion

There is certainty from the literature investigated regarding the necessity of large-scale roughness conditions to be treated as a separate form of flow, and the main obstacle is widely recognised as being the meaningful interpretation of the roughness coefficient. The physical characteristics determining the mechanics of flow resistance need to be included in roughness analyses to provide a more representative and applicable expression, but it is also important that these variables be easily obtainable and measurable. The power form of the roughness equation is preferred to the semi-logarithmic form, as it has various advantages regarding applicability and ease of interpretation.

Table 2.1 summarizes the roughness parameters as discussed in the above sections. At this stage it can be concluded that previous studies, and Simons and Senturk (1992) in particular with Equation (2.27), indicate towards the relative submergence, bed material gradation and slope as significant parameters affecting the resistance coefficient, whereas uncertainty still surrounds the influence of some of the others. Roughness shape can be eliminated for reasons already given in Section 2.2.6.1, and

roughness concentration seems an unlikely contributor that would be difficult to quantify effectively. The effects of channel shape also appears to be limited, while the use of Reynolds and Froude numbers could result in largely spurious correlation. These possibilities will require careful analysis with the help of locally collected data so as to hopefully provide more insight into extreme roughness situations and their successful interpretation, particularly in the Western Cape context. The next logical step is thus the gathering of representative hydraulic data from streams located in this region.

Table 2.1 Parameters identified from literature.

Name	Symbol	Importance
Relative submergence	$\frac{R}{D_{84}}, \frac{R}{D_{50}}, \frac{d}{D_{84}}$	✓
Roughness shape factor	SF	✗
Bed material gradation	$\frac{D_{84}}{D_{50}}, \log\left(\frac{D_{84}}{D_{50}}\right)$	✓
Roughness concentration	λ	✗
Channel shape factors	$\frac{R}{P}, \frac{W}{P}$?
Reynolds number	$\frac{vR}{\nu}$?
Froude number	$\frac{v}{\sqrt{gR}}$?
Slope	S_f, S_0, S_w	✓

Chapter 3: Data collection and processing

3.1 Field work methodology

The acquisition of a representative data set was regarded as an essential prerequisite for the success of the project, and it was realised that meaningful processing and analysis could only proceed once this information was available. The data set was to be of Western Cape origin, a winter rainfall region comprising the south-western part of the Republic of South Africa (see Figure 3.1). This region was chosen mainly because of the existing need for improved measuring techniques for the secluded boulder bed mountain streams that are found there. However, the wider need for more reliable description of large-scale roughness conditions also influenced this choice, since the low summer flows of Western Cape streams present ideal conditions for research on the subject.



Figure 3.1 General map of South Africa.

It was considered important that the typical mountain stream characteristics of the region be reflected. After an investigation as to the possibilities available, four prominent headwater streams from three of the more notable watersheds, namely the Berg, Breede and Eerste River systems, were selected for fieldwork (see Figure 3.2). The approximate location of the rivers is indicated in Figure 3.2 on a map supplied by the University of Stellenbosch: Department of Geography. The required information could then be systematically sampled from these rivers towards obtaining an applicable data set. The collection procedure as well as the basic processing of the gathered information are discussed below.

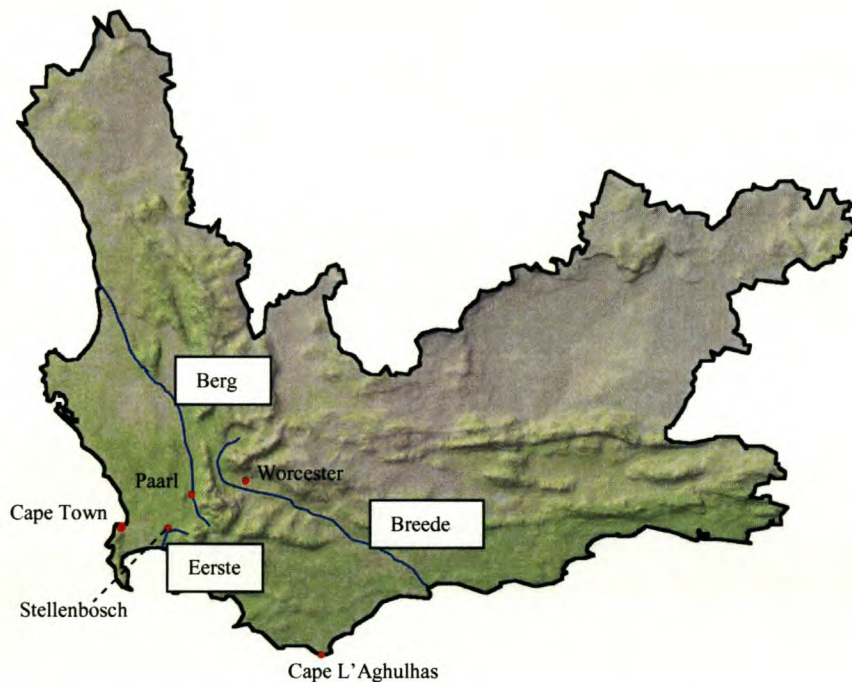


Figure 3.2 General map of the Western Cape Province.

3.1.1 Western Cape mountain stream characteristics

3.1.1.1 Geomorphology

Two geomorphologic ranges can be distinguished in the Western Cape (see Figure 3.3). A Southern Folded Belt is located along the eastern parts parallel to the southern

coastline towards Cape Town, and a Western Folded Belt lies in a north-south direction along the west coast. The two ranges meet in the Worcester area, resulting in a zone of conflict with intricate mountain forms. The typical make up of these mountains is a mixture of quartz, quartzite, minor sandstones, various types of granite and a base of more resistant quartzitic sandstone of the Table Mountain Group (King, 1942; Theron *et al*, 1992). The bed material of the streams that drain these mountains consist of boulders and cobbles that have been eroding from the mountain base for millions of years, and are primarily made up of quartzite.

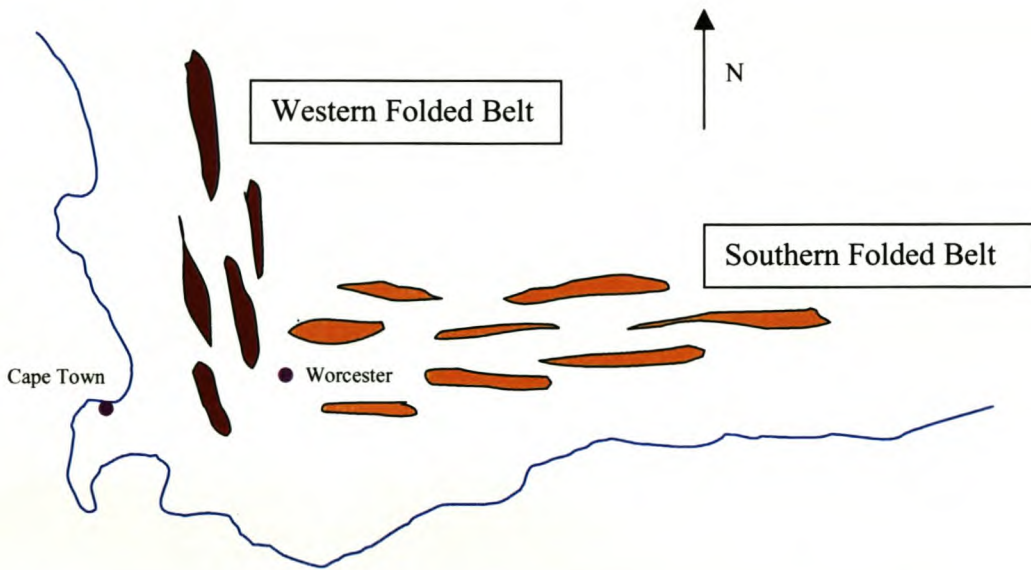


Figure 3.3 Schematic illustration of geomorphologic mountain ranges of the Western Cape (King, 1942).

3.1.1.2 Physical characteristics

Mountain streams in the Western Cape can be typically described as possessing steep gradients and a diverse substrate of quartzite boulders and cobbles. Riffle-pool configurations (Section 2.1.1) can often be identified, although a clear distinction between a riffle-pool or boulder-bed character as defined by Bathurst (1986) does not seem apparent (see also Section 3.1.3). It is thus argued that the Western Cape mountain streams can be described by both these definitions, depending on location and discharge. It is further believed that the riffle-pool sequence is closely linked to

flow rate, where it could appear or disappear as discharge increases, depending on the character of the stream. This would, however, require specific further investigation.

3.1.1.3 Hydraulic characteristics

The boulder bed characteristics of the Western Cape mountain streams cause turbulent flows, particularly during the dry summer months when flows shrink to trickles. Extreme values for friction coefficients such as Chezy and Manning are possible, and effective roughness heights similar in magnitude to the stream depth are not uncommon. These waters are classic examples of mountain streams where large-scale roughness conditions prevail, as described in Section 2.1.4. The processes and parameters that dominate this type of flow are therefore very relevant in the Western Cape context.

Due to the prevalent low summer flows and the rough nature of the bed material, energy dissipation is mainly due to the high flow resistance of the streambed. Most energy is dissipated in the steep and shallow areas of flow and it was decided to concentrate on riffle and run sections for obtaining hydraulic data. Riffle areas have steeper slopes and higher velocities, resulting in high frictional losses. They are generally affected by channel controls rather than specific section controls, which is a necessary prerequisite if the bed resistance is to be the main depicter of the roughness coefficient (Bathurst, 1985). Pools have energy slopes and velocities of close to zero, with many “dead areas” not effectively contributing to the flow, making them less suited to flow calculations. The frictional losses in pools are thus minor and difficult to ascertain accurately, and they were consequently avoided as measuring areas in terms of friction analysis.

Under low flow conditions, Western Cape streams commonly break up into several channels of very shallow flow (see Figure 2.8). These separate channels can be found at substantially different elevations in parallel across a specific section, and the direction of flow of each channel is not necessarily the same as that of the main course of the river. The resultant flow, however, will be. Furthermore, some flow occurs in between and below boulders, which are not accounted for in the measuring process. These flows can normally be ignored, but as water levels fall they increase in

relative importance. The above facts enhance the complex character of the flow, and are some of the reasons why accurate flow calculations are difficult to perform at very low flows.

As mentioned in Section 2, significant variation in resistance to flow with discharge has historically been observed in boulder bed rivers, and a constant value for flow resistance under a wide range of flow rates is recognised to be unrealistic (Simons and Senturk, 1992). In the Western Cape, high winter flow conditions differ drastically from low summer flows, and it was expected that high flows would be affected by roughness mechanisms of a different type and scale than those causing low flow resistance (see Figure 3.4). Whereas a big boulder (say 1 metre in diameter) that is virtually dry in summer has no influence on bed resistance (although still influencing channel shape and thus form resistance), it could make a notable contribution to bed roughness when submerged in winter. Bigger boulders that form part of the roughness geometry in winter could easily be regarded as part of the channel geometry in summer. Bathurst (1978) supported this view by pointing out that the drag influence of smaller and lower lying boulders would decrease as depth increases, while the drag influence of larger and higher lying boulders would increase with depth. The conclusion is thus that it is necessary to distinguish between bed roughness prediction for low flows and bed roughness prediction for higher flows also in the Western Cape context, with this study focusing solely on the lower discharge scenario for reasons already mentioned in Section 1.

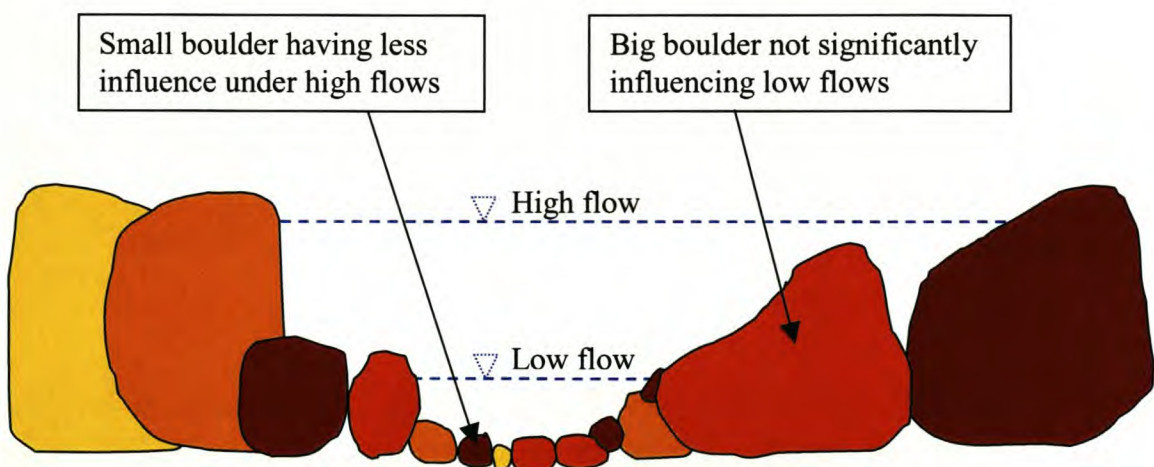


Figure 3.4 Suggested influences of different sized boulders under high and low flow conditions in a typical Western Cape scenario.

3.1.2 General criteria for selecting sites and sections

3.1.2.1 River requirements

Rivers had to be found that are considered typical Western Cape boulder bed rivers. This means that the characteristics described above had to be present and identifiable in the selected catchments. Furthermore, tributaries or headwaters of some of the major river systems of the Western Cape had to be included in the data set, as the goal was after all to obtain a selection of information that is as representative of general Western Cape conditions as possible. This also meant that the streams had to be able to produce noteworthy runoff, which implies importance in terms of utilisation as well as ecology.

The next important consideration was that streams had to be found which are in an undisturbed state. This implies that they are as unaffected by human intervention as possible, so that the existing characteristics of the river could be accepted as natural. The following were considered particularly important:

1. The bed material had to be in natural positions as originally sorted by the river flow, because unnatural changes could affect the roughness to be analysed.
2. The river flows had to be as unaffected by unnatural water abstraction or addition as possible, as the characteristics of a river are undeniably influenced by the prevailing flow rates.
3. The water quality had to be high. In the Western Cape this implies see-through clarity and no heavy sediment loads. If significant enough unnatural sediment deposition had taken place, the effective bed roughness could be notably affected.
4. The streamside vegetation had to be as undisturbed as possible, as it is believed that the natural growth found next to a river keeps the river channel intact and protected from bank erosion, and thus in its original shape. A section where river growth is absent could for instance result in the heavy winter floods causing notable alterations to the original channel shape, because the banks had been exposed by high flows.

3.1.2.2 Logistic considerations

It was imperative that sites be located in the proximity of effectively working gauging weirs as also advocated by Bathurst (1985), so that the discharges obtained from a weir could be regarded as the comparative true flow rates, and thus be used in the calibration process (see Figure 3.5). No water was to enter or leave the system between a weir and the chosen site, as this could jeopardise the mass balance, which would result in inaccuracy. This meant that sites had to be as close to the gauging stations as possible to avoid losses or gains, but still located far enough to be hydraulically unaffected by their presence. Downstream of a weir, the effects of the changed flow pattern are the main concern, and on bigger rivers such as the Berg River, these effects could be present up to 300 metres downstream. On smaller streams though, this distance is much reduced. Upstream of a weir, the weir pool plus any possible backwater effects of high flow conditions had to be avoided. The backwater considered was for the condition until the weir is 100% submerged. Generally, in steep mountain streams this backwater does not progress very far upstream, but to be safe the first 100 metres was regarded as off limits.



Figure 3.5 Photo of gauging weir on the Berg River.

Potential sites also had to be easily accessible. In the first instance this means that a public road or path had to be located close to the stream so that fairly easy entrance under most flow and weather conditions would be possible.

Secondly, the montane areas of the Western Cape are known for their rough and unforgiving nature. It is rocky terrain and quite demanding in terms of steepness and unevenness underfoot, and heavy bush growth in certain areas adds to the possible site related difficulties (see Figure 3.6). Consequently, sections had to be found that are reasonably comfortable to access on a regular basis.



Figure 3.6 Photo showing thick bush on the banks of the Berg River.

Thirdly, due to practical, financial and time limitations the sites had to be located close to Stellenbosch, so that regular visits would be possible. Luckily, many of the premier water carrying streams are found within a reasonable distance of Stellenbosch, and could be used for fieldwork.

The fourth prerequisite was safety. Apart from criminal aspects, which are unfortunately also a reality today, care had to be exercised in selecting rivers and site locations so that the possible risk of injury would be minimised. Aspects taken into consideration include the following:

1. Potentially dangerous terrain e.g. cliffs, sharp and slippery rocks and thorny bush growth.
2. Deep and strong sections of river flow that could be risky to enter on a regular basis.
3. Areas where wild animals abound. Animals considered potentially dangerous in the Western Cape are baboons, leopards and snakes.

3.1.2.3 Sectional hydraulic requirements

In general, uniform flow is required for resistance equations to be applicable. This implies that no change in flow velocity occurs in the direction of flow over a given distance. Strictly speaking, this flow state is not commonly found in natural streams under large-scale roughness conditions. However, no workable alternative to empirical correlation exists at present, and until such time as a better solution to the problem is found, the assumption of uniform flow will have to do. Consequently, fairly straight sections without major changes in slope or width were sought to provide conditions as close to the uniform flow state as possible (Bathurst, 1986; Jarrett, 1984).

The reaches had to be free from obstructions such as driftwood at the flows under consideration, because this could also influence the flow resistance. Chosen reach lengths were further to be characterised by the following:

1. A minimum of bush intrusion for the length of the relatively uniform riffle reach.
2. A reasonably steep channel slope, so that the total fall of the water surface over the reach should significantly exceed the range of error that could arise from measurement of the water surface elevations or uncertainties regarding velocity head. A value of 0.15 metres as a minimum fall height over the reach length in question was implemented by Bathurst (1986), and it was believed that this value could be comfortably accommodated on any of the Western Cape's steep sloped rivers.
3. As mentioned in Section 3.1.2.1, no unnatural disturbance of the substrate should be present, as it was considered important to incorporate the natural distribution of the substrate during data collection.

3.1.2.4 Concluding remarks on site selection criteria

Although the above criteria were applied as far as possible in selecting suitable sites for data collection, it was soon realised that all conditions could not be met at all sites or at all times. The reality is that most significant catchments of the Western Cape

have been affected in some way or another by human intervention. However, it is still believed that an acceptable and representative data set was obtained from rivers that possess typical Western Cape characteristics and are as close to a natural state of flow as possible.

3.1.3 Selected Sites

After multiple trips to various localities, three different catchments were selected. They are the Du Toits Kloof, Jonkershoek and Upper Berg River catchments (see Figures 3.7-3.9). Red dots indicate selected sites, and the available weirs used are also shown. Bathurst (1986) defined two types of reach for data collection purposes in mountain streams. Firstly riffles that are separated by pools in the typical riffle-pool configuration fashion, and secondly areas where boulder beds and steep and shallow flow are found without major pools. In both these cases channel controls define the water levels and the resistance to flow. It is believed that the streams of the Western Cape are a combination of these two types, apart from the Upper Berg River reach that is clearly a riffle-pool site.

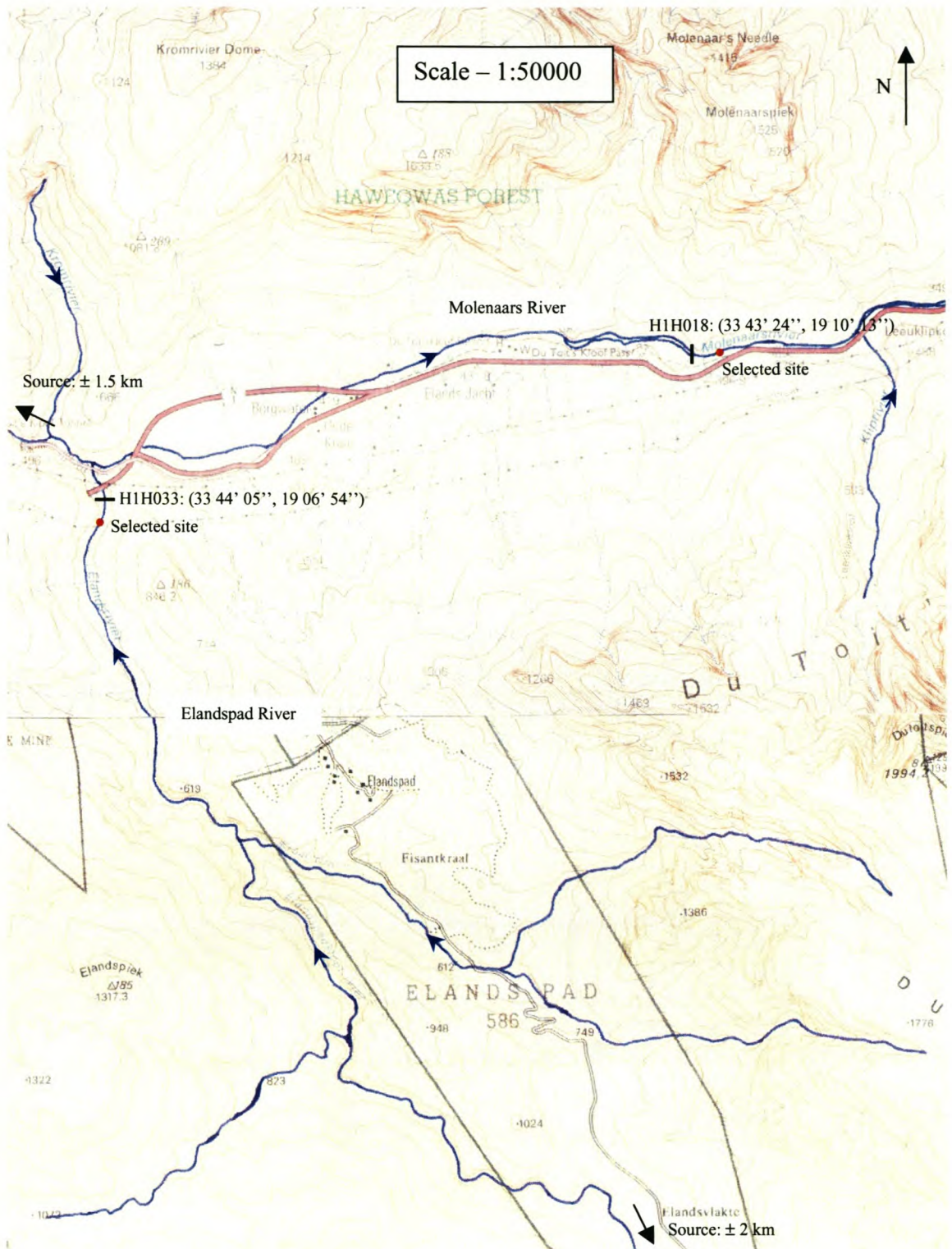


Figure 3.7 Map of Du Toits Kloof catchment showing approximate location of Elandspad and Molenaars sites.

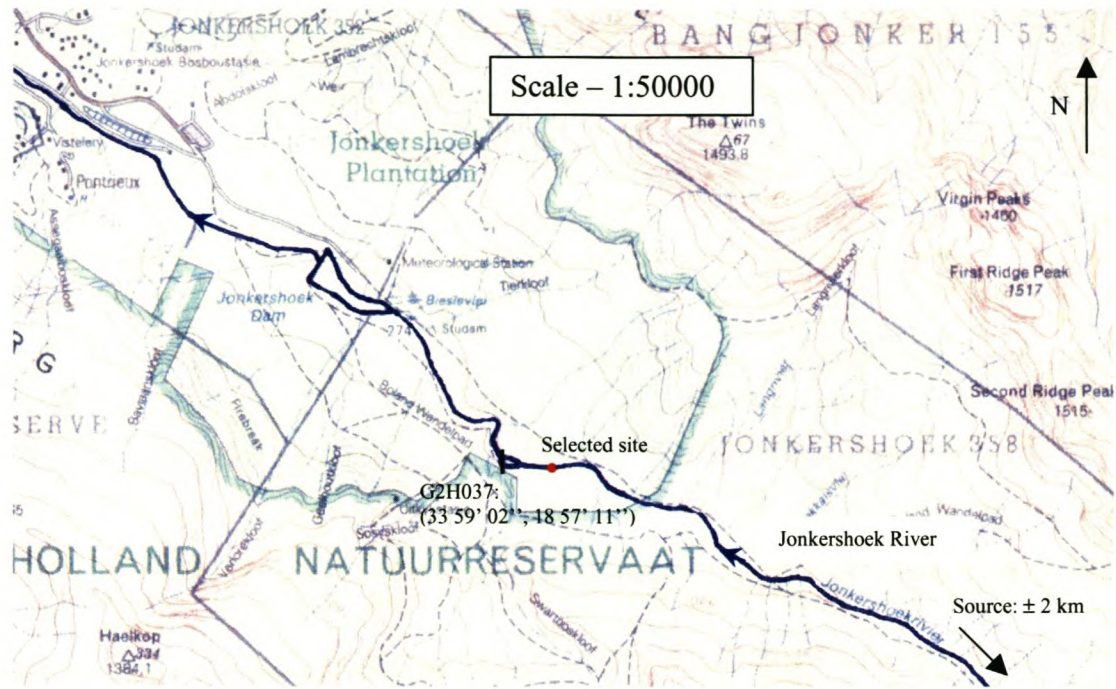


Figure 3.8 Map of Jonkershoek catchment showing approximate location of Jonkershoek site.

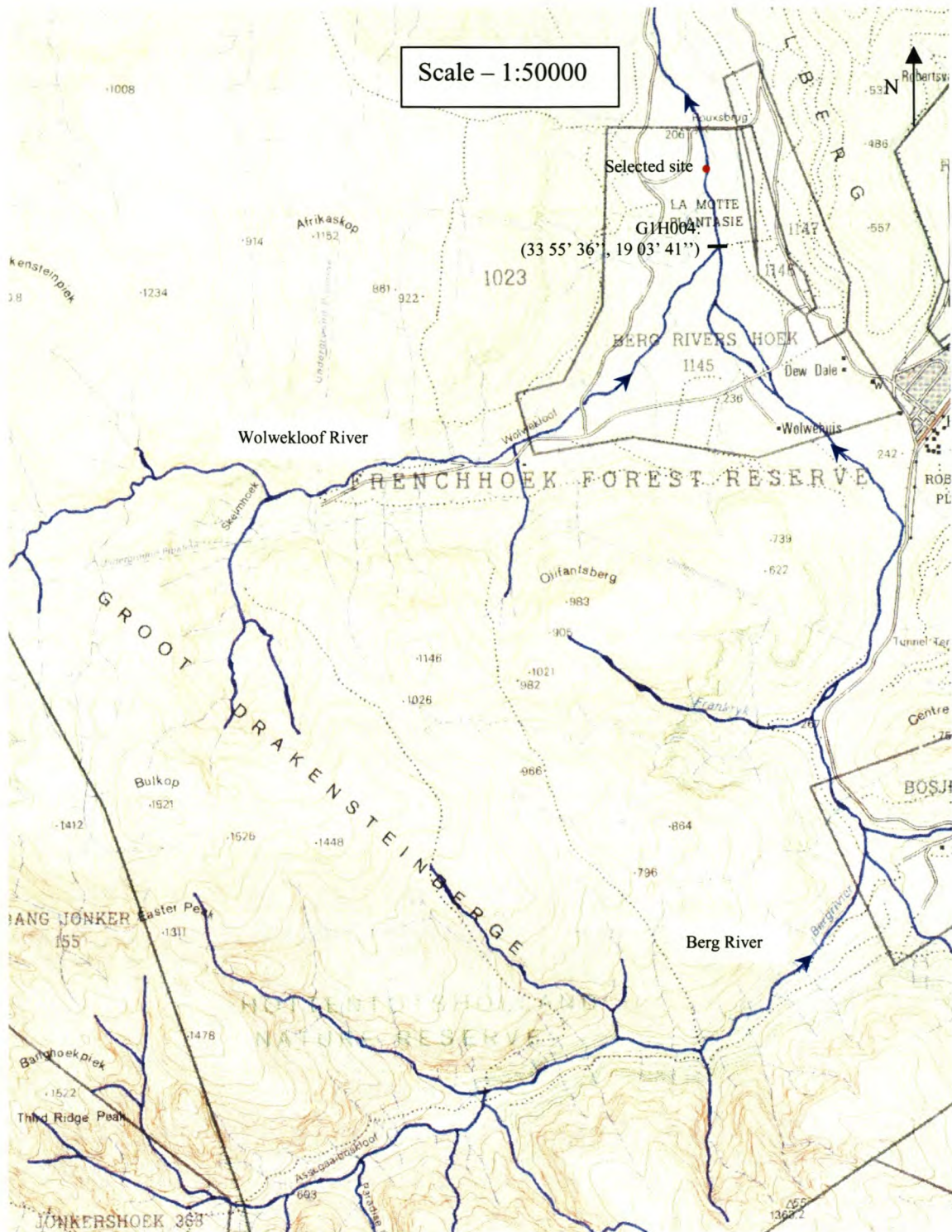


Figure 3.9 Map of Upper Berg River catchment, showing approximate location of Upper Berg site.

Three cross-sections were selected some distance apart at each site (see Figure 3.10). This was done to be able to compare calculated flows after every measurement, to increase the amount of available data for each measured discharge, and to compare an averaged flow rate with the individual results later on. The distance between sections varied from 8 meters on the Jonkershoek River up to 20 meters on the Upper Berg River, with the typical distance around 12 meters. The site and the sections were chosen so that all readings could be taken from a single survey point. Time could be saved and possible complications due to different survey points avoided in this manner. Every specific section at a site was regarded as a separate entity with its own area, perimeter, width, and slope. The only generalized parameter for every site was the boulder size distribution. It was decided that the slope for every section would be found by using water level readings taken in the vicinity of that section, both above and below. Area 1 was selected as the upper section of each site, with areas 2 and 3 downstream in that order. All sections were chosen across relatively shallow areas of reasonably fast flow, with the exception of the Upper Berg River, where deeper flow depths were recorded.

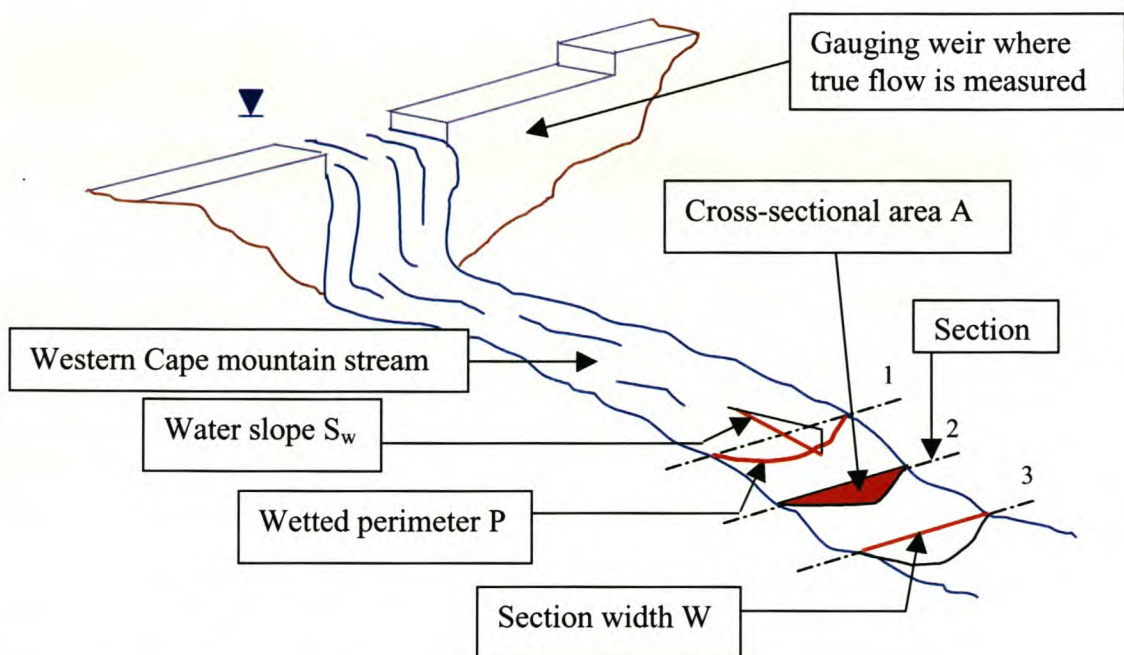


Figure 3.10 Illustration of relevant terms.

3.1.3.1 Elandspad River, Du Toits Kloof (*Gauging Weir: H1H033*)



Figure 3.11 Photo of the Elandspad River looking upstream.

The Elandspad River is situated in the Du Toits Kloof mountain range, and is the main tributary of the Molenaars River that drains into the Breede River system. It is wide (± 15 metres), shallow and fast flowing with pockets of slower water randomly spread in between, and can be considered as being in a pristine condition. Fairly thick bush fringes the waterside, so it was decided to focus primarily on measuring very low flows to avoid the influence of vegetation. Under these low flow conditions, the stream breaks up into several shallow channels of about 0.3 metres in depth, and complications as described in Section 3.1.1.3 arise.

3.1.3.2 Jonkershoek River, Jonkershoek (*Gauging Weir: G2H037*)



Figure 3.12 Photo of Jonkershoek River looking upstream.

The Jonkershoek River is really the upper Eerste River before it reaches Stellenbosch. It is the smallest stream under consideration with an average width of about 4 m, and it has a steep bed slope and very diverse substrate in its upper reaches. It is also quite shallow (± 0.3 metres). Its banks are well vegetated with indigenous bush, but this is kept clear of the water by strong winter floods. Apart from a weir upstream of the site where water is abstracted in summer, this stream is in an undisturbed state.

3.1.3.3 Molenaars River, Du Toits Kloof (*Gauging Weir: H1H018*)



Figure 3.13 Photo of the Molenaars River looking upstream.

The Molenaars River is one of the main tributaries of the Breede River. It is fairly wide (± 10 metres) and shallow, similar to the Elandspad River located further upstream, but it has a higher discharge due to other tributaries having entered the system, and contains larger boulders. The presence of some of the bigger elements found on this section is probably due to the close proximity of high cliffs and steep mountain slopes on its northern bank, from where these rocks probably fragmented through time and found their way down into the river channel. It was expected that under moderate flows the larger bed materials of this stream should have an even more marked disruptive effect on the flow regime than on other large-scale roughness streams. The Molenaars River is a fairly undisturbed stream.

3.1.1.4 Upper Berg River, La Motte (*Gauging Weir: G1H004*)



Figure 3.14 Photo of the Berg River looking upstream.

The Upper Berg River is the largest river of those investigated, and has an average width of about 10 metres in the area under consideration and a depth of up to 1.5 metres in places. It is a very important river in terms of water usage, as it serves as a primary source of water supply for the Greater Cape Town metropolitan area via a tunnel system through the Franschhoek Mountains, and receives compensatory summer irrigation discharge through the same system. Although the flows of the Berg River are unnaturally altered by the tunnel system, abnormally dry conditions during early fieldwork expeditions necessitated the addition of measurements during slightly higher flows. A better spread of data would then be available, from very low flow large-scale roughness conditions to medium flows falling into the intermediate scale roughness range.

Therefore, apart from it being one of the major catchments in the Western Cape, the Berg River site was selected because of the higher summer flows found there. It was also felt that because it is a bigger river and therefore a less fragile system, the changed flow patterns would not have affected its general character as much as in the case of a smaller stream. The rich aquatic life still prevalent in the river seems to support this point. It is a more moderately sloped river and deeper than the other streams (± 0.6 metres deep), with relative submergence values entering the

intermediate scale roughness domain. In its higher reaches it is also a heavily bushed stream that made access particularly difficult (see Figure 3.6).

Apart from the observed characteristics of each site as described above, information was collected from the Department of Water Affairs and Forestry for a better perspective on how the catchments generally compare in terms of size, rainfall etc. The general characteristics of the four sites are thus summarised in Table 3.1, and can be compared accordingly.

Catchment	Distance from origin (km)	Catchment size (km²)	Rainfall (mm/a)	Runoff (Mm³/a)
Elandspad	8	62	1000	102
Jonkershoek	5	21.38	1600	24
Molenaars	20	113	1000	168
Upper Berg	18	70	1900	150

3.1.4 Data collection

3.1.4.1 Data requirements

The main objective of the data collection process was the gathering of hydraulic information that could be used as parameters in friction equations. All the basic data necessary to calculate the parameters identified in Section 2, as well as the true flow rate had to be obtained. The data was necessary not only for implementation in known friction formulae, but also for the possible development of improved expressions. The true flow rates, as was to be recorded from the relevant gauging weirs, were going to be necessary for the calibration processes. The basic data that had to be collected is summarised in Table 3.2.

Table 3.2 Variables to be gathered from field visits.

Weir discharge	Q
Cross-sectional area	A
Wetted perimeter	P
Section width	W
Longitudinal water slope	S_w
Boulder sizes	D_{50}, D_{84}

3.1.4.2 Collection process

During a field trip to a river, the necessary data was collected from the three sections chosen at each site. Apart from boulder size sampling that was done only once for every site, the processes outlined below were repeated at every section on every visit and no use was made of a reference system as advocated by Bathurst (1986). This was done so that possible changes in cross-section and the accuracy of the selected gradient and cross-sectional sampling system could be observed.

Various drawings and photos are included in the descriptions below to demonstrate the methodology followed as graphically and simply as possible:

1. Cross-sectional area A , wetted perimeter P and stream width W

It was decided that a cross-section could be meaningfully and effectively surveyed at 0.5 metre intervals across the section (see Figure 3.15). Surveying took place with the help of a string, a levelling instrument and surveying staff. The instrument was carefully set up in a suitable spot from where readings to all three sections could be comfortably taken (see Figure 3.17). The string, which was colour-marked at 0.5 metre intervals, was spanned across the selected section (see Figure 3.18). A bottom and water level reading was then taken at every 0.5 metres along the marked string from the one dry bank to the other dry bank (see Figures 3.19 and 3.20). Water level readings were taken by holding the bottom of the staff at the water level (see Figure 3.21). Figure 3.15 illustrates a common situation

where more than one area of flow and thus more than one water level occurs across a section. In such a case, a water level for *every separate channel* across the section was found by taking the *average of recorded levels across that specific channel*. Care had to be exercised to disturb the water level as little as possible, and the assistant then had to be positioned either downstream or parallel to the point of measurement. It is important to note that the bottom level readings were taken on the top of boulders (see Figures 3.15 and 3.16). These values were accepted as points on the bottom of the measured cross-section of the channel, and no distinction was made between the channel geometry and the bed material protruding into the flow as advocated by Bathurst (1985). As can be gathered from Figure 3.16, enough gaps and protrusion of boulders generally occur between points to still justify a bed roughness layer along the presumed channel bottom. This method might be considered too general, but it was used from a practical view and lack of better techniques available from literature. Being consistent in applying a certain method was also argued as being more important than the method itself. From the gathered set of bottom and water level values, the cross sectional area A , wetted perimeter P and top stream width W could be determined, as explained further in Section 3.2.

Although the above process was repeated during field trips, in practice an alternative should be used if a specific section is to be visited regularly, whereby the sectional measurements need to be recorded only once in relation to a reference point. On future visits only a reliable water level would then need to be recorded so as to determine the cross-sectional parameters of the section. This should result in a considerable reduction in time and effort necessary for recording purposes.

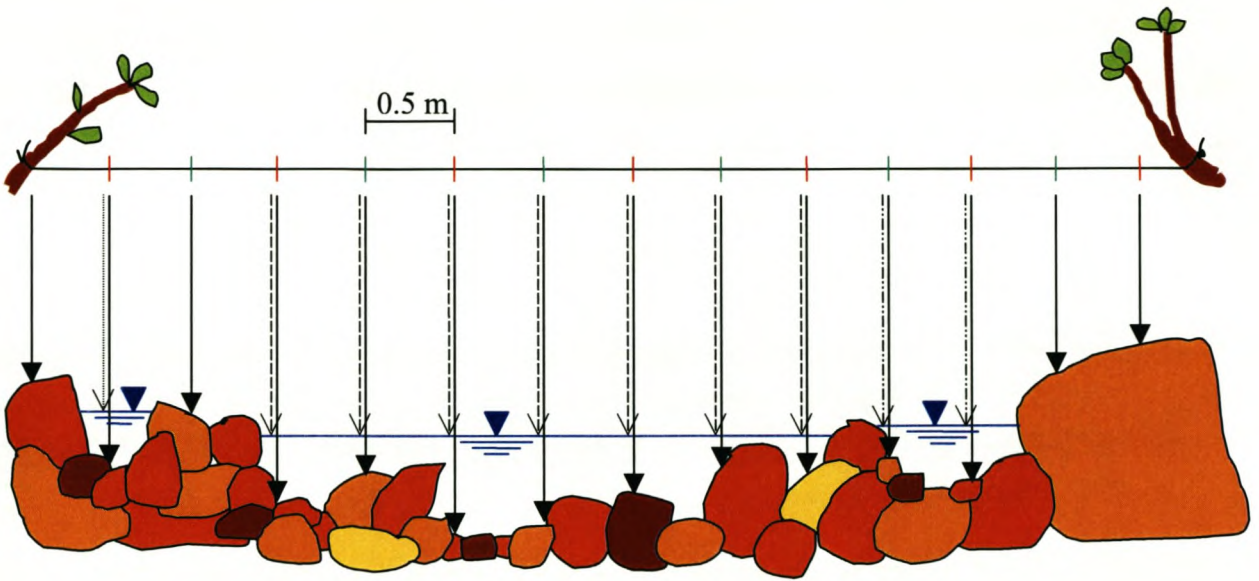


Figure 3.15 Illustration of cross-sectional measurements taken across a section of stream.

where:

- ▶ = Bed level
- ⋯▶ = Water-level 1
- -▶ = Water-level 2
- ·▶ = Water-level 3

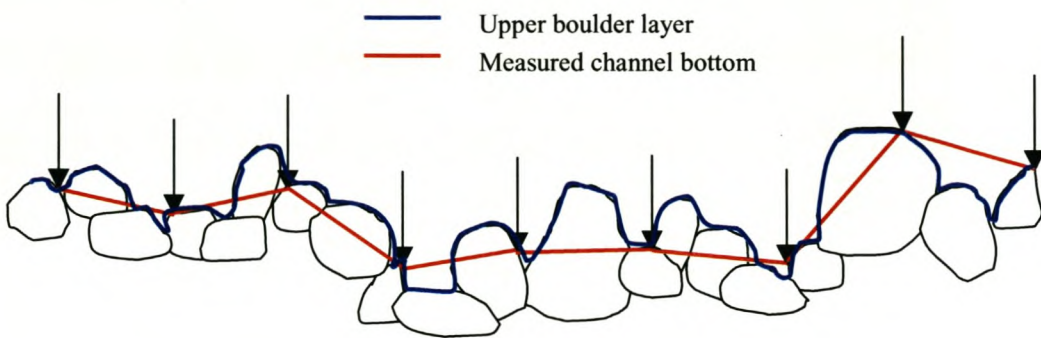


Figure 3.16 Example of measured channel bottom in comparison to the top layer of boulders.



Figure 3.17 Photo showing set up of measuring instruments on the Elandspad River.



Figure 3.18 String spanned across the Molenaars River.



Figure 3.19 A bottom reading being taken.



Figure 3.20 Photo showing a water level reading being taken on the Berg River.



Figure 3.21 Photo showing a close-up view of an estimated water level position being measured.

2. *Slope*

A longitudinal sample of a stretch of river (also defined as a reach) was collected by taking a bottom level, water level and distance reading at each selected interval along the reach, progressing from above section 1 to below section 3 (see Figure 3.22). The total distance along such a reach could vary from 30m to 100m, depending on the size and character of the river. This procedure was used to

determine an average water slope at each of the three sections, and also to give a reflection of the general longitudinal profile of the river reach. Bathurst (1985) used only the three water levels from three chosen sections to calculate an average water slope for the reach. However, this was regarded as too coarse an approach, since the specific slopes of different sections could vary considerably. The average slope of each section was thus calculated by drawing a straight line through three water levels, namely the first level taken above the section, one on the section, and the first one below the section (indicated in red on Figure 3.22). The first levels above and below cross sections were thus to be taken in the close vicinity of the chosen section so as to avoid major jumps or steps that would alter the effective measured height of flow, and thus affect the slope calculation.

The readings were taken in the main channel of flow, because this was regarded as the area that would give the closest representation of the average water level at that particular section (Bray, 1979). In contrast to the above technique, Jarrett (1984) measured water levels on each bank. In retrospect, combining the above methods and taking more than one reading across every section of river may possibly have provided a more reliable water level.

Readings were taken in a straight line and in the main direction of flow as far as possible, so that the recorded distance readings from the levelling instrument are close to the true distances between successive points. Also the line of chosen progression had to be in close proximity to the position of the instrument to avoid errors in distance measurements.

The water slope S_w calculated from this data was assumed to be the energy slope S_f in calculations, because the change in velocity head, which would be the difference between the water head and the friction head, was regarded as negligible compared to water depth and positional energy. This was also argued by Bray (1979) and Bathurst (1985), and is reflected in the longitudinal profile included in the Appendix.

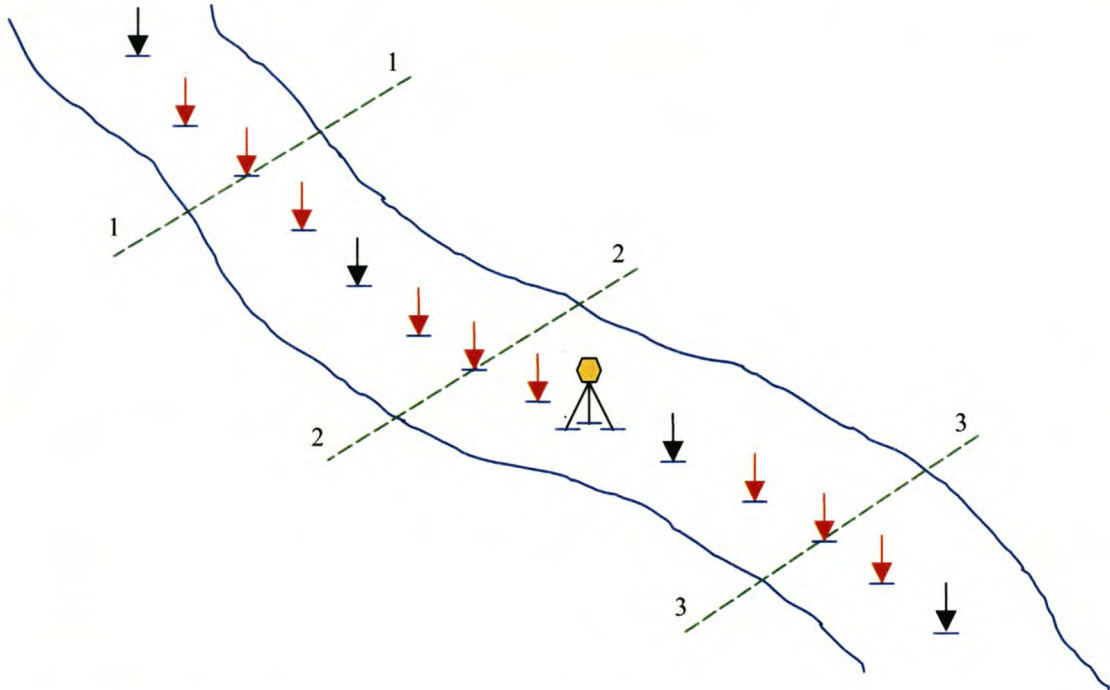


Figure 3.22 Sampling of average water slope along a river reach.

3. Bed material size

A representation of bed roughness was found by sampling boulder size. As explained in 1., the channel bottom measurements were assumed to allow for enough variation in cross-sectional form to warrant the existence of bed roughness independent of the presumed channel bottom (see Figure 3.16). This means that the top layer of boulders could still realistically represent a bottom roughness causing resistance to flow. In-stream boulders and cobbles, that is, the top layer of boulders along the assumed channel bottom, were measured across their median axis in order to find the average grain size distribution to be used in roughness formulae (Hey, 1979; Jarrett, 1984; Bathurst, 1986). The definition of the median axis is illustrated in Figure 3.23. Hey (1979) stated that the use of the median axis to express boulder size is justified because it is easy to measure and widely recognised. Furthermore, it is argued that using other axes provided no apparent improvement in correlation.

The particle sampling procedure was done on a grid system according to Wolman's technique advocated by Hey (1979), Jarrett (1984), Bathurst (1985) and

others, whereby elements are sampled on a standard interval distance (see Figure 3.24). However, the “rough pacing” system used by Bathurst (1986) was regarded as too subjective, and a marked string was once again employed for the task so that a constant interval could be achieved. In this study, 0.5 metre was used as interval distance for the Jonkershoek River and 1 metre for the larger rivers. As there was usually some distance between sections, the sampling areas were concentrated around the selected cross-sections, so that relevant particle sizes close to them could be recorded.

A total of one hundred particles were sampled from every reach. Only smaller cobbles were physically picked up from the streambed, measured and returned. The bigger particles were measured on the streambed without removing them, so that unnecessary disturbance of the flow could be avoided.

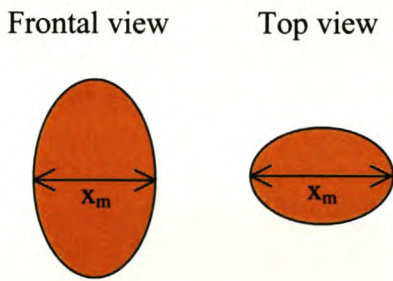


Figure 3.23 The median axis of a boulder.

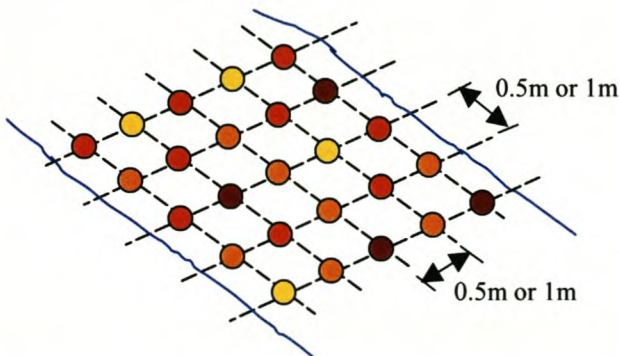


Figure 3.24 Grid system of particle sampling.

The above data collection procedure can be summarised as follows:

1. *Gauge plate at flow gauging weir read off before start of surveying.*
2. *Dumpy level assembled in suitable spot from where all readings could be taken.*
3. *Marker rope spanned across stream at section 1.*
4. *Rod assistant moves into position on the left hand bank looking downstream, for first reading.*
5. *First reading taken on dry bank at first mark.*
6. *A bed and water level reading taken at every 0.5m mark on string ending on dry right hand bank.*
7. *Steps 3 to 6 repeated at sections 2 and 3.*
8. *Starting a reasonable distance above section 1 ($\pm 5-10$ metres), assistant moves into position for first longitudinal reading.*
9. *At each point: bottom and distance readings recorded first after which assistant lifts rod to the water level and a water reading is taken.*
10. *Assistant progresses downstream as readings are taken up to a reasonable distance ($\pm 5-10$ metres) below section 3.*
11. *A Wolman's sample is taken to record boulder sizes.*
12. *Plate at gauging weir rechecked for any change in discharge.*

3.2 Data processing

Following the acquisition of the sets of data from the selected sites, the required hydraulic parameters had to be calculated from the field-recorded data. The techniques used are briefly described below:

1. *Cross-sectional area A , wetted perimeter P and stream width W*

The data points gathered at 0.5 metre intervals across every section was inserted into and sorted on an Excel spreadsheet. An averaged water surface level for every individual channel was then calculated from those recorded, because the rough nature of the streams meant that the water surface level was

often not exactly constant across a specific section. The AutoCAD programme was used subsequently so that a cross-sectional profile could be drawn. A resultant profile as processed in AutoCAD would typically resemble Figure 3.25:

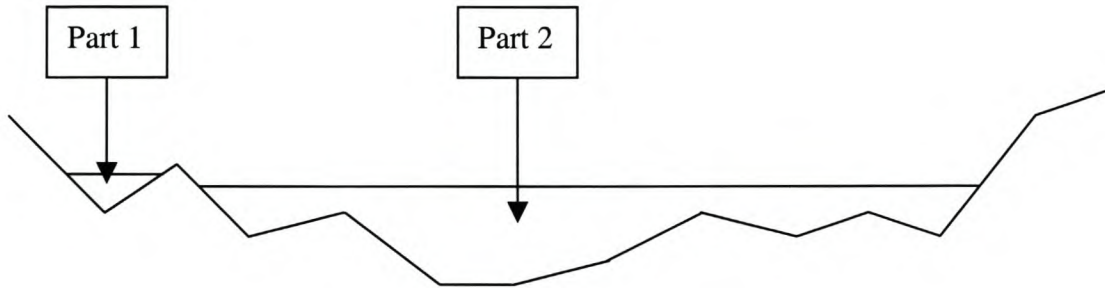


Figure 3.25 Example of typical cross-section drawn with AutoCAD.

The total cross-sectional area A , total wetted perimeter P , and total stream top width W as calculated by AutoCAD was then available for use in further analysis. The word total implies that all individual channels across a section that were separated by dry boulders were first analyzed and then added together. For instance, in the above case, A_1 , P_1 and W_1 from Part 1 would be added to A_2 , P_2 and W_2 from Part 2 to obtain the total values. Sometimes the separation between different channels of flow across a section was not recorded in the sampling process, because the 0.5-meter intervals used excluded the separating dry boulders. In such cases, the error involved was regarded as part of the assumptions involving measuring methodology.

2. Slope

Longitudinal profiles of the reaches were drawn in Excel from the longitudinal elevation data collected (see Figure 3.26). A tangent could then be drawn at each section (using the three water level measurements mentioned in Section 3.1.4.2) and used to determine the prevalent estimated water slope at that section.

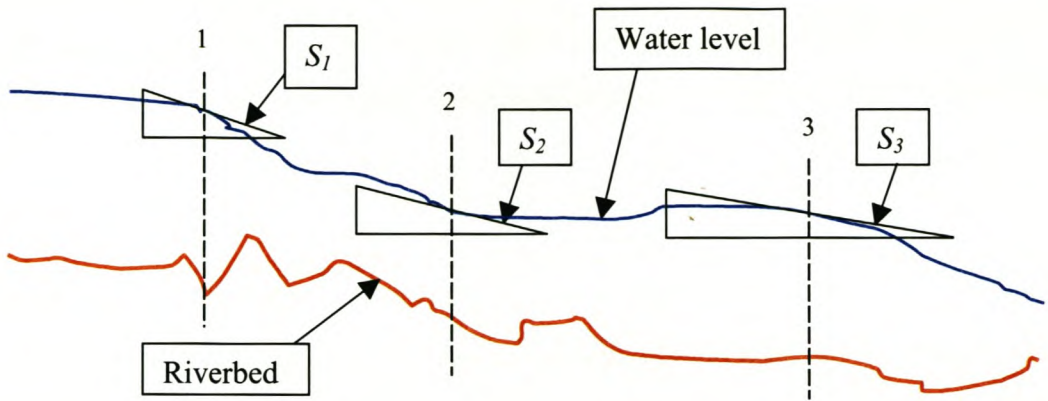


Figure 3.26 Example of a typical longitudinal profile drawn with Excel.

3. Bed material size

The one hundred median particle sizes measured at each reach according to Wolman’s method were recorded in an Excel spreadsheet, after which a graph could be drawn showing the statistic percentile boulder sizes (see Figure 3.27). The relevant sizes could then be read off the graph and implemented in analysis.

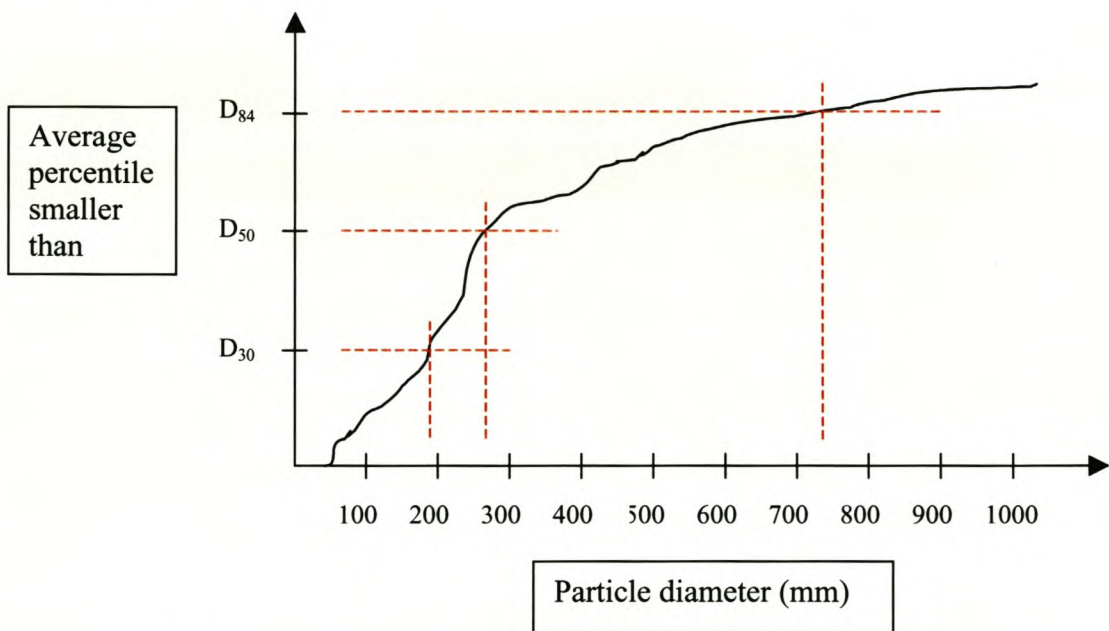


Figure 3.27 Example of typical graph showing average particle sizes.

3.3 The data set

With the completion of the above processes, all necessary hydraulic parameters were available for analysis purposes. These parameters are presented in Table 3.3 and discussed below:

Q_{gauge} : This is the discharge as recorded from a nearby gauging weir. It is assumed in this study to be the true flow, and is used in conjunction with the field-recorded information to calibrate equations. Because all fieldwork was conducted during the warmer months, typical summer low flows were generally recorded, which would give Q_{gauge} a recurrence interval of one.

A : A represents the *total* cross sectional area of the specific section at the specific discharge. In other words, if more than one channel of flow occurs across a section, these are all added to find A .

P : P represents the *total* wetted perimeter of the specific section at the specific discharge. As with A , the perimeters of all separate channels across a section are added together to find P .

W : W represents the total top width of flow of the specific section, which implies the same principle of addition as A and P .

R : The hydraulic radius R is determined by dividing the total area A by the total wetted perimeter P .

d : The hydraulic depth is determined by dividing the total area A by the total top width W .

S_f : S_f represents the energy slope at the specific section, and is calculated as explained in Sections 3.1 and 3.2.

D_{84} : D_{84} is the 84th percentile particle size for a reach as calculated from the 100 particle sizes measured on every river.

D_{50} : D_{50} is the 50th percentile or average particle size for a reach as calculated from the 100 particle sizes collected on every river.

The ranges in which the various parameters fall are also shown in Table 3.3. The same three letters of the alphabet (e.g. three a's) represent the three sections measured during a single trip to a river.

Table 3.3 Hydraulic parameter data set calculated from collected field data.										
		Q_{gauge}	A	P	W	R	d	S_f	D_{84}	D_{50}
Unit		(m^3/s)	(m^2)	(m)	(m)	(m)	(m)		(m)	(m)
Range	Max	4.170	6.23	16.96	15.95	0.51	0.54	0.0167	0.500	0.210
	Min	0.062	0.53	2.40	2.14	0.10	0.11	0.0005	0.300	0.144
Molenaars	a	0.405	1.62	6.28	5.57	0.26	0.29	0.0050	0.500	0.210
	a	0.405	1.22	9.15	8.72	0.13	0.14	0.0022	0.500	0.210
	a	0.405	2.04	8.61	7.91	0.24	0.26	0.0056	0.500	0.210
	b	0.383	1.37	6.37	5.55	0.21	0.25	0.0068	0.500	0.210
	b	0.383	1.56	8.91	8.38	0.17	0.19	0.0036	0.500	0.210
	b	0.383	2.12	10.04	9.38	0.21	0.23	0.0050	0.500	0.210
	c	0.360	1.53	6.70	5.95	0.23	0.26	0.0050	0.500	0.210
	c	0.360	1.58	7.95	7.65	0.20	0.21	0.0042	0.500	0.210
	c	0.360	1.72	8.32	7.51	0.21	0.23	0.0031	0.500	0.210
	d	2.953	3.68	10.93	9.04	0.34	0.41	0.0100	0.500	0.210
	d	2.953	4.26	12.71	11.93	0.34	0.36	0.0045	0.500	0.210
	d	2.953	4.91	13.46	11.93	0.36	0.41	0.0026	0.500	0.210
Upper Berg	a	4.170	4.79	10.28	9.68	0.47	0.49	0.0005	0.300	0.155
	a	4.170	6.23	14.11	13.69	0.44	0.46	0.0005	0.300	0.155
	a	4.170	4.51	16.12	15.61	0.28	0.29	0.0067	0.300	0.155
	b	3.698	5.13	10.02	9.59	0.51	0.54	0.0019	0.300	0.155
	b	3.698	5.92	13.41	12.84	0.44	0.46	0.0007	0.300	0.155
	b	3.698	3.64	13.77	13.24	0.26	0.27	0.0083	0.300	0.155
	c	3.588	5.04	10.28	9.91	0.49	0.51	0.0017	0.300	0.155
	c	3.588	5.98	13.40	12.81	0.45	0.47	0.0011	0.300	0.155
	c	3.588	3.77	14.07	13.65	0.27	0.28	0.0050	0.300	0.155
	d	3.262	4.34	10.27	9.79	0.42	0.44	0.0008	0.300	0.155
	d	3.262	5.97	14.26	13.89	0.42	0.43	0.0010	0.300	0.155
	d	3.262	3.84	13.61	13.26	0.28	0.29	0.0050	0.300	0.155
Jonkershoek	a	0.202	1.24	7.44	7.33	0.17	0.17	0.0067	0.360	0.144
	a	0.202	1.20	7.33	7.04	0.16	0.17	0.0114	0.360	0.144
	a	0.202	1.07	3.51	3.17	0.31	0.34	0.0033	0.360	0.144
	b	0.691	1.76	7.48	7.15	0.24	0.25	0.0050	0.360	0.144
	b	0.691	1.94	7.57	6.87	0.26	0.28	0.0160	0.360	0.144
	b	0.691	1.26	3.78	3.23	0.33	0.39	0.0040	0.360	0.144
	c	0.495	1.54	7.00	6.63	0.22	0.23	0.0050	0.360	0.144
	c	0.495	1.50	6.75	6.33	0.22	0.24	0.0067	0.360	0.144
	c	0.495	1.15	3.56	3.10	0.32	0.37	0.0033	0.360	0.144
	d	0.175	0.97	5.96	5.83	0.16	0.17	0.0033	0.360	0.144
	d	0.175	1.05	6.66	6.20	0.16	0.17	0.0044	0.360	0.144
	d	0.175	0.76	3.15	2.75	0.24	0.28	0.0016	0.360	0.144

		Q_{gauge}	A	P	W	R	d	S_f	D_{84}	D_{50}
		(m ³ /s)	(m ²)	(m)	(m)	(m)	(m)		(m)	(m)
Jonkershoek	e	0.154	0.99	6.33	6.11	0.16	0.16	0.0040	0.360	0.144
	e	0.154	0.97	6.54	6.25	0.15	0.16	0.0020	0.360	0.144
	e	0.154	0.74	3.04	2.68	0.24	0.27	0.0016	0.360	0.144
	f	0.062	0.62	5.75	5.61	0.11	0.11	0.0033	0.360	0.144
	f	0.104	0.73	6.14	5.88	0.12	0.12	0.0020	0.360	0.144
	f	0.146	0.53	2.40	2.14	0.22	0.25	0.0022	0.360	0.144
	g	0.295	1.41	6.67	6.38	0.21	0.22	0.0024	0.360	0.144
	g	0.295	1.14	6.85	6.51	0.17	0.17	0.0020	0.360	0.144
	g	0.295	0.98	3.14	2.79	0.31	0.35	0.0044	0.360	0.144
Elandspad	a	0.190	1.29	8.48	7.81	0.15	0.17	0.0036	0.440	0.170
	a	0.190	1.33	9.31	8.44	0.14	0.16	0.0057	0.440	0.170
	a	0.190	1.49	11.72	10.91	0.13	0.14	0.0167	0.440	0.170
	b	1.115	4.04	12.26	10.65	0.33	0.38	0.0020	0.440	0.170
	b	1.115	3.77	13.01	11.98	0.29	0.31	0.0015	0.440	0.170
	b	1.115	4.24	16.96	15.95	0.25	0.27	0.0040	0.440	0.170
	c	0.433	2.93	10.69	9.23	0.27	0.32	0.0043	0.440	0.170
	c	0.433	2.70	10.95	10.44	0.25	0.26	0.0022	0.440	0.170
	c	0.433	3.11	15.58	14.98	0.20	0.21	0.0100	0.440	0.170
Elandspad	d	0.365	2.76	10.26	9.34	0.27	0.30	0.0033	0.440	0.170
	d	0.365	2.30	10.47	10.07	0.22	0.23	0.0010	0.440	0.170
	d	0.365	2.44	15.84	15.08	0.15	0.16	0.0100	0.440	0.170
	e	0.244	1.14	6.13	5.50	0.19	0.21	0.0033	0.440	0.170
	e	0.244	1.79	9.37	9.10	0.19	0.20	0.0017	0.440	0.170
	e	0.244	1.30	12.47	11.77	0.10	0.11	0.0129	0.440	0.170
	f	0.233	1.88	8.81	7.98	0.21	0.24	0.0033	0.440	0.170
	f	0.233	2.35	9.56	9.25	0.25	0.25	0.0020	0.440	0.170
	f	0.233	1.96	14.49	13.82	0.14	0.14	0.0057	0.440	0.170
	g	0.190	1.33	7.90	7.07	0.17	0.19	0.0022	0.440	0.170
	g	0.190	1.47	9.87	9.47	0.15	0.15	0.0020	0.440	0.170
	g	0.190	1.37	12.65	12.08	0.11	0.11	0.0100	0.440	0.170

Chapter 4: Methodology for deriving flow equation

4.1 Background

The flow equation that is proposed in this section was decided upon after due consideration of the required accuracy of empirical correlation, mathematical and physical validity and practicality of application. Various existing equations as obtained from literature were used for initial indication of significant variables and expressions. Further investigation of the prominent parameters depicting the roughness coefficient was then undertaken through comparative processing using the collected experimental data. After the significant parameters were identified, a mathematical approach was followed to see whether the same parameters would turn up through purely theoretical manipulation of sediment transport expressions. The aim was therefore to attempt to marry empirical and theoretical approaches in deriving a single easily applicable equation. It is believed that this aim was largely achieved.

4.2 Initial testing of existing formulae

Fitting existing friction equations to the local data set was the starting point for indicating the more suitable equation forms and their parameters. These equations preferably had to be applicable under large-scale roughness conditions or on boulder bed streams. As already mentioned, empirical equations calibrated on site-specific data sets with set boundaries have historically been less effective in other situations. With the probability of only limited direct applicability of these existing equations on local streams, the main purpose was thus not the identification of a single suitable equation, but simply to try and differentiate between the more suitable expressions and those that are less so. The formulae were considered and selected according to past research and recommendations from various previous studies. Most of the relevant aspects have been discussed in Section 2. There was also emphasis on investigating equations that differ markedly in form, and both semi-logarithmic and power varieties are represented. The selected equations are discussed shortly and summarised in Table 4.1.

- Bathurst: This was one of the earlier significant equations specifically developed for large-scale roughness conditions. Numerous other studies sprung from this work, and it was therefore considered important to test its relevance under local conditions.
- Chezy: The standard Chezy equation is included, with D_{84} representing k , as it was felt that this commonly used and recognisable equation warrants proper testing under large-scale roughness conditions.
- Griffiths: Although this equation was derived for gravel bed rivers and thus small- and intermediate scale roughness conditions, it was included to see how it would fare under large-scale roughness conditions. It is also a fairly representative example of the many variants and permutations of the semi-logarithmic equation to be found.
- Jarrett: The Jarrett equation was specifically derived for steep sloped, boulder bed rivers, where large-scale roughness conditions would apply most of the time. It was an original and refreshing approach to the problem, utilising only Manning's n , slope and hydraulic radius, and its inclusion was considered essential.
- Simons and
Senturk: As already discussed in Section 2.2.7, the research conducted by Simons and Senturk is particularly relevant to this study, and their large-scale roughness equation is regarded as possibly central to the further improvement of flow measurement accuracy under large-scale roughness conditions.

Originator	Equation	Number
Bathurst (1978)	$\sqrt{\frac{8}{f}} = \left(\frac{R}{0.365D_{84}}\right)^{2.34} \left(\frac{W}{d}\right)^{7(\lambda-0.08)}$	(4.1)
Chezy (Rooseboom <i>et al</i> ,1997)	$C = 5.75\sqrt{g}\text{Log}\left(\frac{12R}{D_{84}}\right)$	(4.2) (also see Equation 2.15)
Griffiths (1981)	$\sqrt{\frac{1}{f}} = 0.76 + 1.98\text{Log}\left(\frac{R}{D_{50}}\right)$	(4.3)
Jarrett (1984)	$n = 0.39S_f^{0.38} R^{-0.16}$	(4.4)
Simons and Senturk (1992)	$\sqrt{\frac{8}{f}} = 1.11\left(\frac{d}{D_{84}}\right)^{0.46} \left(\frac{D_{84}}{D_{50}}\right)^{-0.85} S_f^{-0.39}$	(4.5) (also see Equation 2.27)

The local data was fitted to the above equations to determine roughness coefficients. The accuracies in discharge that resulted from applying these coefficients to discharge calculations are shown in Table 4.2, where the percentage of calculated discharges located within the given margin of the measured discharges is presented.

Number	Within 10%	Within 20%	Within 50%	Within 100%
(4.1)	16.7	28.8	56.1	80.3
(4.2)	6.1	19.7	36.4	63.6
(4.3)	18.2	36.4	54.5	80.3
(4.4)	10.6	15.2	36.4	74.2
(4.5)	10.6	25.8	59.1	90.9

From Table 4.2 it can be gathered that of those tested Equations (4.1), (4.3) and (4.5) show reasonable correlation. Equation (4.3) is the most accurate up to an error of 20%. However, all the equations showed low accuracy under the lower margins of error, so that the performance of Equation (4.3) cannot be regarded as necessarily significant. It is quite surprising, though, that the relatively basic equation of Griffiths, derived for gravel bed rivers under small-scale roughness conditions and utilising

only the relative submergence parameter, should fare so well against some of the other more complex expressions. Under the higher margins of error, Equation (4.5) started to outperform the other equations. It is interesting to note that the two main equation forms, namely the power form of Simons and Senturk and the semi-logarithmic form of Griffiths, should both fit fairly well.

Figure 4.1 illustrates the three best equations graphically, i.e. Bathurst (4.1), Griffiths (4.3) and Simons and Senturk (4.5). The Bathurst and Griffiths versions reveal similar behaviour, with the values spread fairly evenly on both sides of the true value line under low flows but substantially underestimating under higher discharges. Simons and Senturk on the other hand seems to over-predict consistently under lower flow rates, but moves closer to the median as flows increase. Seen on the whole, the Simons and Senturk equation seems to follow the most consistent pattern, with less way-out values than the other two and better correlation under a variety of flow rates.

It is reasonable to assume that the parameters present in the better-correlated equations are significant. It is striking that the relative submergence parameter is present in all three equations, and in fact very much dominant in two of them, namely the Bathurst and Griffiths equations. This would also explain their similar behaviour.

The fact is also highlighted that the more complex Bathurst equation is not more accurate than other simpler equations, and the channel geometry parameter (W/d) does not seem to hold significant advantages. Equation (4.1) was therefore eliminated as a future possibility. Furthermore, it is noteworthy that the Simons and Senturk equation, which contains the energy slope and bed material parameters along with relative submergence, fits the data set quite well. From this investigation there thus seems to be further evidence to suggest that the relative submergence (in some form or another), energy slope and bed material gradation are probably the prominent variables to be included in a large-scale roughness expression.

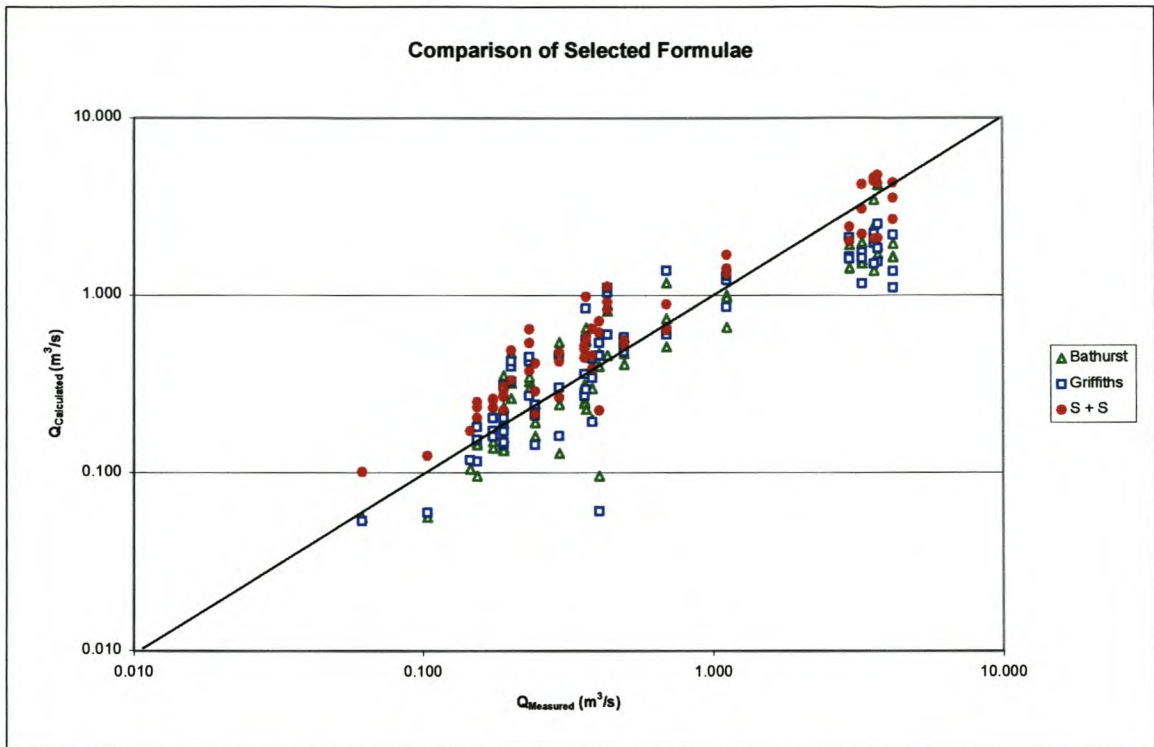


Figure 4.1 Graphic representation of the three more accurate existing equations.

4.3 Empirical approach

The empirical approach focused largely on identifying the most influential mechanisms affecting friction relations by making use of the collected hydraulic information. Calibration of the available hydraulic parameters was used as an indicator of their individual importance. Standard regression techniques were then applied to a number of different combinations. The most prominent variables, expressed as dimensionless parameters, could be identified in this way. The expressions giving the best correlations could then be determined.

It was also important to find an equation that is practical. This meant that the chosen variables had to be easily obtainable, and the equation had to be fairly simple and straightforward so that it could be understood and used by various disciplines.

4.3.1 Initial sediment transport investigation

The possibility of defining relationships between prominent hydraulic variables with similar techniques as used in sediment transport analysis by Basson and Rooseboom (1997), was considered at the start of the empirical investigation. The ratio between applied power along the bed and power required to suspend a particle, v^* / v_{ss} , and an applied stream power term $(gdS_f)^{1.5} / k$, was used in this process. It was hoped that graphs depicting v^* / v_{ss} against $(gdS_f)^{1.5} / k$ would reveal set patterns of the prominent hydraulic parameters already identified, similar to those observed with sand bed rivers (Basson and Rooseboom, 1997; Le Grange and Rooseboom, 2000). The shear velocity v^* is represented by $\sqrt{gdS_f}$. Figure 4.2 displays an example of such a graph. The settling velocity was calculated with the following formula derived for large particles (Simons and Senturk, 1992):

$$v_{ss} = \sqrt{\frac{4}{3} \frac{g}{0.4} \left(\frac{\rho_s - \rho}{\rho} \right) D_{50}} \quad (4.6)$$

where: v_{ss} = Average particle settling velocity (m/s)
 ρ_s = Average mass density of particles (kg/m³)

In the case of the Western Cape, similar quartzite boulders are to be found in all typical mountain streams of the region. The densities of a number of boulders from different streams were determined and found to be fairly constant, as could be expected. Accordingly, an average value of 2450 kg/m³ was used in this study. It would be interesting to see if the particle densities of other areas, such as for example the mountain streams of the Drakensberg, vary substantially from the Western Cape, and if regional averages would generally be possible. Unfortunately, such an investigation is beyond the scope of this study.

As can be gathered from Figure 4.2, a vague z-type curve seems to exist, but no clear pattern as to the behaviour of the relative submergence parameter could be identified. This was also the case with all the other parameters scrutinised in similar fashion. At

this point it was thus decided to discontinue this particular line of investigation, and to first make use of normal regression techniques to evaluate the importance of all likely parameters. However, the applied stream power theory was kept in mind as a mathematical pursuit for a later stage, and for interest's sake the v^*/v_{ss} parameter relevant in power relationships was added to the other hydraulic parameters under investigation.

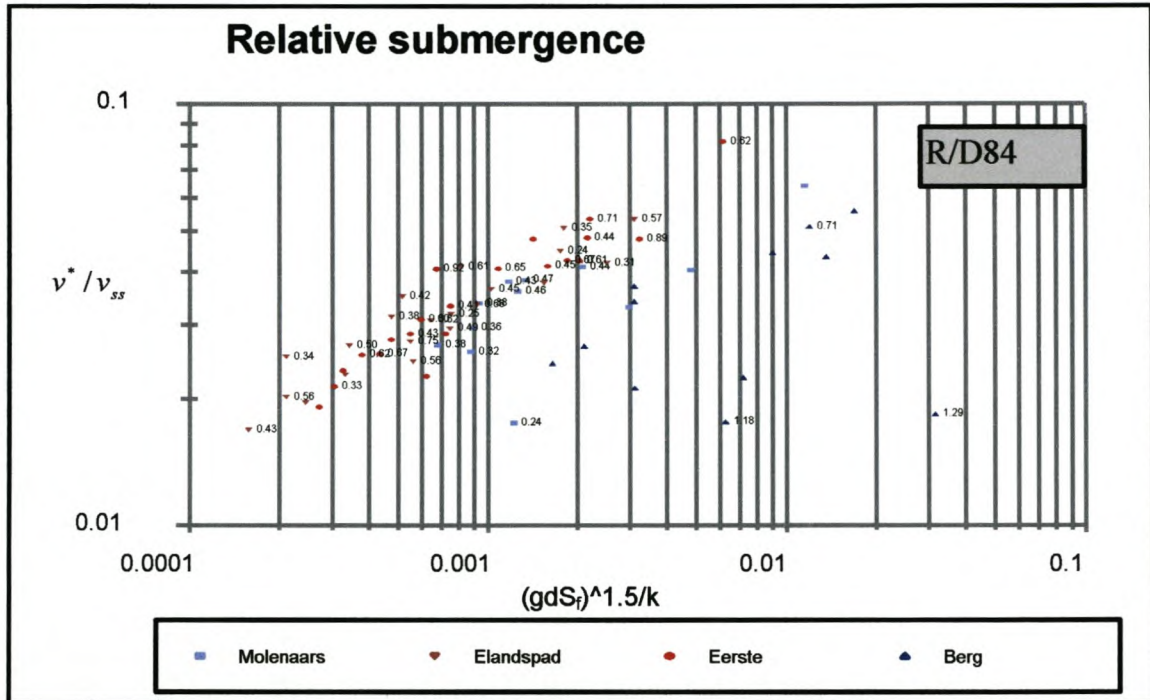


Figure 4.2 v^*/v_{ss} plotted against $(gdS_f)^{1.5}/k$, with relative submergence the variable under observation.

where: x-axis = Applied stream power

$$= \frac{(gdS_f)^{1.5}}{k} \text{ (m}^2/\text{s}^3\text{)}$$

$$\text{y-axis} = \frac{v^*}{v_{ss}}$$

v^* = Shear velocity

$$= \sqrt{gdS_f} \text{ (m/s)}$$

4.3.2 Calibration procedures

A number of different parameters, most of which were already identified through dimensional analysis by previous research, were investigated to evaluate their possible influence on the roughness coefficient. The most important of these, as concluded in Section 2 with the later addition of v^* / v_{ss} , are summarised in Table 4.3:

Table 4.3 Main parameters tested for significance.									
$\frac{R}{D_{84}}$	$\frac{R}{D_{50}}$	$\frac{d}{D_{84}}$	$\frac{D_{84}}{D_{50}}$	S_f	$\frac{\sqrt{gdS_f}}{v_{ss}}$	$\frac{R}{P}$	$\frac{W}{P}$	$\frac{v}{\sqrt{gR}}$	$\frac{vR}{v}$

Multiple regression techniques were applied to a variety of different combinations of the above parameters. Different dimensionless versions of the roughness coefficient were used during calibration, but C/\sqrt{g} proved the most accurate and versatile version. From these tests the following equation forms were thus identified as the most promising for application, i.e.:

$$\frac{C}{\sqrt{g}} = f\left(\left(\frac{R}{D_{84}}\right)\left(\frac{D_{84}}{D_{50}}\right)(S_f)\right) \quad \dots(i)$$

$$\frac{C}{\sqrt{g}} = f\left(\left(\frac{R}{D_{84}}\right)\left(\frac{D_{84}}{D_{50}}\right)\left(\frac{v^*}{v_{ss}}\right)\right) \quad \dots(ii)$$

$$\frac{C}{\sqrt{g}} = f\left(\left(\frac{v^*}{v_{ss}}\right)(S_f)\left(\frac{D_{84}}{D_{50}}\right)\right) \quad \dots(iii)$$

An R^2 value of 0.80 was viewed as the lower limit of required distributional accuracy. Table 4.4 shows the above combinations as calibrated against the data set.

Table 4.4 The three best correlated equations.

Parameters	Equation	R ²	No.
$\frac{R}{D_{84}} ; \frac{D_{84}}{D_{50}} ; S_f$	$\frac{C}{\sqrt{g}} = 14.08 \left(\frac{R}{D_{84}} \right)^{0.25} \left(\frac{D_{84}}{D_{50}} \right)^{-3.59} (S_f)^{-0.31}$	0.81	(4.7)
$\frac{R}{D_{84}} ; \frac{D_{84}}{D_{50}} ; \frac{\sqrt{gdS_f}}{v_{ss}}$	$\frac{C}{\sqrt{g}} = 8.74 \left(\frac{R}{D_{84}} \right)^{0.56} \left(\frac{D_{84}}{D_{50}} \right)^{-3.28} \left(\frac{\sqrt{gdS_f}}{v_{ss}} \right)^{-0.61}$	0.81	(4.8)
$\frac{\sqrt{gdS_f}}{v_{ss}} ; S_f ; \frac{D_{84}}{D_{50}}$	$\frac{C}{\sqrt{g}} = 20.9 \left(\frac{\sqrt{gdS_f}}{v_{ss}} \right)^{0.50} (S_f)^{-0.55} \left(\frac{D_{84}}{D_{50}} \right)^{-3.84}$	0.81	(4.9)

Experimental fitting of parameters to the local data set on purely empirical grounds therefore seemed to suggest the following parameters as particularly significant (Table 4.5):

Table 4.5 Significant parameters.

$\frac{C}{\sqrt{g}}$	$\frac{R}{D_{84}}$	$\frac{D_{84}}{D_{50}}$	S_f	$\frac{\sqrt{gdS_f}}{v_{ss}}$
----------------------	--------------------	-------------------------	-------	-------------------------------

It was, however, considered imperative to find better mathematical and physical justification before an equation form was accepted as suitable. Consequently, the focus was shifted to a fundamental theoretical investigation.

4.4 Hydraulic theory considerations

4.4.1 Sediment transport theory

Sediment transport theory, as derived by applying the law of conservation of power, was chosen as a theoretical approach to selecting the most suitable roughness expression for Western Cape mountain rivers. It was decided that this approach could offer a possibility of successfully describing the roughness mechanisms identified experimentally. The argument was that although the initial mathematical description

of the transport mechanics of sediment had been focused on smaller particles, the same basic laws should theoretically hold for larger bed material as well. It was hoped that similar parameters as those identified through the literature and initial calibration processes would be indicated, and that these could be expressed in a useful and understandable form.

As explained in Section 2.2.1.4, the basic law of conservation of power can be stated as:

$$\int_0^d \rho g S v_e dy = \int_0^d \tau_e \frac{dv}{dy} dy \quad (2.7)$$

If power theory is applied to sediment transport and the critical threshold condition associated with the beginning of particle movement, the transporting capacity of a stream and the required transport effort can be compared.

As also explained in Section 2.2.1.4, rough turbulent conditions lead to the following expression for applied unit stream power at the bed:

$$\left(\tau \frac{dv}{dy} \right)_0 \propto \frac{\rho g S_f d \sqrt{g d S_f}}{\kappa k_s} \quad (4.10)$$

where:

- 0 = “along the bed”
- k_s = Generated eddy size represented by roughness height (m)
- κ = $2R_0$
- κ = Von Karman coefficient, taken as constant = 0.4

The applied power per unit volume required to suspend a particle with density ρ_s and settling velocity v_{ss} in a fluid with density ρ is given as:

$$(\rho_s - \rho) g v_{ss} \quad (4.11)$$

Accordingly the applied power in maintaining motion along a bed has a direct relationship to the applied power required to suspend a particle:

$$\left(\tau \frac{dv}{dy} \right)_0 \propto (\rho_s - \rho) g v_{ss} \quad (4.12)$$

From (4.10) and (4.12):

$$(\rho_s - \rho) g v_{ss} \propto \frac{\rho g S_f d \sqrt{g d S_f}}{k_s} \quad (4.13)$$

Through manipulation the relative roughness can be isolated:

$$\frac{k_s}{d} \propto \frac{\rho g S_f \sqrt{g d S_f}}{(\rho_s - \rho) g v_{ss}} \quad (4.14)$$

As $\frac{\rho}{(\rho_s - \rho)}$ can be regarded as a dimensionless constant for Western Cape rivers, the above equation can take the following form:

$$\frac{k_s}{d} \propto \left(\frac{\sqrt{g d S_f}}{v_{ss}} \right) (S_f) \quad \dots(4.a)$$

It is thus evident that two of the significant parameters identified experimentally are reflected by sediment transport theory.

It is interesting to note that the relative submergence R/D_{84} term is absent from the above theoretical derivation. Seemingly, this would suggest that despite its supposed influence on roughness coefficients, illustrated by its prominence in virtually all known roughness formulae, there is no apparent fundamental justification for its presence in roughness expressions from a sediment transport perspective. This point has also been raised in Section 2, where it was stated that the term seems to have its origin in the logarithmic expression derived from boundary layer theory, which of

course does not apply to large-scale roughness conditions. However, if both the terms k_s/d and $\sqrt{gdS_f}/v_{ss}$ are closely examined, relative submergence or relative roughness does reveal itself in different forms. The following holds true for k_s/d :

$$k_s \propto R_0 \propto D_{84}$$

and:

$$d \propto R$$

Therefore:

$$\frac{k_s}{d} \propto \frac{D_{84}}{R} \quad (4.15)$$

In the case of $\sqrt{gdS_f}/v_{ss}$, it can be seen that for an assumed constant particle density, the settling velocity v_{ss} is determined solely by particle size. With d or R present above the line, it is clear that the relative submergence is to a certain extent incorporated in this parameter as well.

The above would thus explain the influence of the relative submergence or relative roughness term on the roughness coefficient. Nonetheless, it is k_s/d itself and $\sqrt{gdS_f}/v_{ss}$ itself that provide theoretical justification.

4.4.2 Hydraulic depth d versus hydraulic radius R

In shallow mountain streams the hydraulic depth d is almost equal to the hydraulic radius R . This is so because the ratio of width to depth is large. This means that the wetted perimeter P is similar in value to the stream width W (Figure 4.3):

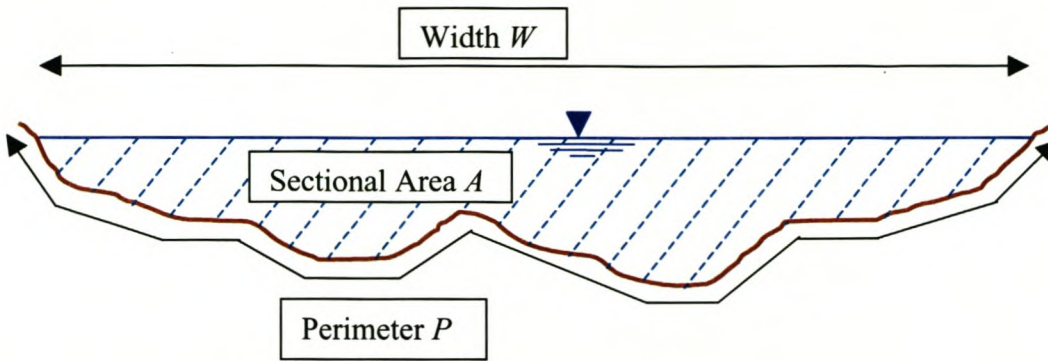


Figure 4.3 Illustration of relevant cross-sectional terms.

Hydraulic radius is given by:

$$R = \frac{A}{P} \quad (4.16)$$

Hydraulic depth is given by:

$$d = \frac{A}{W} \quad (4.17)$$

In shallow, wide streams:

$$P \approx W$$

$$\therefore R \approx d$$

Whereas hydraulic depth appears in Equation (4.a), in channels with very uneven bottoms as those under consideration here, hydraulic radius is the preferred parameter to hydraulic depth, because it gives a more physically meaningful interpretation of the cross-sectional character. Wetted perimeter incorporates the uneven real length of the wetted bottom, whereas stream width does not reflect the nature of the bottom of the river at all. Based on Equation (4.a) and the relevant site data, R correlated similar to d as shown in Table 4.6:

Table 4.6 Hydraulic radius R versus hydraulic depth d as a roughness parameter.			
Parameters	Equation	R²	No.
$\frac{k}{d}; \frac{\sqrt{gdS_f}}{v_{ss}}; S_f$	$\frac{k}{d} = 24 \left(\frac{\sqrt{gdS_f}}{v_{ss}} \right)^{-2.91} (S_f)^{2.17}$	0.57	(4.18)
$\frac{k}{R}; \frac{\sqrt{gRS_f}}{v_{ss}}; S_f$	$\frac{k}{R} = 17.72 \left(\frac{\sqrt{gRS_f}}{v_{ss}} \right)^{-3.09} (S_f)^{2.23}$	0.58	(4.19)

Although hydraulic radius and hydraulic depth would essentially be similar in shallow, wide rivers, it was decided that hydraulic radius would be used in stead of hydraulic depth, because of the reasons given above. Then Equation (4.a) can be written as Equation (4.b):

$$\frac{k_s}{R} \propto \left(\frac{\sqrt{gRS_f}}{v_{ss}} \right) (S_f) \quad \dots(4.b)$$

4.4.3 Bed material size distribution

Although the standard ratio of the bed material size distribution (D_{84} / D_{50}) is not present in the theoretically derived expression, it is clear from experimental evidence that it has such a significant influence on the large-scale roughness coefficient that it cannot be ignored. The ratio originates from the statistical standard deviation of the bed material size, namely $\log(D_{84} / D_{50})$. The standard deviation parameter was however shown by Simons and Senturk (1992) to have practical limitations as a result of the logarithmic format. Therefore the standard ratio parameter is the preferred expression. Under conditions of large-scale roughness, the flow depth is of the same order of magnitude as the size of the bed material, and thus form drag of individual particles plays an important role in affecting flow resistance. Furthermore, in the mountain streams of the Western Cape, a large spread of bed material size is found, from gravel to boulders of more than a metre in diameter. These bigger boulders in particular have significant influence on the flow resistance.

The theory above does not make provision for differences in particle size, and thus ignores the existence of larger boulders. It may therefore be argued that some representative parameter should be added to Equation (4.b) to allow for the presence of different boulder sizes in the river. Simons and Senturk (1992) points out that the bed material gradation represents the coarser portion of the bed material which adds notably to the amount of form drag created, the forming of localised hydraulic jumps, and the energy loss associated with contraction and expansion around the bigger particles. It was also stated that the significance of the gradation coefficient increases with increasing gradient, which supports the argument for its inclusion in frictional expressions of mountain streams. Furthermore, the parameter (D_{84} / D_{50}) implicitly represents the concentration of larger boulders present in the reach. The correlation achieved in calibrating Equation (4.b) was rather disappointing, but if (D_{84} / D_{50}) is added, the correlation improves significantly (see Table 4.7):

Table 4.7 Addition of D_{84}/D_{50} to the roughness equation.

Parameters	Equation	R ²	No.
$\frac{k}{R}; \frac{\sqrt{gRS_f}}{v_{ss}}; S_f; \frac{D_{84}}{D_{50}}$	$\frac{k}{R} = 0.03 \left(\frac{v^*}{v_{ss}} \right)^{-0.63} (S_f)^{0.91} \left(\frac{D_{84}}{D_{50}} \right)^{8.36}$	0.83	(4.20)

It is evident from Table 4.7 that (D_{84} / D_{50}) has a major influence on the roughness coefficient. Due to this fact, it might be worth improving the sampling technique in future, for instance by having a separate boulder size data set for every section instead of for every reach, so that the specific bed character of each section can be evaluated separately.

The conclusion thus far is that the differences between the theoretical flows and the real flows can be diminished significantly by the addition of the size distribution parameter (D_{84} / D_{50}) to the theoretically derived equation, as shown in Table 4.7.

The basic expression of Equation (4.b) has now developed to Equation (4.c):

$$\frac{k_s}{R} \propto \left(\frac{\sqrt{gRS_f}}{v_{ss}} \right) (S_f) \left(\frac{D_{84}}{D_{50}} \right) \dots(4.c)$$

4.4.4 Chezy's C versus relative roughness k/R

As discussed in Section 2.2.4.1, relative submergence, which is the inverse of relative roughness, is incorporated in Chezy's roughness coefficient C as follows:

$$C = 5.75\sqrt{g} \log\left(\frac{12R}{k}\right) \quad (2.14)$$

The factor $\log(12R/k)$ becomes negative when the value of k is higher than that of $12R$. Under low flow conditions in shallow streams, where the roughness height is large compared to the hydraulic radius, this scenario is quite possible. In such cases the value of C could become negative and meaningless, as a negative coefficient is obviously impossible and far removed from reality. It was thus decided that the calibration of C rather than k/R should result in a more widely applicable equation that would eliminate possible problems with the logarithmic function. Because of the above direct relationship between C and relative roughness, this step can be justified as follows:

$$\frac{C}{\sqrt{g}} = f\left(\frac{R}{k}\right) = f'\left(\frac{k}{R}\right)$$

Therefore:

$$\frac{C}{\sqrt{g}} \propto \left(\frac{\sqrt{gRS_f}}{v_{ss}}\right) \left(S_f\right) \left(\frac{D_{84}}{D_{50}}\right) \quad \dots(4.d)$$

The correlation that resulted from the calibration of this equation with the available data set is shown in Table 4.8:

Table 4.8 C instead of k/R as the roughness coefficient.

Parameters	Equation	R ²	No.
$\frac{C}{\sqrt{g}}; \frac{\sqrt{gRS_f}}{v_{ss}}; S_f; \frac{D_{84}}{D_{50}}$	$\frac{C}{\sqrt{g}} = 20.9 \left(\frac{\sqrt{gRS_f}}{v_{ss}} \right)^{0.5} (S_f)^{-0.55} \left(\frac{D_{84}}{D_{50}} \right)^{-3.84}$	0.81	(4.21)

It would thus appear as if one of the equation forms identified empirically, namely Equation (4.9), is indeed close to being a most suitable candidate, both from the mathematical and empirical points of view. Because of the inverse relationship between *C* and *k/R*, the exponents of the factors in the equation are inverted, as expected. The regression still correlates above the threshold R² value of 0.81, but it does fare marginally poorer than the *k/R* relationship (0.83). However, the added versatility of this equation means that it could find wider application under conditions of large-scale roughness.

4.4.5 Comparison to existing formulae

Figure 4.4 graphically illustrates the fitting of Equation (4.21) to the data set in comparison to the existing Equations (4.3) and (4.5) (see Table 4.1). From the graph it is clear that Equation (4.21) gives a significantly better fit to the data set. Lower and higher flows correlate equally well, and few data values are completely wayward. Therefore, there seems to be clear evidence that the locally derived equation holds marked advantage over the foreign ones. Comparing discharge accuracies achieved within given boundaries, as is shown in Table 4.9, further emphasise this. A striking improvement in accuracy can be observed, and lends further weight to the new formula as an effective predictor of flow.

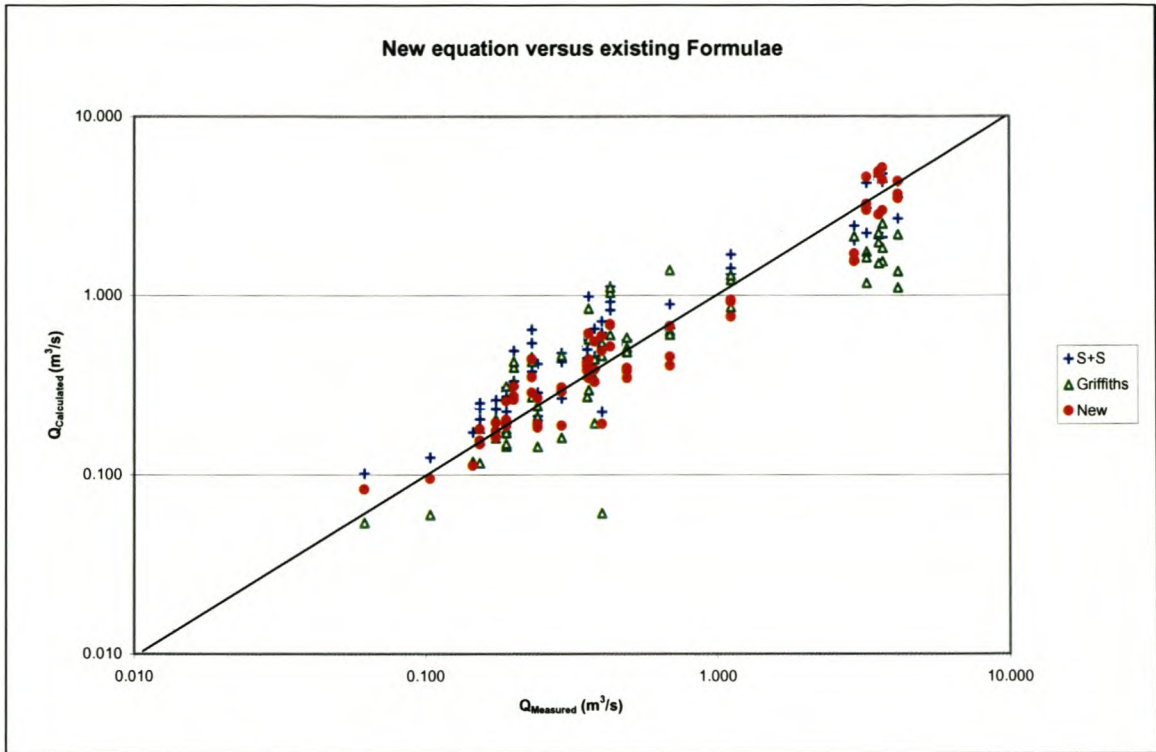


Figure 4.4 Comparison of existing formulae with new equation.

Table 4.9 Accuracies of best existing equations in comparison to new equation.

Number	Within 10%	Within 20%	Within 50%	Within 100%
(4.3)	18.2	36.4	54.5	80.3
(4.5)	10.6	25.8	59.1	90.9
(4.21)	30.3	45.5	80.3	98.5

4.5. Final proposal

After empirical processing and theoretical analysis, Equation (4.d) was selected as the most suitable large-scale roughness equation for Western Cape mountain rivers, with possibly wider application. Although calibration of the variables will still be desirable for site-specific application, the underlying theoretical basis combined with meaningful experimental adjustment will hopefully prove that this formulation is more robust than any other proposal to date. Main parameters are limited to three, and all variables are fairly easy to determine.

Although the preceding discussion and analysis have made plausible the presence of the specific variables in the formulation, the qualitative nature of the dependence of Q on these variables should also be plausible. This is investigated by using the flow equation of Chezy, with the above value of C , i.e:

$$Q = vA = C\sqrt{RSA} \quad (2.12)$$

$$Q = 20.9\sqrt{g} \left(\frac{\sqrt{gRS_f}}{v_{ss}} \right)^{0.5} (S_f)^{-0.55} \frac{D_{84}^{-3.84}}{D_{50}} \sqrt{RS_f} RP \quad (4.22)$$

$$\therefore Q = 115.9 \frac{R^{1.75} S_f^{0.2}}{v_{ss}^{0.5}} \left(\frac{D_{50}}{D_{84}} \right)^{3.84} P \quad (4.23)$$

If the main parameters influencing flow are now isolated, Equation (4.23) results in:

$$\therefore Q \propto R^{1.75} S_f^{0.2} \left(\frac{D_{50}}{D_{84}} \right)^{3.84} P \quad (4.24)$$

The behaviour of Q was then tested quantitatively against these parameters with the help of the graphs shown below in Figures 4.5 – 4.8. Typical values of hydraulic parameters were used to draw the graphs, similar to those found in the data set. It should be kept in mind that the discharge values on the y-axis serve merely to illustrate the *individual behaviour* of the specific parameter towards the flow, and are thus not any indications of true discharge values. The combined effect of all parameters, which determines the resultant discharge behaviour, is another matter entirely.

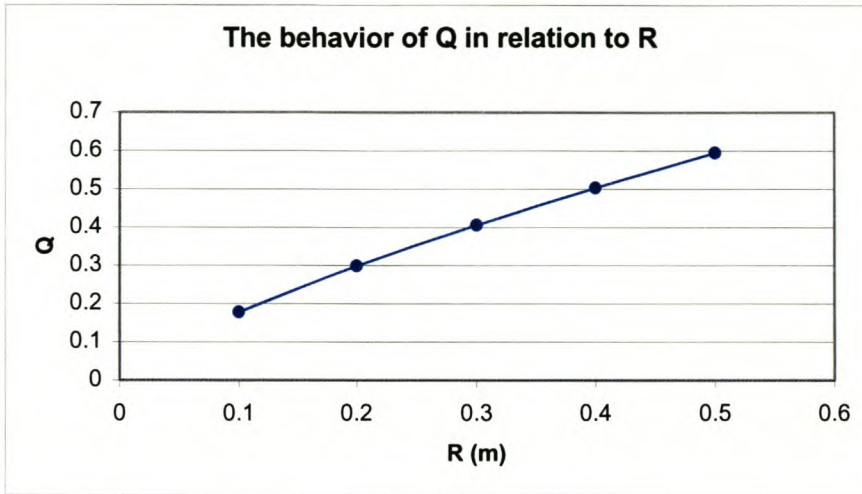


Figure 4.5 The quantitative effect of R on discharge.

From Figure 4.5 it can be deduced that a strong direct relationship exists between the R variable and the flow, as is to be expected. An almost linear increase in the discharge results from an increase in R , and the dependence of Q on the hydraulic radius is clearly significant.

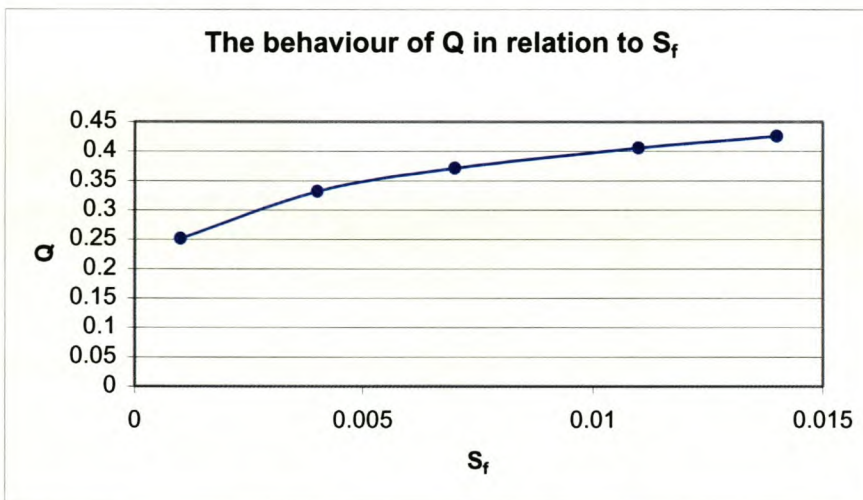


Figure 4.6 The quantitative effect of S_f on flow.

Figure 4.6 shows a much flatter curve that appears to be moving towards some horizontal asymptote as the energy slope increases. This could be linked to the fact that although turbulence and energy loss is more severe under higher flows, the variation as such will be less than under lower flows. The direct relationship is to be expected, as it makes sense that flow will increase with slope, but the underlying

conclusion that can be drawn from this graph is that the dependence of Q on slope is not nearly as significant as might have been anticipated. In fact, the dependence is very weak indeed. If Equation (4.21) is closely examined along with Equation (2.12), it becomes apparent that the slope term in (4.21) almost cancels out the slope term of (2.12) when implemented. Considering the rough nature of flow in the mountain streams examined, where the irregular bed material has a very disruptive effect on flow and slope as such, it is not completely surprising that the influence of slope is so low. It holds definite advantages concerning field measurements, because an exact water slope would not be required to calculate the discharge accurately. This aspect is examined further in Section 5.

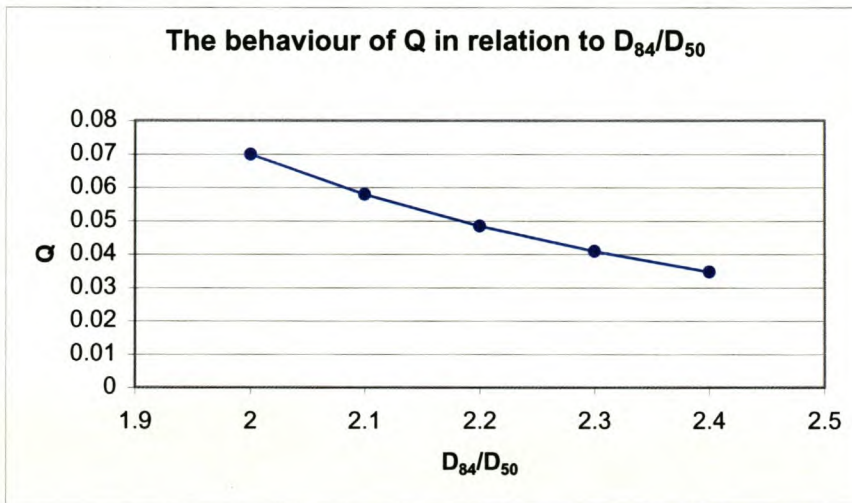


Figure 4.7 The quantitative effect of D_{84}/D_{50} on flow.

Figure 4.7 displays the steep inverse relationship between discharge and particle gradation. The inverse dependence also makes sense, because as the diversity and thus the number of large boulders increase, so will the resistance to flow. It is apparent that under conditions of large-scale roughness the bed material size distribution has a major influence on the discharge, and its inclusion in the roughness expression is therefore justified.

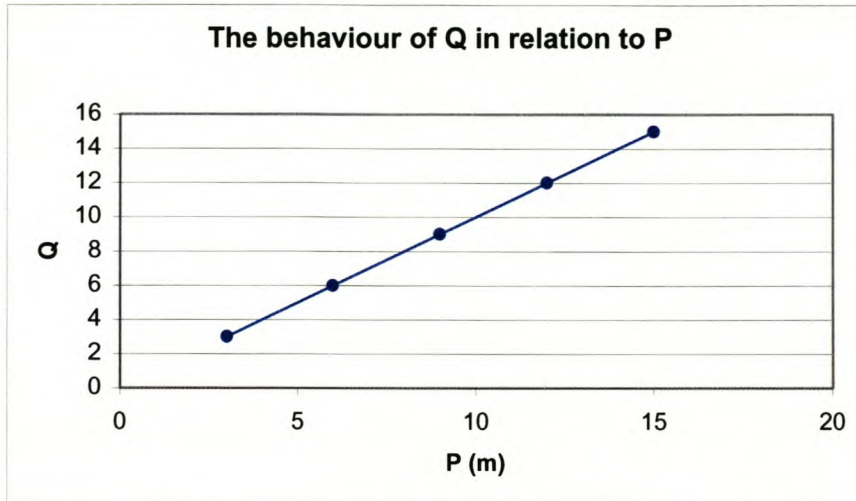


Figure 4.8 The quantitative effect of P on flow.

A linear direct relationship exists between flow and wetted perimeter according to Figure 4.8. This was to be expected, as flow will increase with the wetted perimeter, which is closely associated with the cross-sectional area and the hydraulic radius, both of which are also direct indicators of the amount of water passing a certain point.

From the above it does appear as if the reaction of Q to all parameters makes sense and can be duly explained. Equation (4.21) is therefore acceptable.

The final three useful expressions can thus be summarised as follows:

- General expression for Chezy's roughness coefficient suited for mountain stream roughness calculation:

$$\therefore \frac{C}{\sqrt{g}} = f \left\{ \left(\frac{\sqrt{gRS_f}}{v_{ss}} \right) \left(S_f \right) \left(\frac{D_{84}}{D_{50}} \right) \right\} \quad \dots(4.d)$$

- Calibrated equation for Chezy's roughness coefficient suited for Western Cape mountain stream roughness calculation:

$$\frac{C}{\sqrt{g}} = 20.9 \left(\frac{\sqrt{gRS_f}}{v_{ss}} \right)^{0.5} (S_f)^{-0.55} \left(\frac{D_{84}}{D_{50}} \right)^{-3.84} \quad (4.21)$$

- Discharge equation suited for Western Cape mountain stream flow calculation:

$$\therefore Q = 115.9 \frac{R^{1.75} S_f^{0.2}}{v_{ss}^{0.5}} \left(\frac{D_{50}}{D_{84}} \right)^{3.84} P \quad (4.23)$$

In closing, it is believed that the above expressions, and particularly Equation (4.d), could form the basis of generally applicable equations that should prove to be more reliable than any other proposed to date, especially under diverse flow conditions such as those prevalent in the mountain streams of the Western Cape. However, if wide applicability and effective usage is to be ensured, more research and also field data is required so that more general calibration can be undertaken.

Although much more research and practical investigation will be needed, some exploratory testing was undertaken in this regard, particularly concerning the sensitivity of the slope parameter and the practical application of Equation (4.21). This is presented in the next section.

Chapter 5: Variations on a theme

After the derivation of the most promising expression was completed, it was decided to investigate two aspects surrounding its usage. In the first instance, the effective measuring of an energy slope was singled out as a major obstacle during data sampling. The sensitivity of this variable was thus to be investigated so as to work towards equating it effectively and accurately. Secondly, because three sections were measured at every recorded discharge, an averaged flow rate could be calculated to see if any further improvement in the results is possible. Both of these investigations revealed significant results.

5.1 Sensitivity of slope in the chosen formulation

From the literature study conducted on large-scale roughness conditions and friction formulae in general, various different viewpoints and techniques were found concerning the sampling and calculation of the energy slope parameter. Some studies advocated the channel gradient (Afzalimehr and Anctil, 1998), whereas others made use of the water level to determine slope (Bathurst, 1985). A multitude of different sampling methods were also employed. The fact remains that slope is a very difficult variable to determine accurately, particularly where low flows and boulder beds are concerned.

Against the background of conflicting views, the equation calibrated on the local data set, namely Equation (4.21), showed slope to have remarkably little influence on the flow rate (see Figure 4.6). It is accepted that this has a lot to do with the rough nature of the streams concerned, where other effects such as the disruptive influence of large boulders could easily override the effects of slope. This limited influence is further demonstrated with the help of Figure 5.1 and Table 5.1, where a variety of averaged and even guessed slope values gave similar results, as expected.

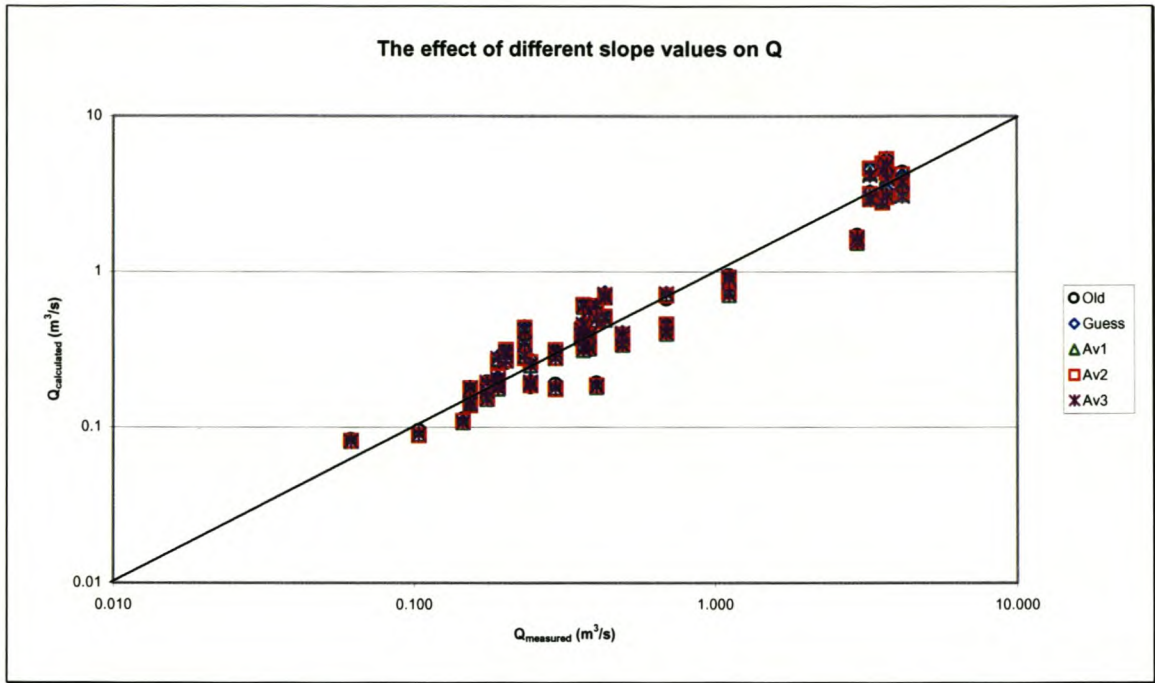


Figure 5.1 Graph illustrating the minor influence of different slope values on the discharge calculated with Equation (4.21).

Number	Within 10%	Within 20%	Within 50%	Within 100%
Old	30.3	45.5	80.3	98.5
Guess	27.3	47.0	78.8	98.5
Av1	30.3	43.9	80.3	98.5
Av2	24.2	47.0	78.8	98.5
Av3	27.3	42.4	80.3	98.5

where:

- Old = Original slope values used
- Guess = Improvised slope values used
- Av1 = Averaged reach slope values used
- Av2 = Averaged cross-sectional slope values used
- Av3 = Averaged data set slope value used

The fact that slope is of lesser importance is a big plus for the current formulation, because complicated and time-consuming water level measuring exercises can thus be avoided. It is advocated that as long as an average water slope that seems more or less

realistic for the reach under consideration is used in calculations, satisfactory results should be achieved. From experience, in the Western Cape context realistic would mean between 0.001 and 0.01, with the average for low summer flows in typical reaches around 0.005. This scenario could however be very different in other streams with smaller-scale roughness conditions, and it is recommended that recalibration of Equation (4.d) be done before application in streams with markedly different characteristics takes place.

As mentioned in Section 4.5, the slope parameter of the roughness formulation cancels out the slope parameter of the discharge formulation to a large extent. Consequently, the inclusion of the energy slope in the roughness equation is necessary, not only because the theory requires it, but also because its importance as a determinant of flow rates is effectively diminished.

5.2 Averaged values of calculated discharge

Because of the diverse and random nature of the river channels in the mountain streams under investigation, flow characteristics also change continually along a reach. No two sections are the same, and individual characteristics prevalent across one section could affect the flow quite differently from another section with its own unique character. With this in mind, it was deduced that an averaged flow calculation, consisting of more than one sectional measurement, could possibly further improve the reliability of flow prediction.

As already explained in Section 3, the hydraulic data of three different sections were collected with every recorded discharge rate. The average of the three discharges calculated for every measured discharge could thus be determined, and compared to the original results. Figure 5.2 and Table 5.2 illustrate the outcome of this process. A significant improvement is discernable in the fitting of the data in Figure 5.2, and Table 5.2 presents clear evidence that better accuracy is achieved when applying this technique.

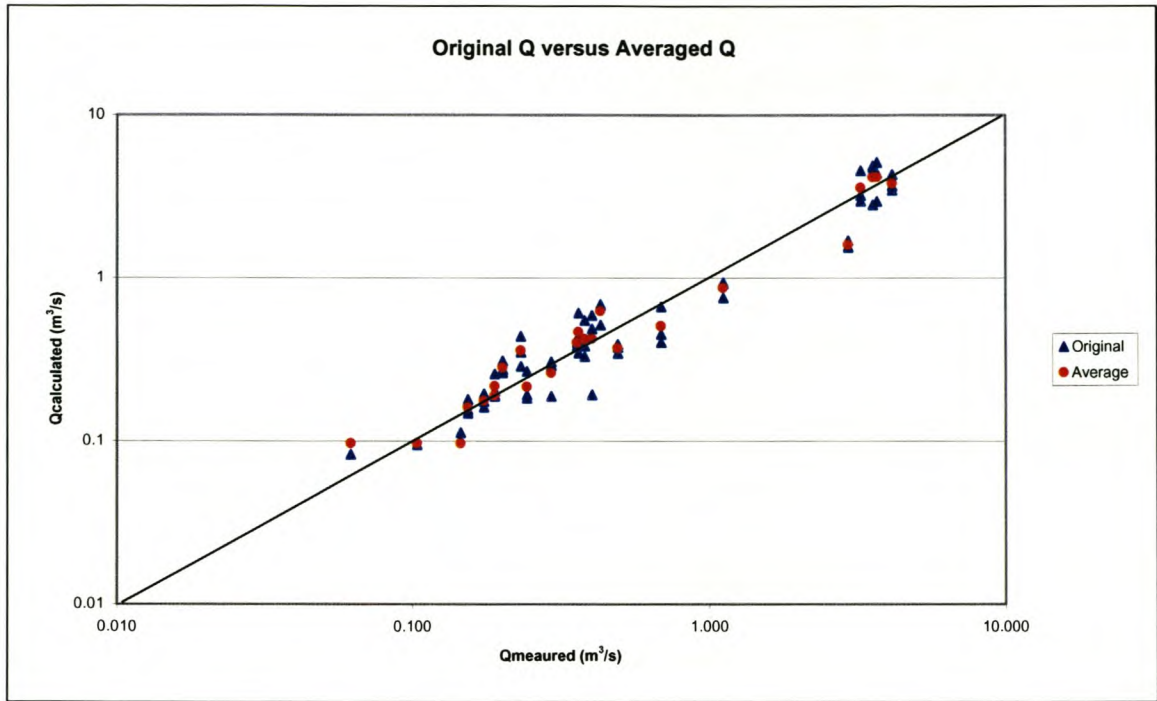


Figure 5.2 Graph illustrating averaged discharge prediction in comparison to normal discharge prediction.

Number	Within 10%	Within 20%	Within 50%	Within 100%
Original	30.3	45.5	80.3	98.5
Averaged	28.8	60.6	87.9	100

The conclusion from the above is that there is a distinct advantage in measuring more than one section and determining the average flow rate. The different characteristics affecting flow along different sections of stream can be accommodated this way, and it is strongly recommended that an averaging technique be employed in practice.

Although reasonable results have been achieved by the above tests, proper verification using independent data still needs to be done so as to test the general applicability of Equation (4.21). This aspect is discussed in the next section.

Chapter 6: Verification of derived equation

6.1 Background

It was considered important that the chosen large-scale roughness equation be verified against an independent set of data, so that its general applicability could be tested. An independent local dataset would preferably be the starting point for such an investigation, but unfortunately no other set of applicable Western Cape data existed at the time of writing. Therefore, the necessary information had to be obtained from international studies conducted on large-scale roughness conditions. This was not ideal for the following reasons:

- The proposed equation of this paper was derived first and foremost for application in the Western Cape, and as such it would have been preferable to test it on the streams that it is to be applied on.
- Despite apparently similar conditions, the characteristics of streams from other regions could be quite different from those of the Western Cape. For example, the density of bed particles could be different because of the individual geological characteristics of an area, and this is information not readily supplied with a set of hydraulic data.
- Since the exact measuring techniques used in foreign collection processes are not known, results and consequent accuracies could differ substantially from the locally applied sampling techniques.
- It was regarded as important to use information that falls within the relevant parameter boundaries applicable to the calibrated equation, so that figuratively speaking apples could be compared to apples. Unfortunately, few samples from other datasets could be found that conform to all the relevant requirements.

Due to the above reasons, a proper verification could not be conducted, and it is recommended that this be done at some point in the future.

6.2 Verification results

Despite the limitations discussed above, a few samples of suitable data (Bathurst,1985; Jarrett, 1984; Thorne and Zevenbergen, 1985) were found and selected to serve as a first indication of the merit of the chosen formula. The data points chosen all fell within or close to the applicable parameter boundaries, and are shown in Table 6.1. The density of the bed particles was assumed to be the same as in the Western Cape, as this information was not available from the literature.

Table 6.1 Suitable data obtained from literature.											
		Q_{gauge}	A	R	d	S_f	D_{84}	D_{50}	d/D_{84}	R/D_{84}	D_{84}/D_{50}
Unit		(m ³ /s)	(m ²)	(m)	(m)		(m)	(m)			
Dataset	Max	5.270	5.92	0.470	0.488	0.0340	0.55	0.18	0.850	1.196	3.096
	Min	0.315	1.02	0.142	0.142	0.0060	0.15	0.06	0.434	0.434	2.250
Required	Max	4.170	6.23	0.512	0.535	0.0167	0.50	0.21	1.783	1.707	2.588
	Min	0.062	0.53	0.104	0.110	0.0005	0.30	0.14	0.251	0.237	1.935
Bathurst	1	0.315	1.84	0.142	0.142	0.0145	0.33	0.12	0.434	0.434	2.66
	2	1.550	2.78	0.261	0.261	0.0098	0.31	0.12	0.850	0.850	2.60
Jarrett	3	1.501	3.99	0.311	0.311	0.0150	0.55	0.18	0.567	0.567	3.00
	4	0.878	1.95	0.268	0.268	0.0300	0.43	0.15	0.629	0.629	2.80
	5	0.368	1.02	0.152	0.152	0.0160	0.15	0.06	1.000	1.000	2.50
Thorne & Zevenbergen	6	2.050	3.67	0.349	0.355	0.0143	0.39	0.16	0.903	0.888	2.43
	7	3.280	4.37	0.404	0.412	0.0151	0.39	0.16	1.048	1.028	2.43
	8	5.270	5.32	0.470	0.488	0.0163	0.39	0.16	1.242	1.196	2.43
	9	2.050	3.96	0.289	0.296	0.0183	0.34	0.13	0.878	0.858	2.59
	10	3.340	4.70	0.331	0.338	0.0193	0.34	0.13	1.003	0.982	2.59
	11	4.280	5.10	0.352	0.359	0.0189	0.34	0.13	1.065	1.045	2.59
	12	5.270	5.92	0.389	0.397	0.0190	0.34	0.13	1.178	1.154	2.59

Table 6.2 shows the accuracy of the above data set in comparison to the Western Cape data set used for calibration. As can be seen the foreign set compares favourably with the local set. Thus there seems to be reasonable evidence to suggest the wider application of Equation (4.21), as long as the parameters fall within reasonably similar ranges as those used in the calibration of Equation (4.21).

Table 6.2 Accuracies of best existing equations in comparison to new equation.		
Number	Within 50%	Within 100%
(4.21): Foreign data	75	100
(4.21): Local data	80.3	98.5

For interest's sake, a number of data points that vary substantially from the ranges of the Western Cape set were also investigated, and are shown in Table 6.3.

Table 6.3 Unsuitable data obtained from literature.											
		Q_{gauge}	A	R	d	S_f	D_{84}	D_{50}	d/D_{84}	R/D_{84}	D_{84}/D_{50}
Unit		(m^3/s)	(m^2)	(m)	(m)		(m)	(m)			
Dataset	Max	4.350	7.650	0.417	0.417	0.037	0.610	0.305	0.834	1.089	4.333
range	Min	0.340	1.301	0.146	0.146	0.003	0.240	0.091	0.597	0.369	1.644
Required	Max	4.170	6.23	0.512	0.535	0.0167	0.50	0.21	1.783	1.707	2.588
range	Min	0.062	0.53	0.104	0.110	0.0005	0.30	0.14	0.251	0.237	1.935
Bathurst	1	4.350	7.65	0.417	0.417	0.01360	0.500	0.251	0.834	0.834	1.99
	2	2.000	3.81	0.277	0.277	0.03730	0.464	0.263	0.597	0.597	1.76
	3	2.380	4.15	0.191	0.191	0.01560	0.240	0.146	0.796	0.796	1.64
Jarrett	4	1.104	3.62	0.201	0.201	0.00300	0.396	0.213	0.508	0.508	1.86
	5	0.340	1.30	0.146	0.146	0.01100	0.396	0.091	0.369	0.369	4.33
	6	2.661	3.25	0.332	0.332	0.01600	0.396	0.091	0.838	0.838	4.33
Thorne & Zevenbergen	7	4.190	6.32	0.390	0.390	0.01900	0.610	0.305	0.640	0.640	2.00
	8	1.359	2.97	0.180	0.180	0.02600	0.366	0.122	0.492	0.492	3.00
	9	2.605	4.27	0.250	0.250	0.02600	0.366	0.122	0.683	0.683	3.00
	10	1.982	4.46	0.299	0.299	0.00900	0.274	0.152	1.089	1.089	1.80

An accuracy of within 100% was achieved 0% of the time! This disturbing result illustrates the dangers involved in attempting to apply calibrated equations to unsuitable parameter ranges. It would appear as if the bed material size ratio is the most sensitive to change, as it is the only parameter differing notably from that of the data set of Table 6.1 and the original set. This makes sense, because the bed material size ratio is such a dominant parameter under large-scale roughness conditions. Slope also differs substantially, but that was also the case in Table 6.1, which compared satisfactorily with the Western Cape set. The results of this test as well as that of the data set of Table 6.1 is graphically illustrated in Figure 6.1.

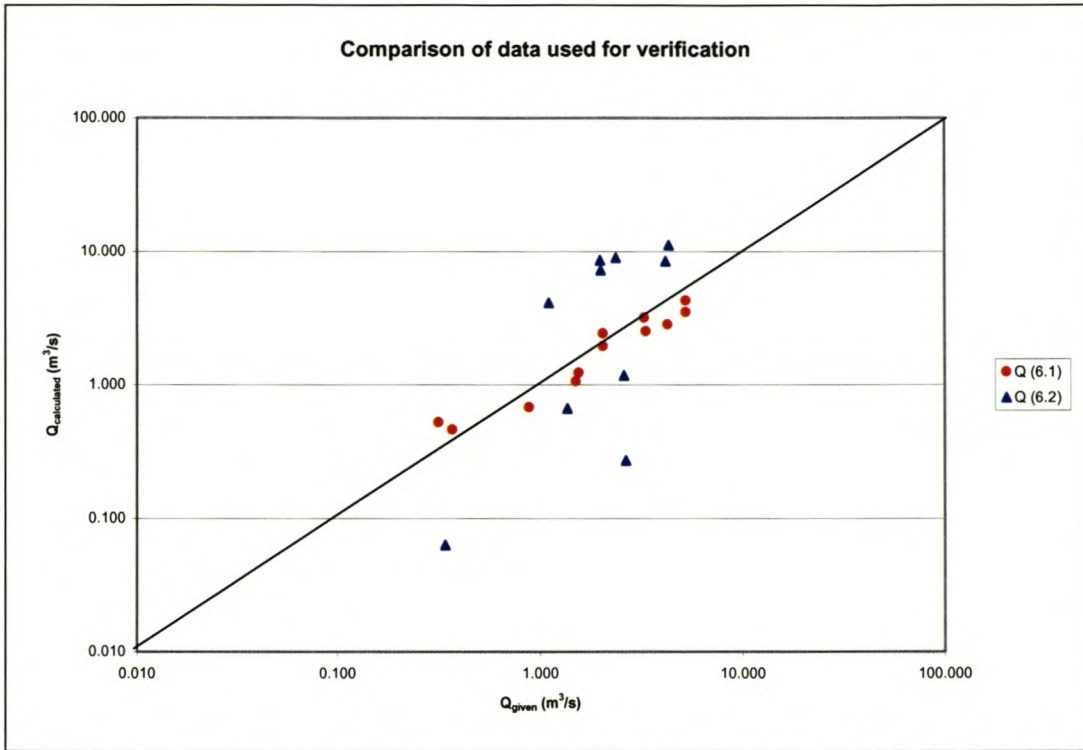


Figure 6.1 Graph illustrating the fitting of the independent data sets from Tables 6.1 and 6.3.

Figure 6.1 shows clearly the difference in results between the two sets of data. It is accordingly recommended that Equation (4.d) be tested and calibrated on as wide a range of local data as possible, so that its format for different conditions can be determined and the range of its applicability evaluated. As far as Equation (4.21) is concerned, the respectable result achieved with the dataset of Table 6.1 and graphically illustrated in Figure 6.1, supports its recommendation as a directly applicable formula on streams and reaches that fall within or close to the required ranges of the individual hydraulic parameters, with particular attention to the bed material size ratio parameter.

Chapter 7: Conclusions and recommendations

7.1 Conclusions

The main goal of this study was the development of an improved expression for calculating roughness coefficients and flow rates in Western Cape mountain streams, preferably with the support of empirical fitting, fundamental derivation and physical justification. It is believed that this goal was achieved. A low impact, user friendly equation was derived through sediment transport principles applied in combination with empirical adjustment. The expression was shown to outperform other existing equations, and provides a much-needed alternative to existing calculation techniques. Significant potential also exists for its wider application, provided further research is done. Conclusions drawn concerning all different aspects of the study are discussed below:

The following main conclusions were drawn from the study as a whole:

- Mountain stream flow conditions are unique and undeniably determined by the physical characteristics of the river reach, and in particular the bed roughness, with the bed material size having a dominant influence. A distinctive approach incorporating these physical characteristics will thus always be necessary for flow calculation under similar flow conditions.
- Empirical friction equations from previous studies on different continents have limited applicability on Western Cape mountain streams, underlining the unique character of these streams. A locally derived and calibrated formula is more suitable for the purposes of friction and flow calculations.
- Relative submergence, energy slope, bed material size ratio and the ratio between applied power and power required to suspend a particle ($\sqrt{gRS_f} / v_{ss}$) are the significant parameters influencing the roughness coefficient under Western Cape large-scale roughness conditions.

- A reasonably accurate and easily applicable alternative to existing mountain stream measuring techniques exists, encompassing a simple combination of physical parameters related in a power function, that is soundly supported on physical and fundamental grounds.

Secondary conclusions concerning specific aspects are summarized as follows:

- Sediment transport theory successfully describes a roughness expression in power form containing the energy slope term and the power ratio term $\sqrt{gRS_f} / v_{ss}$.
- $\sqrt{gRS_f} / v_{ss}$, energy slope S_f and bed material size ratio D_{84}/D_{50} make up the most suitable parameter combination for a roughness expression for Western Cape mountain streams.
- The inclusion of energy slope in the roughness expression effectively diminishes its influence in the flow calculation.
- Taking the average of three independent discharge calculations, simultaneously recorded across three sections on the same river, increases the accuracy of flow determination.
- Parameter boundaries similar to those used in the calibration process are necessary for accurate application of the chosen expression, with bed material size ratio revealing particular sensitivity to this aspect.

7.1 **Recommendations**

During the field work process and the analyses that followed, various possible improvements or alternatives were identified and are considered and recommended below:

- It is recommended that the boulder sampling procedure be refined to include a set of 100 particles for every individual section. Large differences between boulder sizes of specific sections exist, and this step will result in a more scientifically reliable reflection of the influence of particle size on the roughness of specific sections.
- A larger set of Western Cape stream data is required for further calibration and refining of Equation (4.21). The need also exists to test its effectiveness on as many sections of Western Cape mountain stream as possible, so that proper verification could be done.
- A more streamlined method of data recording needs to be developed, particularly for sections that are to be used regularly in flow calculation, so that repetitive measuring can be avoided. It is suggested that a reference point system be implemented, so that a reliable water level could be measured. This would mean a specific cross-section could be recorded once, after which only a water level reading would have to be taken in future to calculate the necessary parameters.
- The range of applicability of the derived equation needs to be investigated. For instance, as depth increases in relation to particle size, the bed material gradation term will become less dominant until its influence disappears completely, such as in a sand bed river. The threshold values of applicability need to be determined if Equation (4.d) is to be utilized to its full potential.

“Now this is not the end. It is not even the beginning of the end. But it is, perhaps, the end of the beginning.”

- Winston Churchill

Chapter 8: References

1. Aberle, J., Dittrich, A., Nestmann, F., 1999. "Discussion: Estimation of Gravel-Bed River Flow Resistance", Journal of the Hydraulics Division, ASCE, Vol. 125, No. 12.
2. Afzalimehr, H., Anctil, F., 1998. "Estimation of Gravel-Bed River Flow Resistance", Journal of the Hydraulics Division, ASCE, Vol. 124, No. 10.
3. Basson, G.R., Rooseboom, A., 1997. "Dealing with Reservoir Sedimentation", WRC Report No. TT 91/97, Water Research Commission, RSA.
4. Bathurst, J.C., 1978. "Flow Resistance of Large-Scale Roughness", Journal of the Hydraulics Division, ASCE, Vol. 104, No. HY12.
5. Bathurst, J.C., Li, R., Simons, D.B., 1981. "Resistance Equation for Large-Scale Roughness", Journal of the Hydraulics Division, ASCE, Vol. 107, No. HY12.
6. Bathurst, J.C., Hey, R.D., Thorne, C.R., 1982. "Gravel-Bed Rivers", John Wiley and Sons, New York.
7. Bathurst, J.C., 1985. "Flow Resistance Estimation in Mountain Rivers", Journal of the Hydraulics Division, ASCE, Vol. 111, No. 4.
8. Bathurst, J.C., 1986. "Slope-Area Discharge Gaging in Mountain Rivers", Journal of the Hydraulics Division, ASCE, Vol. 112, No. 5.
9. Bathurst, J.C., 1987. "Closure: Discussion: Flow Resistance Estimation in Mountain Rivers", Journal of the Hydraulics Division, ASCE, Vol. 113, No. 6.
10. Bray, D.I., 1979. "Estimating Average Velocity in Gravel-Bed Rivers", Journal of the Hydraulics Division, ASCE, Vol. 105, No. HY9.
11. Chow, V.T., 1959. "Open Channel Hydraulics", McGraw-Hill, New York.
12. Chow, V.T., 1979. "An Introduction to Computational Fluid Mechanics", John Wiley and Sons, New York.
13. Featherstone, R.E., Nalluri, C., 1995. "Civil Engineering Hydraulics", Third Edition, Blackwell Science Ltd., Osney Mead, Oxford OX2 0EL.
14. Ferro, V., Giordano, G., 1991. "Experimental Study of Flow Resistance in Gravel-Bed Rivers", Journal of the Hydraulics Division, ASCE, Vol. 117, No. 10.
15. Ferro, V., Baiamonte, G., 1994. "Flow Velocity Profiles in Gravel-Bed Rivers", Journal of the Hydraulics Division, ASCE, Vol. 120, No. 1.

16. Ferro, V., 1999. "Friction Factor for Gravel-Bed Channel with High Boulder Concentration", *Journal of the Hydraulics Division, ASCE*, Vol. 125, No. 7.
17. Graf, W.H., 1987, "Discussion: Flow Resistance Estimation in Mountain Rivers", *Journal of the Hydraulics Division, ASCE*, Vol. 113, No. 6.
18. Griffiths, G.A., 1981. "Flow Resistance in Coarse Gravel Bed Rivers", *Journal of the Hydraulics Division, ASCE*, Vol. 107, No. HY7.
19. Hey, R.D., 1979. "Flow Resistance in Gravel-Bed Rivers", *Journal of the Hydraulics Division, ASCE*, Vol. 105, No. HY4.
20. Hey, R.D., Thorne, C.R., 1983. "Accuracy of Surface Samples from Gravel Bed Material", *Journal of the Hydraulics Division, ASCE*, Vol. 109, No. 6.
21. Jarrett, R.D., 1984. "Hydraulics of High-Gradient Streams", *Journal of the Hydraulics Division, ASCE*, Vol. 110, No. 11.
22. Kennedy, J.F., 1983. "Reflections on Rivers, Research, and Rouse", *Journal of the Hydraulics Division, ASCE*, Vol. 109, No. 10.
23. King, L.C., 1942. "South African Scenery: A Textbook of Geomorphology", Oliver and Boyd Ltd, London.
24. Le Grange, A., Rooseboom, A., 2000. "The hydraulic resistance of sand streambeds under steady flow conditions", *Journal of Hydraulic Research, IAHR*, Vol. 38, No. 1.
25. Lopez, J.L., Falcon, M.A., 1999. "Calculation of Bed Changes in Mountain Streams", *Journal of the Hydraulics Division, ASCE*, Vol. 125, No. 3.
26. Massey, B.S., 1989. "Mechanics of Fluids", Van Nostrand Reinhold, London.
27. Myers, W.R.C., 1991. "Influence of Geometry on Discharge Capacity of Open Channels", *Journal of the Hydraulics Division, ASCE*, Vol. 117, No. 5.
28. Miller, B.A., Wenzel, H.G., 1985. "Analysis and Simulation of Low Flow Hydraulics", *Journal of the Hydraulics Division, ASCE*, Vol. 111, No. 12.
29. National Water Act, 1998. Department of Water Affairs and Forestry, RSA.
30. Rennie, C.D., Millar, R.G., 1999. "Discussion: Estimation of Gravel-Bed River Flow Resistance", *Journal of the Hydraulics Division, ASCE*, Vol. 125, No. 12.
31. Rooseboom, A., 1992. "Sediment Transport in Rivers and Reservoirs – A South African Perspective", WRC Report No. 297/1/92, Water Research Commission, RSA.

32. Rooseboom, A. et al., 1997. "National Transport Commission Road Drainage Manual", Department of Transport, RSA.
33. Rooseboom, A. et al, 2001. Classnotes: Advanced Hydraulics Course, Department of Civil Engineering, University of Stellenbosch, RSA.
34. Rosso, M., Schiara, M., Berlamont, J., 1990. "Flow Stability and Friction Factor in Rough Channels", Journal of the Hydraulics Division, ASCE, Vol. 116, No. 9.
35. Rouse, H., 1938. "Fluid Mechanics for Hydraulic Engineers", Dover Publications, New York.
36. Rouse, H., 1965. "Critical Analysis of Open-Channel Resistance", Journal of the Hydraulics Division, ASCE, Vol. 91, No. HY4.
37. Simons, D.B., Al-Shaikh-Ali, K.S., Li, R., 1979. "Flow Resistance in Cobble and Boulder Riverbeds", Journal of the Hydraulics Division, ASCE, Vol. 105, No. HY5.
38. Simons, D.B., Senturk, F., 1992. "Sediment Transport Technology", Water Resources Publications, Colorado.
39. Smart, F., 1999. "Turbulent Velocity Profiles and Boundary Shear in Gravel Bed Rivers", Journal of the Hydraulics Division, ASCE, Vol. 125, No. 2.
40. Theron, J.N., Gresse, P.G., Siegfried, H.P., Rogers, J., 1992. "The Geology Of The Cape Town Area", Department of Mineral and Energy Affairs, RSA.
41. Thorne, C.R., Zevenbergen, L.W., 1985. "Estimating Mean Velocity in Mountain Rivers", Journal of the Hydraulics Division, ASCE, Vol. 111, No. 4.

Appendix

1. Low flow Western Cape mountain stream field data

1.1. Cross-sectional measurements

River: Elandspad

Cathment: Breede

Weir: H1H033

Area no. Description: Interval:	No.	1 run 0.5 m		2 run 0.5 m		3 run 0.5 m	
		Bottom	Water	Bottom	Water	Bottom	Water
1(a) 11/04/2000	1	0.430	0.000	1.090	0.000	0.799	0.000
	2	1.885	1.702	1.759	1.562	1.526	1.415
	3	1.860	1.709	1.554	0.000	1.556	1.415
	4	1.885	1.705	1.720	1.555	1.501	1.410
	5	1.912	1.710	1.511	0.000	1.581	1.410
	6	1.947	1.721	1.550	0.000	1.389	0.000
	7	1.839	1.720	1.724	1.566	1.941	1.418
	8	1.924	1.729	1.918	1.570	1.715	1.421
	9	1.696	0.000	1.773	1.575	1.709	1.438
	10	2.005	1.722	1.684	1.569	1.709	1.439
	11	1.940	1.718	1.669	1.570	1.278	0.000
	12	1.600	0.000	1.735	1.585	1.489	1.410
	13	1.723	0.000	1.395	0.000	1.305	0.000
	14	1.949	1.725	2.150	1.585	1.635	1.401
	15	2.119	1.712	1.790	1.591	1.615	1.400
	16	1.711	0.000	1.740	1.596	1.420	1.400
	17	1.648	0.000	1.769	1.600	1.481	1.400
	18	1.926	1.779	1.459	0.000	1.589	1.405
	19	1.640	0.000	1.729	1.595	1.540	1.400
	20	1.787	0.000	1.811	1.603	1.260	0.000
	21	1.995	1.821	1.712	1.600	1.359	0.000
	22	1.853	1.829	1.551	0.000	1.299	0.000
	23	1.999	1.835	1.415	0.000	1.141	0.000
	24	1.850	1.815	1.199	0.000	0.948	0.000
	25	1.791	0.000	1.410	0.000	1.449	0.000
	26	1.711	0.000	1.325	0.000	0.713	0.000
	27	1.840	1.825	1.471	0.000	0.871	0.000
	28	1.805	0.000	1.330	0.000	0.875	0.000
	29	1.916	1.843	1.400	0.000		
	30	1.978	1.835	1.029	0.000		
	31	1.920	1.841				
	32	1.881	1.830				

1(a)		33	1.431	0.000				
		34	1.181	0.000				
1(b)	06/10/2000	1	0.612	0.000	1.014	0.000	1.022	0.000
		2	1.579	0.954	1.584	1.192	1.691	1.385
		3	1.613	0.953	1.377	1.185	1.658	1.382
		4	1.563	0.955	1.555	1.183	1.629	1.385
		5	1.467	0.945	1.342	1.195	1.685	1.381
		6	1.142	0.958	1.551	1.199	1.635	1.379
		7	1.676	0.960	1.526	1.198	1.526	1.381
		8	1.477	0.958	1.706	1.195	1.624	1.378
		9	1.279	0.960	1.600	1.193	1.684	1.379
		10	1.263	0.962	1.404	1.196	1.777	1.384
		11	1.648	0.947	1.466	1.198	1.587	1.386
		12	0.968	0.000	1.813	1.202	1.512	1.391
		13	0.940	0.000	1.827	1.198	1.533	1.426
		14	1.525	0.947	1.735	1.193	1.922	1.425
		15	1.546	0.948	1.589	1.194	1.983	1.419
		16	1.405	0.952	1.625	1.202	1.520	1.406
		17	1.322	0.963	1.475	1.199	1.674	1.412
		18	1.427	0.948	1.213	0.000	1.431	0.000
		19	1.269	0.952	1.724	1.197	1.418	0.000
		20	0.941	0.000	1.571	1.202	1.821	1.475
		21	1.148	0.961	1.464	1.199	1.816	1.457
		22	1.014	0.953	1.300	1.195	1.752	1.453
		23	0.968	0.000	1.342	1.195	1.766	1.445
		24	0.638	0.000	1.020	0.000	1.602	1.459
		25			1.100	0.000	1.850	1.456
		26			1.104	0.000	1.749	1.464
		27			1.317	1.185	1.805	1.462
		28			1.261	1.177	1.796	1.461
		29			0.845	0.000	1.744	1.464
		30					1.806	1.467
		31					1.588	1.462
		32					1.805	1.471
		33					1.675	1.456
		34					1.181	0.000
1(c)	03/11/2000	1	0.654	0.000	1.308	0.000	1.225	0.000
		2	1.744	1.210	1.679	1.404	1.803	1.580
		3	1.620	1.220	1.619	1.412	1.769	1.585
		4	1.659	1.221	1.590	1.411	1.779	1.586
		5	1.558	1.219	1.471	1.426	1.839	1.588
		6	1.249	0.000	1.696	1.436	1.846	1.585
		7	1.844	1.232	1.726	1.435	1.586	0.000
		8	1.625	1.230	1.754	1.436	1.814	1.585
		9	1.827	1.225	1.785	1.438	1.800	1.591
		10	1.365	1.227	1.703	1.434	1.798	1.586
		11	1.466	1.216	1.689	1.438	1.925	1.585

1(c)		12	1.604	1.225	1.916	1.436	1.631	1.614
		13	1.055	0.000	1.849	1.436	1.705	1.614
		14	1.520	1.221	1.824	1.435	1.881	1.615
		15	1.667	1.222	1.655	1.434	1.985	1.611
		16	1.620	1.220	1.703	1.433	1.814	1.609
		17	1.521	1.220	1.643	1.432	1.856	1.605
		18	1.336	1.221	1.409	0.000	1.545	0.000
		19	1.514	1.217	1.803	1.434	1.827	1.687
		20	1.394	1.225	1.787	1.434	2.001	1.676
		21	1.124	0.000	1.631	1.434	1.955	1.677
		22			1.584	1.433	1.991	1.684
		23			1.121	0.000	1.891	1.682
		24					1.861	1.683
		25					1.964	1.690
		26					1.974	1.691
		27					1.895	1.695
		28					1.933	1.695
		29					1.900	1.692
		30					1.864	1.689
		31					1.902	1.690
	32					1.703	0.000	
1(d)	29/11/2001	1	0.639	0.000	1.331	0.000	1.268	0.000
		2	1.554	1.255	1.504	1.441	1.811	1.614
		3	1.494	1.256	1.420	0.000	1.761	1.613
		4	1.510	1.263	1.514	1.451	1.736	1.614
		5	1.537	1.256	1.636	1.467	1.845	1.615
		6	1.244	0.000	1.475	0.000	1.814	1.616
		7	1.774	1.264	1.618	1.467	1.614	0.000
		8	1.614	1.260	1.854	1.468	1.819	1.612
		9	1.672	1.262	1.714	1.466	1.691	1.615
		10	1.859	1.263	1.670	1.467	1.901	1.614
		11	1.740	1.261	1.763	1.465	1.895	1.615
		12	1.835	1.257	1.881	1.466	1.706	1.629
		13	1.412	1.257	1.931	1.467	1.660	0.000
		14	1.506	1.256	1.876	1.465	1.845	1.634
		15	1.713	1.255	1.693	1.464	1.960	1.638
		16	1.541	1.260	1.728	1.467	1.641	0.000
		17	1.540	1.258	1.662	1.465	1.845	1.633
		18	1.265	0.000	1.331	0.000	1.595	0.000
		19	1.379	1.259	1.695	1.464	1.755	1.711
		20	1.391	1.260	1.696	1.467	2.029	1.705
		21	1.090	0.000	1.639	1.468	1.951	1.700
		22			1.617	1.464	1.945	1.708
		23			1.561	1.467	1.911	1.709
		24			1.120	0.000	1.724	0.000
		25					1.961	1.720
		26					1.920	1.723

1(d)	27					1.861	1.725	
	28					1.931	1.730	
	29					1.959	1.723	
	30					1.860	1.718	
	31					1.876	1.718	
	32					1.700	0.000	
	33					1.721	1.694	
	34					1.314	0.000	
1(e)	24/01/2001	1	0.800	0.000	1.260	0.000	1.065	0.000
		2	1.222	0.000	1.434	0.000	1.745	1.595
		3	1.245	0.000	1.575	1.437	1.718	1.590
		4	1.032	0.000	1.571	1.440	1.657	1.600
		5	1.415	1.250	1.513	1.455	1.732	1.590
		6	1.143	0.000	1.395	0.000	1.660	1.595
		7	1.630	1.265	1.577	1.445	1.525	0.000
		8	1.697	1.275	1.777	1.455	1.603	0.000
		9	1.843	1.275	1.642	1.445	1.730	1.575
		10	1.475	1.270	1.745	1.445	1.763	1.605
		11	1.528	1.265	1.695	1.445	1.605	1.570
		12	1.135	0.000	1.808	1.455	1.350	0.000
		13	1.161	0.000	1.864	1.445	1.300	0.000
		14	1.240	0.000	1.805	1.450	1.780	1.605
		15	1.463	1.275	1.770	1.445	2.000	1.620
		16	1.290	1.265	1.640	1.445	1.648	1.590
		17	1.226	0.000	1.530	1.450	1.625	1.580
		18	1.426	1.250	1.258	0.000	1.653	1.605
		19	1.395	1.255	1.328	0.000	1.445	0.000
		20	1.122	0.000	1.647	1.450	1.605	0.000
		21			1.568	1.445	1.870	1.670
		22			1.540	1.445	1.645	0.000
		23			1.462	1.435	1.890	1.680
		24			1.052	0.000	1.777	1.680
		25					1.775	1.685
		26					1.885	1.690
		27					1.901	1.710
		28					1.660	0.000
		29					1.862	1.700
		30					1.763	1.705
		31					1.670	0.000
		32					1.755	1.675
		33					1.134	0.000
1(f)	31/01/2001	1	0.500	0.000	0.905	0.000	0.990	0.000
		2	1.310	1.180	1.408	1.330	1.707	1.520
		3	1.354	1.190	1.373	1.345	1.670	1.520
		4	1.360	1.175	1.470	1.335	1.630	1.515
		5	1.493	1.180	1.342	0.000	1.620	1.510
		6	1.105	0.000	1.582	1.375	1.640	1.523

1(f)		7	1.740	1.195	1.690	1.375	1.722	1.520	
		8	1.464	1.190	1.570	1.375	1.645	1.515	
		9	1.560	1.195	1.524	1.375	1.675	1.510	
		10	1.728	1.200	1.482	1.375	1.560	1.510	
		11	1.610	1.185	1.463	1.380	1.665	1.523	
		12	1.475	1.190	1.702	1.385	1.790	1.515	
		13	1.348	1.190	1.692	1.380	1.445	0.000	
		14	1.380	1.185	1.710	1.380	1.435	0.000	
		15	1.250	1.175	1.527	1.370	1.715	1.535	
		16	1.260	1.190	1.515	1.385	1.838	1.545	
		17	1.163	0.000	1.423	1.380	1.638	1.545	
		18	1.442	1.185	1.452	1.380	1.718	1.530	
		19	0.910	0.000	1.303	0.000	1.415	0.000	
		20			1.543	1.390	1.690	1.615	
		21			1.512	1.390	1.890	1.605	
		22			1.205	0.000	1.680	1.610	
		23					1.820	1.630	
		24					1.775	1.625	
		25					1.610	0.000	
		26					1.843	1.645	
		27					1.838	1.640	
		28					1.770	1.630	
		29					1.795	1.640	
		30					1.853	1.635	
		31					1.615	0.000	
		32					1.725	1.635	
		33					1.555	0.000	
	1(g)	13/02/2001	1	0.730	0.000	1.194	0.000	1.300	0.000
			2	1.440	1.345	1.510	1.500	1.813	1.680
			3	1.422	1.345	1.582	1.520	1.766	1.670
			4	1.421	1.345	1.634	1.520	1.748	1.675
			5	1.250	0.000	1.662	1.540	1.815	1.670
			6	1.265	0.000	1.590	1.535	1.715	1.670
7			1.921	1.350	1.655	1.540	1.795	1.665	
8			1.656	1.365	1.895	1.540	1.510	0.000	
9			1.665	1.365	1.742	1.540	1.557	0.000	
10			1.860	1.367	1.535	0.000	1.840	1.674	
11			1.440	1.350	1.584	1.537	1.710	1.672	
12			1.595	1.350	1.948	1.535	1.696	1.678	
13			1.305	0.000	1.888	1.532	1.660	0.000	
14			1.490	1.350	1.846	1.535	1.975	1.690	
15			1.431	1.355	1.677	1.535	2.112	1.692	
16			1.634	1.345	1.608	1.537	1.703	1.695	
17			1.405	1.345	1.588	1.540	1.767	1.692	
18	1.297	0.000	1.370	0.000	1.635	0.000			
19	1.405	1.355	1.777	1.545	1.808	1.790			
20	1.060	0.000	1.787	1.540	1.945	1.780			

1(g)	21			1.622	1.545	1.973	1.780
	22			1.570	1.542	1.908	1.770
	23			1.180	0.000	1.895	1.790
	24					1.640	0.000
	25					1.875	1.783
	26					1.968	1.790
	27					1.867	1.785
	28					1.916	1.780
	29					1.865	1.782
	30					1.945	1.780
	31					1.750	0.000
	32					1.575	0.000

River: Jonkershoek
Cathment: Eerste
Weir: G2H037

Area no. Interval:	1 0.5 m		2 0.5 m		3 0.5 m		
	No.	Bottom	Water	Bottom	Water	Bottom	Water
2(a) 17/08/2000	1	0.953	0.000	1.307	0.000	1.730	0.000
	2	1.208	0.975	1.483	1.398	2.240	1.840
	3	1.213	0.980	1.483	1.360	2.277	1.835
	4	1.176	0.970	1.550	1.355	2.165	1.835
	5	1.141	0.965	1.558	1.357	2.270	1.835
	6	1.103	0.940	1.693	1.355	2.176	1.830
	7	1.163	0.940	1.602	1.360	2.136	1.835
	8	1.198	0.930	1.502	1.345	1.590	0.000
	9	1.116	0.935	1.552	1.352		
	10	1.126	0.925	1.482	1.355		
	11	1.168	0.930	1.384	1.345		
	12	1.042	0.930	1.438	1.345		
	13	1.030	0.935	1.023	0.000		
	14	1.040	0.945	1.085	0.000		
	15	1.038	0.955	1.508	1.340		
	16	0.900	0.000	1.717	1.355		
	17			1.530	1.350		
	18			1.300	0.000		
2(b) 28/09/2000	1	0.732	0.000	1.058	0.000	1.305	0.000
	2	1.201	0.830	1.500	1.202	1.656	0.000
	3	1.150	0.832	1.452	1.211	2.175	1.665
	4	1.196	0.833	1.515	1.206	2.234	1.659
	5	1.159	0.827	1.610	1.203	1.970	1.648
	6	1.125	0.828	1.628	1.217	2.218	1.625
	7	1.099	0.825	1.399	1.203	2.140	1.642
	8	1.148	0.810	1.563	1.204	1.660	1.645
	9	1.020	0.824	1.518	1.208	1.630	0.000

2(b)		10	1.071	0.818	1.494	1.212		
		11	1.004	0.844	1.404	1.205		
		12	1.093	0.828	1.435	1.203		
		13	0.908	0.848	1.042	0.000		
		14	1.002	0.836	0.989	0.000		
		15	1.048	0.854	1.683	1.205		
		16	0.616	0.000	1.558	1.188		
		17			1.108	0.000		
2(c)	07/10/2000	1	0.875	0.000	1.139	0.000	1.329	0.000
		2	1.301	0.957	1.580	1.330	1.814	0.000
		3	1.262	0.956	1.560	1.332	1.753	0.000
		4	1.261	0.955	1.555	1.334	2.247	1.794
		5	1.239	0.957	1.622	1.331	2.351	1.789
		6	1.132	0.949	1.685	1.329	2.144	1.805
		7	1.278	0.944	1.654	1.333	2.336	1.791
		8	1.286	0.940	1.720	1.336	2.220	1.790
		9	1.194	0.938	1.568	1.338	1.755	0.000
		10	1.151	0.954	1.586	1.339		
		11	1.146	0.946	1.465	1.328		
		12	1.127	0.953	1.545	1.331		
		13	0.944	0.000	1.054	0.000		
		14	1.227	0.973	1.124	0.000		
		15	0.779	0.000	1.319	0.000		
		16			1.613	1.320		
		17			1.171	0.000		
2(d)	18/10/2000	1	0.911	0.000	1.200	0.000	1.783	0.000
		2	1.322	1.071	1.589	1.438	2.304	1.949
		3	1.289	1.072	1.595	1.439	2.334	1.950
		4	1.315	1.075	1.676	1.439	2.090	1.945
		5	1.250	1.071	1.671	1.443	2.316	1.949
		6	1.250	1.068	1.710	1.441	2.310	1.945
		7	1.212	1.044	1.730	1.436	1.871	0.000
		8	1.260	1.048	1.605	1.437		
		9	1.231	1.049	1.421	0.000		
		10	1.181	1.046	1.612	1.443		
		11	1.176	1.048	1.461	1.433		
		12	1.164	1.049	1.536	1.440		
		13	0.969	0.000	1.124	0.000		
		14	1.141	1.094	1.111	0.000		
		15	0.790	0.000	1.789	1.450		
		16			1.638	1.443		
		17			1.231	0.000		
2(e)	24/10/2000	1	0.864	0.000	1.326	0.000	1.724	0.000
		2	1.273	1.012	1.525	1.374	2.252	1.886
		3	1.235	1.010	1.594	1.376	2.254	1.890
		4	1.247	1.013	1.587	1.377	2.054	1.891
		5	1.150	1.013	1.604	1.375	2.269	1.892

2(e)		6	1.139	0.995	1.631	1.379	2.200	1.893
		7	1.164	0.983	1.489	1.379	1.736	0.000
		8	1.248	0.985	1.508	1.383		
		9	1.168	0.985	1.465	1.381		
		10	1.074	0.986	1.425	1.378		
		11	1.127	0.991	1.528	1.375		
		12	1.143	0.990	1.036	0.000		
		13	0.916	0.000	1.092	0.000		
		14	1.167	1.031	1.384	0.000		
		15	0.715	0.000	1.683	1.382		
		16			1.561	1.375		
		17			1.146	0.000		
2(f)	27/10/2000	1	0.779	0.000	1.241	0.000	1.657	0.000
		2	1.194	0.996	1.434	1.339	2.210	1.864
		3	1.148	1.001	1.422	1.337	2.210	1.869
		4	1.175	1.001	1.651	1.336	2.127	1.865
		5	1.118	0.999	1.481	1.335	2.129	1.866
		6	1.071	0.984	1.550	1.335	1.757	0.000
		7	1.077	0.969	1.449	1.334		
		8	1.196	0.969	1.428	1.335		
		9	1.039	0.970	1.389	1.335		
		10	1.060	0.974	1.380	1.336		
		11	1.011	0.965	1.400	1.341		
		12	1.029	0.971	0.980	0.000		
		13	0.824	0.000	1.161	0.000		
		14	1.079	1.014	1.288	0.000		
		15	0.666	0.000	1.592	1.344		
		16			1.447	1.343		
		17			1.072	0.000		
2(g)	01/06/2001	1	1.065	0.000	1.355	0.000	1.952	0.000
		2	1.477	1.195	1.544	0.000	2.435	2.065
		3	1.472	1.190	1.778	1.570	2.535	2.065
		4	1.495	1.200	1.784	1.576	2.525	2.060
		5	1.366	1.205	1.803	1.570	2.395	2.055
		6	1.365	1.180	1.880	1.575	2.465	2.065
		7	1.506	1.160	1.800	1.570	1.960	0.000
		8	1.470	1.160	1.758	1.575		
		9	1.421	1.165	1.738	1.585		
		10	1.374	1.167	1.785	1.580		
		11	1.405	1.165	1.538	0.000		
		12	1.388	1.170	1.736	1.573		
		13	1.140	0.000	1.318	0.000		
		14	1.358	1.195	1.532	0.000		
		15	0.983	0.000	1.600	1.577		
		16			1.892	1.570		
		17			1.735	1.572		
		18			1.500	0.000		

River: Molenaars
Cathment: Breede
Weir: H1H018

Area no. Description: Interval:	1 run 0.5 m		2 run 0.5 m		3 run 0.5 m		
	No.	Bottom	Water	Bottom	Water	Bottom	Water
3(a) 28/02/2001	1	0.275	0.000	1.658	0.000	1.652	0.000
	2	1.020	0.930	1.820	1.775	2.330	2.040
	3	1.037	0.932	1.877	1.775	2.250	2.030
	4	1.204	0.938	1.817	1.775	2.040	0.000
	5	1.073	0.940	2.017	1.775	2.186	2.035
	6	0.617	0.000	1.733	0.000	2.628	2.040
	7	0.762	0.000	2.138	1.774	2.526	2.045
	8	1.540	1.045	2.145	1.785	2.643	2.030
	9	1.496	1.045	1.901	1.780	2.492	2.040
	10	1.406	1.055	1.842	1.774	2.234	2.035
	11	1.538	1.045	1.992	1.768	2.315	2.035
	12	1.510	1.055	1.890	1.772	2.252	2.032
	13	1.467	1.050	1.964	1.765	2.091	2.030
	14	1.181	1.045	2.021	1.772	2.042	0.000
	15	0.662	0.000	1.888	1.772	1.833	0.000
	16	0.948	0.000	1.735	0.000	1.956	0.000
	17	1.220	1.050	1.915	1.765	2.155	2.037
	18	0.390	0.000	1.792	1.740	2.270	2.035
	19			1.813	1.735	2.350	2.030
	20			1.722	0.000	1.928	0.000
3(b) 07/03/2001	1	0.324	0.000	1.526	0.000	1.820	0.000
	2	0.770	0.000	1.743	1.710	2.036	1.940
	3	0.786	0.000	1.615	0.000	2.137	1.955
	4	0.705	0.000	1.620	0.000	1.930	0.000
	5	0.890	0.810	1.902	1.685	2.532	1.935
	6	0.240	0.000	1.732	1.682	2.427	1.925
	7	0.166	0.000	2.084	1.675	2.536	1.925
	8	0.876	0.824	2.126	1.675	2.268	1.940
	9	0.943	0.835	1.859	1.673	2.367	1.940
	10	0.985	0.835	1.975	1.677	2.180	1.937
	11	0.940	0.835	1.930	1.670	2.090	1.935
	12	0.550	0.000	1.862	1.680	2.097	1.940
	13	0.550	0.000	1.848	1.670	2.002	1.940
	14	0.860	0.000	1.931	1.665	1.962	1.925
	15	1.370	0.940	1.868	1.665	2.031	1.935
	16	1.262	0.943	1.895	1.675	1.970	1.930
	17	1.397	0.950	1.660	0.000	2.178	1.940
	18	1.390	0.955	1.772	1.645	2.070	1.940

3(b)		19	1.302	0.950	1.603	0.000	2.149	1.935
		20	1.333	0.953	1.728	1.633	2.155	1.935
		21	0.620	0.000	1.450	0.000	1.655	0.000
		22	0.653	0.000	1.703	1.565		
		23	1.245	0.965	1.168	0.000		
		24	0.490	0.000				
3(c)	14/03/2001	1	0.772	0.000	1.510	0.000	1.760	0.000
		2	0.925	0.845	1.695	0.000	2.140	1.970
		3	0.893	0.845	1.583	0.000	2.080	1.974
		4	0.950	0.850	1.681	0.000	2.170	1.975
		5	1.020	0.850	1.975	1.715	2.145	1.970
		6	0.580	0.000	2.032	1.720	2.470	1.965
		7	0.802	0.000	1.994	1.705	2.492	1.970
		8	1.507	0.965	2.117	1.705	2.440	1.975
		9	1.465	0.955	1.982	1.705	2.420	1.970
		10	1.255	0.965	1.993	1.703	1.939	0.000
		11	1.318	0.965	1.945	1.705	2.185	1.960
		12	1.370	0.965	1.953	1.705	1.980	1.960
		13	1.485	0.955	1.800	1.710	1.735	0.000
		14	1.085	0.960	1.825	1.695	2.230	1.960
		15	0.608	0.000	1.937	1.705	1.875	0.000
		16	0.900	0.000	1.936	1.705	1.940	0.000
		17	1.117	0.950	1.600	0.000	2.038	1.970
		18	0.240	0.000	1.837	1.665	2.160	1.960
		19			1.723	1.670	2.275	1.970
		20			1.603	0.000	1.780	0.000
		21			1.715	1.670		
		22			1.308	0.000		
3(d)	12/06/2001	1	0.245	0.000	1.460	0.000	1.552	0.000
		2	0.723	0.670	1.620	1.570	2.190	1.815
		3	0.923	0.670	1.735	1.580	2.220	1.835
		4	1.016	0.685	1.812	1.580	2.194	1.835
		5	0.451	0.000	1.652	1.570	2.333	1.830
		6	0.450	0.000	1.860	1.585	2.810	1.870
		7	1.020	0.725	2.140	1.580	2.705	1.810
		8	0.915	0.720	2.027	1.575	2.780	1.810
		9	0.930	0.725	1.920	1.570	2.700	1.820
		10	0.696	0.000	2.300	1.575	2.180	1.825
		11	1.047	0.825	2.242	1.545	2.183	1.825
		12	0.715	0.000	2.073	1.550	2.230	1.830
		13	1.445	0.840	1.945	1.570	1.750	0.000
		14	1.465	0.830	2.100	1.570	2.265	1.830
		15	1.455	0.830	1.820	1.575	2.420	1.820
		16	1.606	0.800	2.083	1.565	1.973	1.825
		17	1.616	0.805	2.058	1.575	2.180	1.820
		18	1.610	0.815	2.015	1.560	2.395	1.815
		19	1.550	0.815	1.850	1.560	2.455	1.825

3(d)	20	1.140	0.835	1.885	1.550	2.090	1.820
	21	0.556	0.000	1.960	1.545	1.910	1.810
	22	1.135	0.785	1.742	1.555	1.860	1.800
	23	1.468	0.780	1.913	1.545	1.760	0.000
	24	0.440	0.000	1.630	1.540	1.705	0.000
	25			1.744	1.540	1.755	0.000
	26			1.390	0.000	2.010	1.825
	27					1.895	1.810
	28					1.970	1.820
	29					1.600	0.000

River: Upper Berg
Cathment: Berg
Weir: G1H004

Area no. Interval:	No.	1 0.5 m		2 0.5 m		3 0.5 m	
		Bottom	Water	Bottom	Water	Bottom	Water
4(a) 26/01/2001	1	0.650	0.000	0.750	0.000	0.565	0.000
	2	0.945	0.780	1.067	0.805	1.343	0.845
	3	1.080	0.780	1.128	0.804	1.306	0.840
	4	1.170	0.785	1.292	0.810	1.315	0.845
	5	1.060	0.785	1.168	0.804	1.295	0.845
	6	1.053	0.785	1.162	0.805	1.252	0.845
	7	1.340	0.785	1.150	0.795	1.076	0.845
	8	1.500	0.790	1.157	0.805	1.227	0.843
	9	1.535	0.780	1.251	0.804	1.223	0.847
	10	1.455	0.780	1.198	0.805	1.141	0.842
	11	1.360	0.780	1.196	0.800	1.300	0.840
	12	1.390	0.790	1.247	0.800	1.229	0.847
	13	1.078	0.780	1.346	0.800	1.303	0.850
	14	1.425	0.780	1.340	0.803	1.198	0.842
	15	1.460	0.780	1.390	0.806	1.012	0.848
	16	1.375	0.795	1.527	0.802	1.094	0.850
	17	1.453	0.790	1.315	0.801	1.022	0.855
	18	1.380	0.775	1.510	0.802	1.067	0.852
	19	1.315	0.795	1.309	0.795	1.253	0.840
	20	1.165	0.780	1.537	0.795	1.232	0.845
	21	0.700	0.000	1.488	0.800	1.203	0.845
	22			1.400	0.800	1.195	0.845
	23			1.452	0.800	1.168	0.841
	24			1.330	0.795	1.025	0.845
	25			1.184	0.795	1.078	0.845
	26			1.080	0.795	1.067	0.860
	27			1.087	0.795	0.997	0.842
	28			0.936	0.798	0.920	0.840
	29			0.690	0.000	0.995	0.840

4(a)		30					0.920	0.845
		31					0.930	0.830
		32					0.900	0.830
		33					0.803	0.000
4(b)	16/02/2001	1	0.630	0.000	0.700	0.000	0.710	0.000
		2	0.750	0.710	1.206	0.725	1.183	0.780
		3	0.978	0.705	1.140	0.735	1.301	0.780
		4	1.163	0.705	1.118	0.730	1.246	0.785
		5	1.215	0.710	1.046	0.730	1.025	0.780
		6	1.185	0.705	1.117	0.740	1.212	0.785
		7	1.305	0.710	1.103	0.730	1.002	0.780
		8	1.450	0.710	1.113	0.730	1.137	0.785
		9	1.423	0.705	1.163	0.735	1.167	0.780
		10	1.320	0.700	1.234	0.730	1.155	0.785
		11	1.237	0.708	1.237	0.725	1.153	0.790
		12	1.367	0.714	1.261	0.735	1.083	0.790
		13	1.410	0.715	1.204	0.740	1.013	0.790
		14	1.394	0.720	1.398	0.730	0.878	0.800
		15	1.340	0.716	1.373	0.732	1.045	0.805
		16	1.350	0.720	1.369	0.735	0.866	0.795
		17	1.380	0.715	1.078	0.730	0.980	0.795
		18	1.137	0.705	1.291	0.730	1.190	0.800
		19	1.280	0.708	1.459	0.730	1.184	0.790
		20	1.110	0.710	1.452	0.735	1.018	0.780
		21	0.635	0.000	1.294	0.725	1.074	0.795
		22			1.368	0.730	0.998	0.795
		23			1.097	0.730	0.984	0.795
		24			1.080	0.730	1.056	0.790
		25			1.043	0.732	1.020	0.790
		26			0.900	0.728	1.002	0.785
		27			0.672	0.000	0.860	0.785
		28					0.750	0.000
4(c)	27/02/2001	1	0.820	0.000	0.790	0.000	0.820	0.000
		2	0.860	0.820	1.110	0.835	1.370	0.900
		3	1.140	0.825	1.278	0.840	1.370	0.890
		4	1.240	0.810	1.218	0.840	1.335	0.900
		5	1.305	0.805	1.226	0.845	1.235	0.890
		6	1.302	0.815	1.188	0.840	1.256	0.890
		7	1.315	0.810	1.178	0.840	1.246	0.895
		8	1.486	0.805	1.194	0.840	1.205	0.890
		9	1.542	0.815	1.250	0.840	1.273	0.885
		10	1.427	0.805	1.328	0.842	1.312	0.895
		11	1.490	0.810	1.362	0.840	1.214	0.885
		12	1.425	0.820	1.422	0.842	1.225	0.885
		13	1.480	0.810	1.322	0.840	1.100	0.895
		14	1.490	0.815	1.464	0.840	1.157	0.896
		15	1.423	0.815	1.452	0.845	1.146	0.895

4(c)		16	1.430	0.816	1.551	0.838	1.068	0.890
		17	1.455	0.817	1.393	0.841	1.072	0.895
		18	1.237	0.810	1.151	0.835	1.120	0.900
		19	1.345	0.820	1.623	0.835	1.208	0.890
		20	1.185	0.815	1.566	0.837	1.223	0.890
		21	0.730	0.000	1.442	0.835	1.126	0.890
		22			1.478	0.835	1.205	0.892
		23			1.412	0.830	1.088	0.890
		24			1.161	0.834	0.983	0.885
		25			1.132	0.825	1.105	0.895
		26			1.063	0.835	1.115	0.890
		27			0.773	0.000	0.915	0.885
		28					1.025	0.890
	29					0.715	0.000	
4(d)	01/06/2001	1	0.965	0.000	0.960	0.000	0.930	0.000
		2	1.060	0.950	1.265	0.980	1.480	1.035
		3	1.372	0.955	1.268	0.980	1.470	1.030
		4	1.455	0.955	1.310	0.980	1.533	1.025
		5	1.450	0.960	1.278	0.985	1.432	1.025
		6	1.510	0.953	1.277	0.975	1.405	1.020
		7	1.485	0.955	1.256	0.980	1.427	1.030
		8	1.482	0.952	1.300	0.980	1.295	1.030
		9	1.480	0.950	1.374	0.981	1.400	1.025
		10	1.385	0.953	1.299	0.980	1.376	1.025
		11	1.275	0.955	1.437	0.980	1.350	1.020
		12	1.555	0.950	1.446	0.984	1.350	1.020
		13	1.515	0.956	1.478	0.980	1.340	1.020
		14	1.527	0.960	1.462	0.985	1.312	1.035
		15	1.470	0.955	1.580	0.982	1.311	1.040
		16	1.580	0.953	1.506	0.975	1.322	1.040
		17	1.510	0.960	1.763	0.978	1.203	1.040
		18	1.200	0.955	1.713	0.978	1.152	1.030
		19	1.290	0.960	1.620	0.977	1.364	1.023
		20	1.300	0.955	1.706	0.980	1.366	1.025
		21	0.700	0.000	1.653	0.980	1.308	1.025
		22			1.643	0.978	1.257	1.025
		23			1.462	0.980	1.240	1.030
		24			1.542	0.980	1.216	1.035
		25			1.274	0.976	1.172	1.026
		26			1.170	0.975	1.245	1.035
		27			1.202	0.980	1.132	1.023
		28			1.115	0.970	0.985	0.000
		29			0.955	0.000		

1.2. Longitudinal profile measurements

River: Elandspad
Cathment: Breede
Weir: H1H033
Date: 11/04/2000
Sample : 1(a)

No.	Bottom		Water
	Middle	Top	Middle
	Average		Average
1	1.549	1.721	1.376
2(1)	1.584	1.685	1.407
3	1.744	1.790	1.470
4	1.827	1.850	1.494
5(2)	1.791	1.810	1.591
6	1.811	1.851	1.605
7	1.952	2.025	1.630
8(3)	2.041	2.161	1.720
9	2.305	2.495	2.108
Weirflowheigth 0.05 m			
Weirflow 0.1901 m³/s			

Date: 06/10/2000
Sample : 1(b)

No.	Bottom		Water
	Middle	Top	Middle
	Average		Average
1	1.218	1.331	0.930
2	1.259	1.364	0.958
3(1)	1.477	1.575	0.961
4	1.506	1.594	0.968
5	1.684	1.719	1.072
6	1.576	1.588	1.203
7(2)	1.843	1.861	1.202
8	1.696	1.727	1.203
9	1.815	1.877	1.248
10	1.835	1.944	1.418
11(3)	1.894	2.013	1.411
12	1.857	1.981	1.425
13	1.873	2.010	1.518
Weirflowheigth 0.17+ m			
Weirflow 1.1145 m³/s			

Date: 03/11/2000
Sample : 1(c)

No.	Bottom		Water
	Middle	Top	Middle
	Average		Average
1	1.747	1.890	1.195
2	1.625	1.741	1.198
3(1)	1.841	1.937	1.227
4	1.410	1.475	1.234
5	1.460	1.495	1.314
6	1.825	1.834	1.444
7(2)	1.847	1.868	1.433
8	1.603	1.642	1.464
9	1.810	1.876	1.484
10	2.044	2.138	1.635
11(3)	1.930	2.045	1.679
12	2.005	2.135	1.719
13	2.018	2.180	1.748
Weirflowheigth 0.09 m			
Weirflow 0.4327 m³/s			

Date: 29/11/2000
Sample : 1(d)

No.	Bottom		Water
	Middle	Top	Middle
	Average		Average
1	1.605	1.754	1.240
2	1.594	1.721	1.251
3(1)	1.745	1.841	1.267
4	1.646	1.726	1.278
5	1.503	1.542	1.339
6	1.781	1.791	1.464
7(2)	1.910	1.931	1.461
8	1.830	1.863	1.465
9	1.736	1.812	1.548
10	1.879	1.978	1.680
11(3)	1.895	2.010	1.715
12	2.085	2.205	1.743
13	2.049	2.199	1.768
Weirflowheigth 0.08 m			
Weirflow 0.3652 m³/s			

Date: 24/01/2001

Sample : 1(e)

No.	Bottom		Water
	Middle	Top	Middle
	Average		Average
1	1.615	1.755	1.245
2	1.738	1.862	1.250
3(1)	1.587	1.678	1.270
4	2.068	2.150	1.275
5	1.636	1.672	1.330
6	1.802	1.813	1.455
7(2)	1.831	1.853	1.460
8	1.863	1.897	1.465
9	1.823	1.878	1.495
10	1.919	2.022	1.605
11(3)	2.005	2.124	1.720
12	2.050	2.183	1.715
13	1.968	2.128	1.750
Weirflowheigth		0.06	m
Weirflow		0.2437	m³/s

Date: 31/01/2001

Sample : 1(f)

No.	Bottom		Water
	Middle	Top	Middle
	Average		Average
1	1.463	1.616	1.170
2	1.632	1.765	1.170
3(1)	1.609	1.706	1.192
4	1.714	1.795	1.203
5	1.767	1.819	1.336
6	1.679	1.688	1.385
7(2)	1.710	1.725	1.390
8	1.678	1.707	1.392
9	1.925	1.985	1.430
10	1.799	1.895	1.570
11(3)	1.800	1.910	1.605
12	1.885	2.020	1.670
13	2.038	2.195	1.675
Weirflowheigth		0.058	m
Weirflow		0.23298	m³/s

Date: 13/02/2001

Sample : 1(g)

No.	Bottom		Water
	Middle	Top	Middle
	Average		Average
1	1.826	1.985	1.340
2	1.822	1.949	1.342
3(1)	1.692	1.790	1.365
4	2.077	2.147	1.370
5	1.773	1.811	1.415
6	1.884	1.894	1.545
7(2)	1.833	1.848	1.545
8	1.791	1.836	1.570
9	2.008	2.078	1.590
10	1.958	2.066	1.690
11(3)	2.130	2.250	1.690
12	2.065	2.189	1.810
13	2.140	2.292	1.840
Weirflowheigth		0.05	m
Weirflow		0.1901	m³/s

River: Jonkershoek
Cathment: Eerste
Weir: G2H037

Date: 17/08/2000

Sample : 2(a)

No.	Bottom		Water
	Middle	Top	Middle
	Average		Average
1	1.195	1.255	0.830
2	1.167	1.200	0.900
3(1)	1.178	1.205	0.935
4	1.203	1.218	0.925
5	1.845	1.865	1.295
6	1.893	1.913	1.350
7(2)	1.605	1.638	1.360
8	1.590	1.628	1.405
9	1.708	1.762	1.590
10	1.935	2.012	1.780
11(3)	2.270	2.366	1.835
12	2.142	2.245	1.835
13	2.370	2.500	1.845
Weirflowheigth		0.066	m
Weirflow		0.202	m³/s

Date: 28/09/2000

Sample : 2(b)

No.	Bottom		Water
	Middle	Top	Middle
	Average		Average
1	1.112	1.150	0.778
2	1.109	1.139	0.812
3(1)	1.065	1.090	0.818
4	1.114	1.133	0.824
5	1.241	1.251	0.956
6	1.606	1.586	1.183
7(2)	1.645	1.671	1.203
8	1.519	1.548	1.218
9	1.794	1.855	1.458
10	2.133	2.221	1.645
11(3)	2.155	2.251	1.642
12	2.152	2.252	1.646
13	2.161	2.268	1.654
Weirflowheigth		0.15	m
Weirflow		0.6912	m³/s

Date: 07/10/2000

Sample : 2(c)

No.	Bottom		Water
	Middle	Top	Middle
	Average		Average
1	1.169	1.207	0.904
2	1.198	1.229	0.926
3(1)	1.157	1.180	0.953
4	1.161	1.179	0.946
5	1.539	1.547	1.264
6	1.516	1.534	1.334
7(2)	1.639	1.666	1.339
8	1.483	1.515	1.357
9	1.723	1.761	1.391
10	2.196	2.279	1.786
11(3)	2.266	2.360	1.801
12	2.255	2.364	1.792
13	2.250	2.368	1.785
Weirflowheigth		0.12	m
Weirflow		0.4945	m³/s

Date: 18/10/2000

Sample : 2(d)

No.	Bottom		Water
	Middle	Top	Middle
	Average		Average
1	1.261	1.300	1.014
2	1.216	1.249	1.056
3(1)	1.264	1.290	1.049
4	1.256	1.275	1.054
5	1.555	1.563	1.421
6	1.604	1.624	1.441
7(2)	1.679	1.705	1.443
8	1.600	1.633	1.467
9	1.822	1.876	1.702
10	2.210	2.295	1.945
11(3)	2.324	2.419	1.947
12	2.281	2.391	1.952
13	2.271	2.394	1.951
Weirflowheigth		0.06	m
Weirflow		0.1748	m³/s

Date: 24/10/2000

Sample : 2(e)

No.	Bottom		Water
	Middle	Top	Middle
	Average		Average
1	1.101	1.141	0.971
2	1.132	1.166	0.995
3(1)	1.224	1.250	1.005
4	1.210	1.229	1.007
5	1.689	1.697	1.370
6	2.026	2.047	1.402
7(2)	1.647	1.679	1.408
8	1.551	1.592	1.409
9	1.689	1.740	1.577
10	2.147	2.232	1.918
11(3)	2.314	2.411	1.911
12	2.264	2.368	1.910
13	2.335	2.460	1.909
Weirflowheigth		0.055	m
Weirflow		0.1539	m³/s

Date: 27/10/2000

Sample : 2(f)

No.	Bottom		Water
	Middle	Top	Middle
	Average		Average
1	1.034	1.071	0.867
2	1.128	1.164	0.899
3(1)	1.092	1.117	0.913
4	1.164	1.182	0.914
5	1.483	1.492	1.261
6	1.830	1.849	1.292
7(2)	1.452	1.481	1.293
8	1.495	1.534	1.290
9	1.591	1.632	1.376
10	2.046	2.131	1.862
11(3)	2.174	2.270	1.865
12	2.146	2.257	1.871
13	2.189	2.314	1.869
Weirflowheigth		0.03	m
Weirflow		0.0618	m³/s

Date: 01/06/2001

Sample : 2(g)

No.	Bottom		Water
	Middle	Top	Middle
	Average		Average
1	1.355	1.400	1.140
2	1.352	1.383	1.165
3(1)	1.457	1.485	1.165
4	1.402	1.421	1.163
5	1.927	1.936	1.515
6	2.237	2.258	1.580
7(2)	1.887	1.922	1.580
8	1.786	1.828	1.580
9	2.263	2.334	2.010
10	2.385	2.475	2.050
11(3)	2.549	2.646	2.065
12	2.443	2.550	2.065
13	2.538	2.660	2.070
Weirflowheigth		0.085	m
Weirflow		0.2951	m³/s

River: Molenaars
Cathment: Breede
Weir: H1H018

Date: 28/02/2001

Sample : 3(a)

No.	Bottom		Water
	Middle	Top	Middle
	Average		Average
1	1.238	1.376	0.805
2	1.127	1.214	1.015
3(1)	1.510	1.592	1.005
4	1.554	1.621	1.065
5	1.937	1.985	1.555
6	2.005	2.100	1.745
7(2)	2.131	2.243	1.775
8	2.220	2.344	1.785
9	2.703	2.871	2.020
10	2.850	3.069	2.015
11(3)	2.672	2.920	2.040
12	2.648	2.944	2.085
13	2.590	2.935	2.140
Gauge plate		0.078	m
Weir flow		0.40487	m³/s

Date: 07/03/2001

Sample : 3(b)

No.	Bottom		Water
	Middle	Top	Middle
	Average		Average
1	0.949	1.101	0.700
2	1.163	1.283	0.948
3(1)	1.255	1.360	0.950
4	1.382	1.475	0.960
5	1.423	1.454	1.100
6	2.116	2.184	1.655
7(2)	1.899	1.987	1.680
8	2.036	2.133	1.680
9	2.616	2.753	1.920
10	2.640	2.825	1.915
11(3)	2.520	2.740	1.935
12	2.492	2.754	1.980
13	2.543	2.842	2.043
Gauge plate		0.075	m
Weir flow		0.38264	m³/s

Date: 14/03/2001

Sample : 3(c)

No.	Bottom		Water
	Middle	Top	Middle
	Average		Average
1	1.050	1.215	0.720
2	1.320	1.437	0.960
3(1)	1.320	1.432	0.975
4	1.387	1.490	1.170
5	1.445	1.485	1.400
6	2.186	2.196	1.685
7(2)	2.008	2.093	1.715
8	2.359	2.452	1.710
9	2.593	2.718	1.950
10	2.603	2.785	1.955
11(3)	2.603	2.815	1.970
12	2.433	2.657	1.980
13	2.580	2.855	2.030
Gauge plate		0.072	m
Weir flow		0.36041	m³/s

Date: 12/06/2001

Sample : 3(d)

No.	Bottom		Water
	Middle	Top	Middle
	Average		Average
1	1.235	1.392	0.775
2	1.540	1.684	0.798
3(1)	1.575	1.710	0.810
4	1.350	1.475	0.835
5	1.700	1.770	1.040
6	2.145	2.194	1.580
7(2)	2.134	2.194	1.580
8	2.135	2.207	1.565
9	2.852	2.980	1.810
10	2.638	2.818	1.820
11(3)	2.840	3.027	1.825
12	2.624	2.820	1.830
13	2.583	2.792	1.835
Gauge plate		0.3	m
Weir flow		2.9530	m³/s

River: Upper Berg
Cathment: Berg
Weir: G1H004

Date: 26/01/2001

Sample : 4(a)

No.	Bottom		Water
	Middle	Top	Middle
	Average		Average
1	1.233	1.543	0.735
2	1.405	1.667	0.770
3(1)	1.501	1.717	0.775
4	1.560	1.726	0.775
5	1.727	1.835	0.780
6	1.776	1.820	0.790
7(2)	1.441	1.456	0.797
8	1.240	1.295	0.805
9	1.375	1.460	0.825
10	1.196	1.300	0.830
11(3)	1.280	1.401	0.855
12	1.161	1.330	0.925
13	1.294	1.503	0.980
Weirflowheigth		0.42	m
Weirflow		4.17	m³/s

Date: 16/02/2001

Sample : 4(b)

No.	Bottom		Water
	Middle	Top	Middle
	Average		Average
1	1.202	1.587	0.675
2	1.22	1.481	0.695
3(1)	1.47	1.684	0.710
4	1.386	1.557	0.726
5	1.625	1.722	0.720
6	1.7	1.726	0.730
7(2)	1.327	1.340	0.730
8	1.363	1.405	0.742
9	1.237	1.325	0.747
10	1.015	1.117	0.775
11(3)	1.18	1.295	0.795
12	1.087	1.235	0.850
13	1.161	1.354	0.890
Weirflowheigth		0.4	m
Weirflow		3.698	m³/s

Date: 27/02/2001

Sample : 4(c)

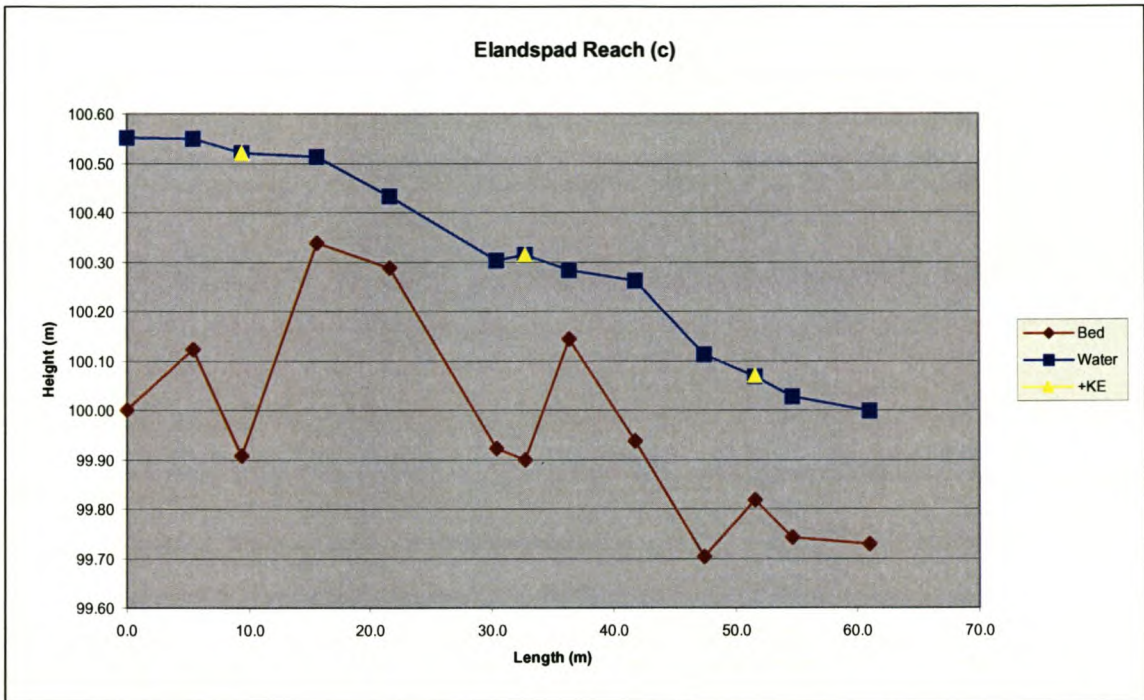
No.	Bottom		Water
	Middle	Top	Middle
	Average		Average
1	1.213	1.532	0.765
2	1.410	1.678	0.790
3(1)	1.590	1.805	0.815
4	1.450	1.612	0.825
5	1.773	1.865	0.830
6	1.723	1.748	0.833
7(2)	1.435	1.448	0.840
8	1.470	1.515	0.845
9	1.230	1.313	0.852
10	1.255	1.357	0.880
11(3)	1.240	1.354	0.890
12	1.307	1.454	0.925
13	1.300	1.480	0.980
Weirflowheigth		0.395	m
Weirflow		3.5875	m³/s

Date: 01/06/2001

Sample : 4(d)

No.	Bottom		Water
	Middle	Top	Middle
	Average		Average
1	1.607	1.870	0.940
2	1.588	1.835	0.955
3(1)	1.543	1.773	0.955
4	1.535	1.750	0.960
5	1.735	1.910	0.970
6	1.838	1.862	0.975
7(2)	1.484	1.504	0.980
8	1.482	1.528	0.990
9	1.499	1.581	1.000
10	1.411	1.522	1.015
11(3)	1.360	1.483	1.025
12	1.355	1.490	1.038
13	1.408	1.568	1.095
Weirflowheigth		0.380	m
Weirflow		3.262	m³/s

Typical example of longitudinal profile, showing the minor influence of kinetic energy at the three sections in comparison to flow depth:

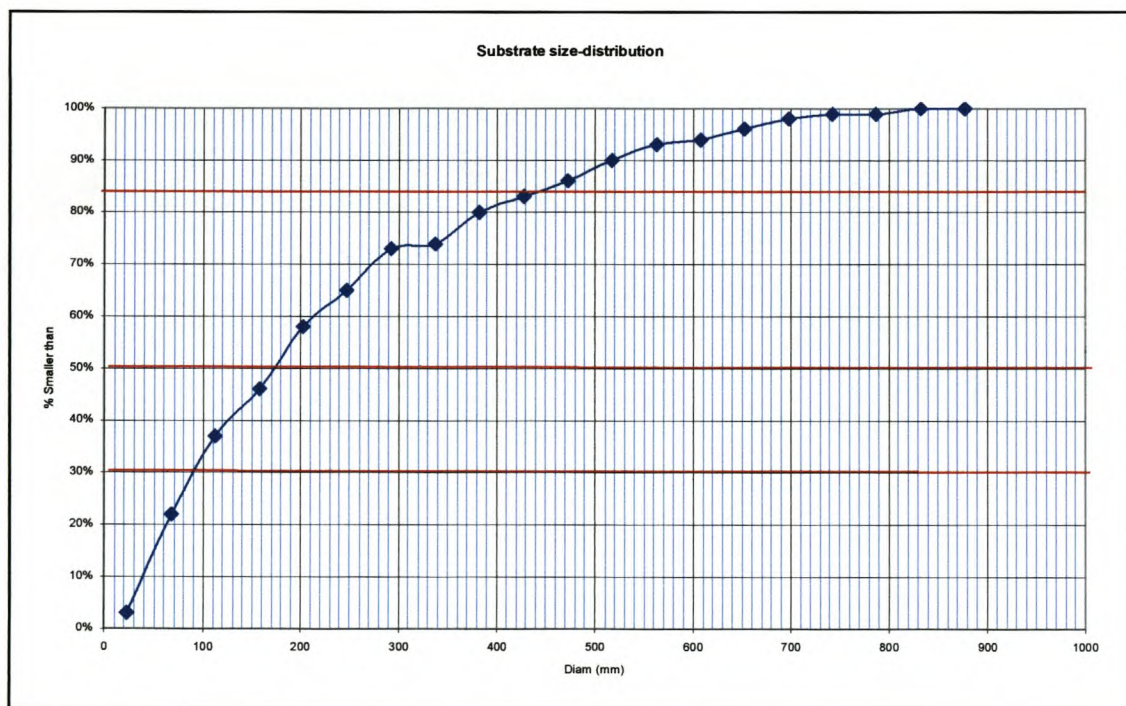


1.3. Sampled particle sizes

WOLMAN SAMPLE: Elandspad River

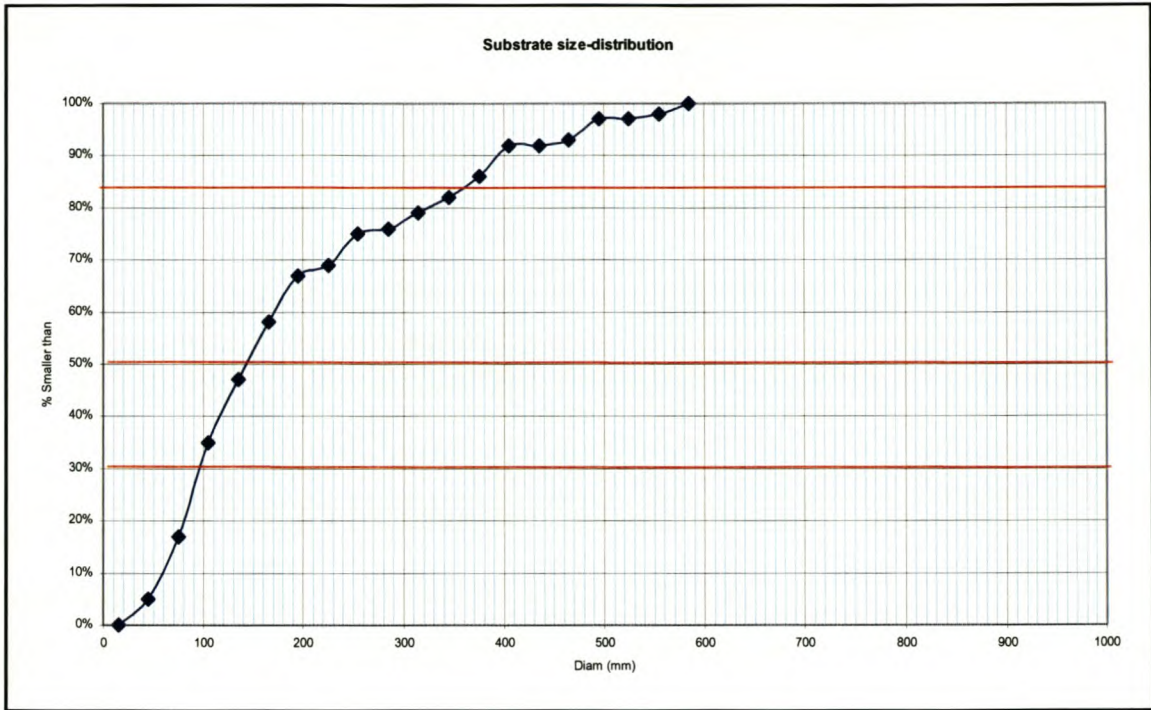
No.	Diameter (mm)	No.	Diameter (mm)	No.	Diameter (mm)
1	70	39	240	77	420
2	300	40	60	78	130
3	380	41	240	79	70
4	120	42	110	80	50
5	170	43	380	81	100
6	810	44	200	82	90
7	540	45	100	83	50
8	360	46	750	84	160
9	50	47	80	85	280
10	180	48	210	86	110
11	140	49	670	87	650
12	180	50	690	88	60
13	200	51	510	89	140
14	60	52	140	90	280
15	360	53	130	91	380
16	100	54	230	92	260
17	40	55	60	93	280

18	50	56	220	94	60
19	100	57	310	95	300
20	130	58	420	96	90
21	490	59	210	97	60
22	70	60	190	98	180
23	120	61	280	99	250
24	410	62	70	100	80
25	250	63	150		
26	510	64	550		
27	170	65	460		
28	620	66	80		
29	150	67	470		
30	80	68	210		
31	60	69	40		
32	280	70	200		
33	250	71	40		
34	320	72	190		
35	510	73	130		
36	370	74	510		
37	140	75	680		
38	120	76	540		



WOLMAN SAMPLE:
Jonkershoek River

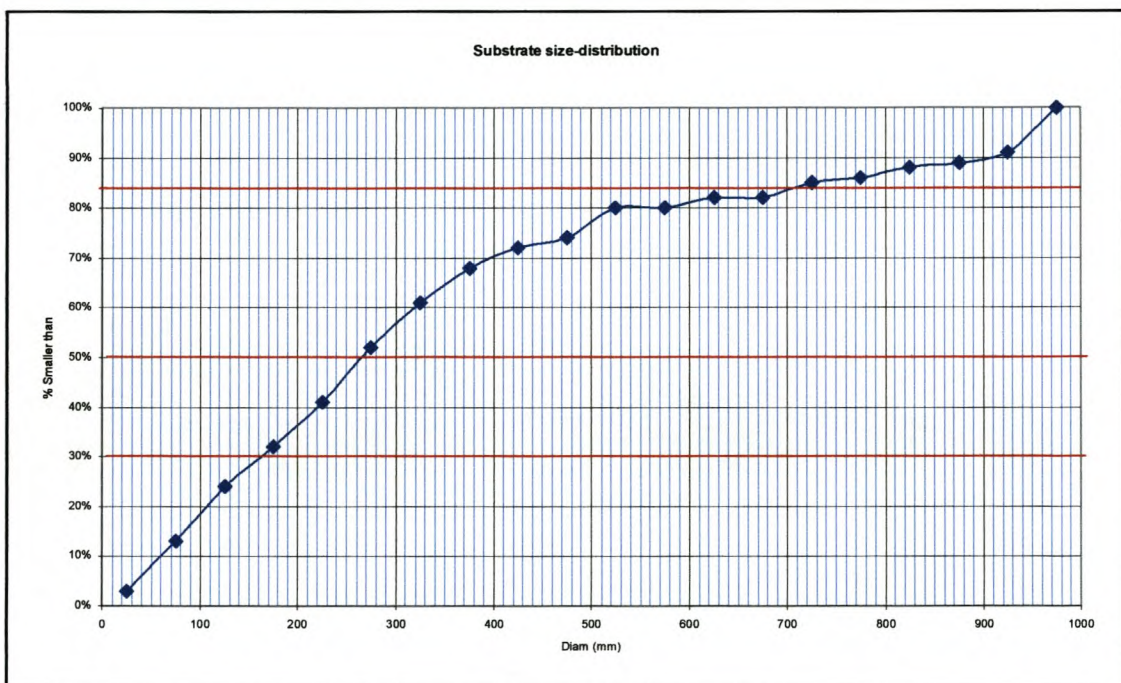
No.	Diameter (mm)	No.	Diameter (mm)	No.	Diameter (mm)
1	400	39	100	77	150
2	150	40	60	78	250
3	100	41	120	79	140
4	80	42	300	80	100
5	150	43	180	81	550
6	250	44	380	82	150
7	80	45	80	83	140
8	200	46	450	84	280
9	100	47	100	85	100
10	130	48	140	86	90
11	200	49	400	87	60
12	80	50	40	88	60
13	250	51	250	89	200
14	150	52	90	90	190
15	350	53	120	91	130
16	200	54	400	92	70
17	80	55	130	93	100
18	40	56	150	94	180
19	50	57	40	95	250
20	100	58	90	96	380
21	100	59	170	97	90
22	250	60	200	98	120
23	100	61	80	99	340
24	360	62	100	100	50
25	500	63	100		
26	480	64	150		
27	230	65	150		
28	230	66	60		
29	80	67	100		
30	500	68	100		
31	150	69	300		
32	380	70	130		
33	400	71	600		
34	130	72	150		
35	400	73	400		
36	600	74	130		
37	300	75	500		
38	350	76	180		



WOLMAN SAMPLE:
Molenaars River

No.	Diameter (mm)	No.	Diameter (mm)	No.	Diameter (mm)
1	1000	39	500	77	150
2	200	40	1000	78	350
3	200	41	700	79	140
4	70	42	900	80	200
5	100	43	300	81	400
6	1000	44	350	82	120
7	250	45	80	83	280
8	30	46	250	84	150
9	450	47	90	85	150
10	50	48	100	86	1000
11	250	49	270	87	300
12	500	50	200	88	200
13	250	51	1000	89	300
14	20	52	180	90	250
15	200	53	1000	91	500
16	200	54	130	92	400
17	600	55	600	93	350
18	100	56	40	94	300
19	500	57	160	95	250
20	150	58	350	96	400
21	1000	59	80	97	250
22	300	60	300	98	350

22	300	60	300	98	350
23	500	61	80	99	300
24	150	62	50	100	500
25	100	63	140		
26	130	64	1000		
27	1000	65	300		
28	750	66	400		
29	800	67	850		
30	130	68	450		
31	800	69	900		
32	200	70	80		
33	250	71	700		
34	200	72	700		
35	300	73	350		
36	350	74	100		
37	180	75	60		
38	80	76	250		



WOLMAN SAMPLE:
Berg River

No.	Diameter (mm)	No.	Diameter (mm)	No.	Diameter (mm)
1	80	39	200	77	190
2	180	40	180	78	90
3	140	41	250	79	100
4	220	42	170	80	100
5	360	43	350	81	80
6	150	44	330	82	140
7	300	45	300	83	250
8	100	46	240	84	250
9	190	47	130	85	300
10	130	48	120	86	270
11	80	49	250	87	80
12	250	50	60	88	60
13	100	51	400	89	400
14	220	52	200	90	280
15	140	53	150	91	420
16	80	54	250	92	120
17	90	55	370	93	70
18	130	56	100	94	450
19	100	57	250	95	380
20	70	58	300	96	70
21	340	59	50	97	300
22	120	60	250	98	280
23	190	61	150	99	150
24	400	62	60	100	240
25	260	63	140		
26	320	64	270		
27	100	65	80		
28	330	66	200		
29	140	67	160		
30	130	68	200		
31	260	69	50		
32	70	70	120		
33	50	71	100		
34	80	72	70		
35	60	73	190		
36	140	74	100		
37	100	75	200		
38	80	76	300		

